MINISTERE DE L'ENSEIGNEMENT SUPERIEUR ET DE LA RECHERCHE SCIENTIFIQUE
UNIVERSITE MOHAMED KHIDER - BISKRA
FACULTE DES SCIENCES ET DE LA TECHNOLOGIE
DEPARTEMENT DE GENIE ÉLECTRIQUE

Thèse de Doctorat

En vue de l'obtention du diplôme de docteur LMD en génie électrique

Contribution à l'étude du diagnostic du vieillissement d'une pile à combustible PEMFC.

Réalisé par: **Hichem kahia**

Soutenue publiquement le: 21/12/2023

Devant le jury composé de:

Bahri Mubarak	Professeur	Université de Biskra	Président
Saadi Aicha	MCA	Université de Biskra	Rapporteur
Rouina Abdelhafid	MCA	Université de Biskra	Examinateur
Ziet Lahcene	Professeur	Université de Sétif	Examinateur

Année Universitaire 2022/2023

MINISTERE DE L'ENSEIGNEMENT SUPERIEUR ET DE LA RECHERCHE SCIENTIFIQUE
UNIVERSITE MOHAMED KHIDER - BISKRA
FACULTE DES SCIENCES ET DE LA TECHNOLOGIE
DEPARTEMENT DE GENIE ÉLECTRIQUE

Thèse de Doctorat

En vue de l'obtention du diplôme de docteur LMD en génie électrique

Contribution to the study of the diagnosis of the aging of a PEM fuel cell.

Réalisé par: **Hichem kahia**

Soutenue publiquement le: 21/12/2023

Devant le jury composé de:

Bahri Mubarak	Professeur	Université de Biskra	Président
Saadi Aicha	MCA	Université de Biskra	Rapporteur
Rouina Abdelhafid	MCA	Université de Biskra	Examinateur
Ziet Lahcene	Professeur	Université de Sétif	Examinateur

Année Universitaire 2022/2023

العنوان: المساهمة في دراسة تشخيص شيخوخة خلية وقود PEMFC

الخلاصة:

لصالح الانبعاثات المنخفضة والكفاءة العالية لخلية الوقود ، تعتبر خلايا الوقود بمثابة أجهزة توليد الطاقة من الجيل التالي في المدن الذكية والتنقل المستدام. تقوم خلايا الوقود بتحويل الطاقة الكيميائية المخزنة في الوقود إلى كهرباء بطريقة كهروكيميائية. مطلوب تشخيص مناسب لتحديد الأخطاء المختلفة التي قد تحدث في أنظمة خلايا الوقود. تعتبر قضية إدارة المياه مهمة بشكل خاص في خلية الوقود. يتمثل دور دائرة الترطيب في ترطيب الغازات التي تدخل خلية الوقود ، بشكل عام من الماء الذي تنتجه الخلية ، والذي يتم استعادته بواسطة مكثف. يقلل تجفيف الغشاء أو الترطيب الزائد من إنتاج الطاقة الكهربائية ويحد من عمر خلية الوقود. لضمان التشغيل السليم (سلامة خلية الوقود ، وقت الاستجابة ، القيود الميكانيكية ، إلخ) ، من الضروري أن يكون لديك نظام تحكم عالمي يعمل على فهم واكتشاف وتشخيص وعزل كل من أوضاع الفشل هذه في خلية الوقود. يركز هذا العمل على إيجاد طريقة مناسبة وفعالة وسهلة الاستخدام ، لتلافي الأخطاء المتكررة التي تنتج عن ضعف تدفق الماء داخل خلية الوقود أثناء تشغيلها ، وقد أوضحت هذه الدراسة أن الرطوبة النسبية ترتبط مع معلمات التحليل الطيفي للمعاوقة الكهروكيميائية ، ونموذج التحكم في شبكة الخلايا العصبية الاصطناعية فعالة في التقدير الصحي لخلية الوقود وتشخيص المشكلات المتعلقة بإدارة المياه التي تسبب تدهور الأداء والمتانة. توفر الطرق المعروضة في هذه الدراسة العديد من المزايا مقارنة بالتقنيات الأخرى التي تتطلب عددًا كبيرًا من قواعد البيانات والأدوات ، وهذا ما يبرره التحليل من حيث سرعة الإنذار وسرعة التنفيذ والتكلفة المنخفضة.

الكلمات الأساسية: خلايا وقود غشاء التبادل البروتوني (PEMFC) ، الشبكة العصبية الاصطناعية ، الحالة الصحية (SOH) ، الذكاء الاصطناعي (AI).

Titre : Contribution à l'étude du diagnostic du vieillissement d'une pile à combustible PEMFC

Résumé : En faveur des faibles émissions et du haut rendement de la pile à combustible, la pile à combustible est considérée comme un dispositif d'alimentation de nouvelle génération dans les villes intelligentes et la mobilité durable. Les piles à combustible convertissent l'énergie chimique stockée dans les combustibles en électricité de manière électrochimique. Un diagnostic adapté est nécessaire pour identifier les différents défauts pouvant survenir dans les systèmes de pile à combustible. La question de la gestion de l'eau est particulièrement importante dans la pile à combustible. Le rôle du circuit d'humidification est d'humidifier les gaz entrant dans la pile à combustible, généralement à partir de l'eau produite par la pile, récupérée au moyen d'un condenseur. Le séchage ou le surmouillage de la membrane diminue la production d'énergie électrique et limite la durée de vie de la pile à combustible. Pour assurer un bon fonctionnement (rendement, sécurité de la pile à combustible, temps de réponse, contraintes mécaniques, etc.), il est nécessaire de disposer d'un système de contrôle global qui agit sur la compréhension, la détection, le diagnostic et l'isolement de chacun de ces modes de défaillance dans la pile à combustible. Ce travail se concentre sur la recherche d'une méthode appropriée, efficace et facile à utiliser, pour éviter les erreurs fréquentes qui sont présentées par le mauvais écoulement de l'eau à l'intérieur de la pile à combustible pendant son fonctionnement. Cette étude a démontré que l'humidité relative passée et présente est en corrélation avec les paramètres de spectroscopie d'impédance électrochimique, et un modèle de contrôle de réseau de neurones artificiels est efficace dans l'estimation de la santé des piles à combustible et le diagnostic des problèmes liés à la gestion de l'eau qui entraînent une détérioration des performances et de la durabilité. Les méthodes présentées dans cette étude offrent de nombreux avantages par rapport à d'autres techniques qui nécessitent un grand nombre de bases de données et d'instruments, et cela justifié par l'analyse en termes de pronostic précis rapide, rapide à mettre en œuvre et à faible coût.

Mots clés : Piles à combustible à membrane échangeuse de protons (PEMFC), Réseau de neurones artificiels, État de santé (SOH), Intelligence artificielle (IA).

Title : Contribution to the study of the diagnosis of the aging of a PEM fuel cell.

Abstract :

In favor low emissions and high efficiency of fuel cell (FC), Fuel cell is regarded as next generation power devices in smart cities and sustainable mobility. Fuel cells convert the chemical energy stored in fuels to electricity in an electrochemically way. A suitable diagnostic is required to identify the different faults that may occur in fuel cell systems. The water management issue is particularly important in PEMFC. The role of the humidification circuit is to humidify the gases entering the fuel cell, generally from the water produced by the cell, recovered by means of a condenser. Drying or overwetting the membrane decreases electrical energy production and limits FC life. To ensure proper operation (yield, FC safety, response time, mechanical constraints, etc.), it is necessary to have a global control system that acts on understanding, detection, diagnosis and isolation of each of these failure modes in the PEMFC. This work focuses in finding a suitable, effective, and easy to use method, to avoid the frequent mistakes that are presented by the poor flow of water inside the fuel cell during its operation.This study demonstrated that past and present relative humidity correlates with the electrochemical impedance spectroscopy parameters (EIS), and an ANN control model is effective in health estimation of PEMFC and diagnosing water management related problems that cause performance deterioration, durability. The presented methods in this study provides many advantages compared to other techniques that require a large number of database and instruments, and this justified by the analysis in term of fast accurate prognostic, quick to implement and low cost.

Key words : Proton exchange membrane fuel cells (PEMFC), Artificial neural network, State of health (SOH), Artificial intelligence (AI).

Publications

✓ **Hichem Kahia**, S. Aicha, D. Herbadji, A. Herbadji, and S. Bedda, "Neural network based diagnostic of PEM fuel cell"
J. New Mater. Electrochem. Syst., vol. 23, no. 4, pp. 225-234, 2020, doi: 10.14447/JNMES.V23I4.A02.

✓ **Hichem Kahia**, Saadi, A., Herbadji, A., Herbadji, D., Ramadhan, H.M. (2023). "Accurate estimation of PEMFC state of health using modified hybrid artificial neural network models"
Journal of New Materials for Electrochemical Systems, Vol. 26, No. 1, pp. 32-41. https://doi.org/10.14447/jnmes.v26i1.a05

Conferences

✓ **Hichem Kahia**, Saadi Aicha, Abderrahmane Herbadji and Djamel Herbadji "PEM fuel cell Diagnosis using Convolutional Neural Networks"
4thInternational Conference on Applied Engineering and Natural Sciences, November 10-13, 2022, Konya, Turkey.
(https://drive.google.com/file/d/170fpXifUv0TH4q7IHFhE7iLIo lAvo33/view usp=sharing).

✓ **Hichem Kahia**, Saadi Aicha, Djamel Herbadji and Abderrahmanel Herbadji, Aissa Belmeguenai, "An improved approach towards PEM fuel cell water management using artificial neural network"
Fourth International Conference on Technological Advances in Electrical Engineering (ICTAEE 23.), May 23-24 2023, skikda, Algeria.

✓ **Hichem Kahia**, Saadi Aicha, Abderrahmane Herbadji and Djamel Herbadji "Overview of PEM fuel cell diagnosis"
National Seminar of Physics, Chemistry and Their Applications (NSPCA 23), Mohamed El Bachir El Ibrahimi University, Bordj-Bou-Arreridj, March 6th-7th, 2023.
https://sites.google.com/univ-bba.dz/nspca23/publications.

✓ **Hichem Kahia**, Saadi Aicha, Djamel Herbadji and Abderrahmane Herbadji "Artificial intelligence and fuel cells: diagnosis of flooding and drying in PEMFC using neural networks"
3rd National Conference on Applied Physics And Chemistry (3rdNCAPC23), Ecole Normale Superieure de Laghouat Laghouat, Algeria, March 12-13, 2023.

✓ **Hichem Kahia**, Saadi Aicha, Djamel Herbadji and Abderrahmane Herbadji "Recent advances in PEM fuel cell diagnosis: accomplishments and challenges"
3rd National Conference on Applied Physics And Chemistry (3rdNCAPC23), Ecole Normale Superieure de Laghouat Laghouat, Algeria, March 12-13, 2023.

Acknowledgements

First and above all, I would like to express my heartfelt gratitude to ALLAH, the merciful, for blessing me with the mental and physical strength and enlightening me on the right path to conclude my PhD studies successfully.

I owe my gratitude to my advisor ***Dr. Saadi Aicha*** for the guidance, supervision, motivation, and support. This excellent support and guidance have indeed helped me find a proper direction in my work.

I would like to express my appreciation to my thesis committee members:

Pr. (Bahri Mubarak), Professor at the University of biskra, finds here the expression of my most sincere thanks for having accepted to chair this thesis.

Pr. (Ziet Lahcene), Professor at University of Setif-1, for the interest shown in our work and his participation in the jury as an examiner.

Dr. (Rouina abdelhafid), Lecturer A at the University of biskra, for having accepted to be an examiner as well as for his great assistance in the administrative matters.

I would like to express my deepest gratitude to ***Mr. Abderrhamane Herbadji***, University of Msila, ***Mr. Djamel Herbadji***, University of Skikda. their dedication, thirst for novelty, guidance, and commitment to quality were inspirations to honing my research skills in the field the artifcial intelegence and deep learning.

Finally, I would like to express my gratitude and appreciation to all of my family for their support, encouragement, and help.

Hichem Kahia
21/12/ 2023

Contents

List of Figures

List of Tables

Glossary of Important Terms

✓ **ANN**: Artificial neuron network

✓ **bi**: bias vector of neural network identifier

✓ **CPE**: Constant Phase Elements

✓ **D**: Diffusion coefficient

✓ **F**: Faraday constant ($Asmol^{-(1)}$)

✓ **FCOV**: Fuel cell output voltage

✓ **N**: Number of electrons

✓ **Q**: Parameter of the CPE

✓ **qwin**: Molar flow air in the inlet (mol/s)

✓ **R**: Perfect gas constant ($Jmol^{-(1)}K^{-(1)}$)

✓ **Rd**: Electrical resistance [Ohm]

✓ **RH**: Relative humidity

✓ **Rm**: Membrane resistance [Ohm]

✓ **Rp**: Polarisation resistance [Ohm]

✓ **S**: Active area (m^2)

✓ **T**: Temperature (K)

✓ **tm**: Membrane thickness (m)

✓ **u**: Equation of hidden layer's input

✓ **V cel**: Cell voltage (V)

✓ **W**: Weights of ANN output layer

✓ **Z**: Fuel cell impedance [Ohm]

✓ **ZCPE**: CPE impedance

✓ **Zw**: Warburg impedance [Ohm]

✓ **SVM**: Support Vector Machines

- ✓ α: Power of the CPE
- ✓ δ: Diffusion layer width (m)
- ✓ τ_d: The time constant of diffusion (s)
- ✓ w: Pulsation ($rads^{-(1)}$)

Chapter 1

General Introduction

1.1 Introduction

No alternative fuel today meets public acceptance for competing with traditional fossil fuels, which have benefited from nearly a century of continuous improvement by the oil industry. Currently, the energy crisis and the increase in the level of pollution are major problems worldwide. New renewable and clean energy sources must, therefore, be considered and this will be one of the eminent challenges in these years, both economically and environmentally [13].

Soon, fuel cell technology will be considered as a renewable primary energy source. The fuel cell will generate electrical energy from hydrogen; this is why it has become one of the key energy converters for the future, whether for stationary and on-board applications (laptops, cars, buses, planes, scooters, boats, and submarines) [14].

There are various types of fuel cells which are classified based on the nature of the electrolyte and/or the operating temperature. Among these categories of the fuel cell, we find PEM (Polymer Exchange Membrane) fuel cell. The electrolyte (i.e. polymer membrane) allows the transport of protons to the cathode side from the anode side. The electrons, meanwhile, move inside external load, thereby producing useful electrical power.

Currently, many researchers revolve around augmenting the service life and understanding the aging mechanisms in a fuel cell system, e.g. modifying air flow rate, humidifying gases, etc. to confirm the proper functioning of the PEMFC. Therefore, the diagnosis of PEMFC (i.e. the technique of detection and identification of faults) are treated essentially in the literature, for instance, the works in [15, 16, 17, 18, 19].

The fuel cell must operate under conditions where the speed of evaporation and evacuation of water is slower than its production's speed to keep the membrane hydrated. Some operating conditions applied to the fuel cell may lead to produce two types of antagonistic faults (drowning and drying).

Generally, the detected faults are linked to the management of water in the membrane [20, 21, 22, 23]. Among the most used methods for characterization is electrochemical impedance spectroscopy (EIS). This method is employed to measure the value of the electrical resistance or for monitoring degradation [24, 12, 25, 26, 27]. During each degradation phase, EIS can be carried out to characterize the impedance and describe its evolution of the parameters in order to allow differencing between drying and flooding.

There are a significant amount of methodological approaches to identify and diagnose a fuel cell system, which can be classified into five families, i.e. semi-empirical models, knowledge models, black-box models, empirical approaches, and finally information processing techniques.

These methodologies can be normally divided into two groups: so-called static methods or so-called dynamic methods. The static approach is particularly interesting to make a technological choice concerning like the catalyst or to size components of the cell). While, dynamic

methods are preferable when one wishes to analyze transient phenomena such as a sudden change of a set point or a parameter.

1.2 Goals of this Thesis

The proton exchange membrane (PEM) fuel cell has attracted much attention due to its high efficiency and environmental friendliness, of which the only reaction product is water. Water state and transport always have a significant effect on the output characteristics and reliability of the fuel cell under various conditions (e.g. cold start and normal operation). PEM fuel cell failure modes' diagnosis (flooding & drying) is very important to the normal operation of the PEMFC, since dehydration hinders the proton delivery in the membrane and thereby the performance will be limited. In addition, the water accumulation is generally lead to the flooding inside the fuel cell, this flooding might prevent the reactant transport and result in the gas starvation.

PEM fuel cell diagnosis has been extensively adopted in the literature primarily thanks to straightforwardness in easy identification of water state in fuel cell. The State of Health and the service life of fuel cells are related to the fault diagnosis strategy of the PEMFC system. The existing PEM fuel cell diagnosis methods can normally be grouped into five classes: semi-empirical, empirical, physical, analytical and the black-box models.

The semi-empirical, empirical, physical, analytical-based diagnosis techniques are remarkably affected by several factors. For instance, computationally expensive, the need for experimental and invasive instrumentation, large number of characteristic quantities, slowness of the temporal resolution [5], inserting the sensors into the PEMFC stack changes its intrinsic behavior which makes difficulties to distinguish between the effect of the fault and presence of this sensor. One of the potential solutions to vanquish these drawbacks is developing new schemes that should accurately and efficiently distinguish normal and different degrees of two typical fault states (flooding and drying) of the stack.

To this end, in this doctoral thesis, we suggest to deploy Artificial Intelligence for water management failure in PEMFC that it directly affects the durability and stability of fuel cells. The main idea behind using ANNs for PEMFC diagnostic is that neural network approach presents a high sensitivity to identify the parameters of the Randles model and capable to predict response of voltage under a sudden change in relative humidity.

The benefit of this work is summed up in the demonstration of the existence in a simple way that helps to define the state of health of the fuel cell by contributing to obtaining a good diagnosis without the need for expensive equipment.

1.3 Thesis organisation

The thesis is organised as follows. Chapter 2 discusses the basic issues of PEMFC (Fondamentals, materials and applications). Chapter 3 reports recent advances in PEM fuel cell diagnosis, i.e. the accomplishments and the challenges. Artificial intelligence technologies based proposed method for PEMFC diagnosis are described in chapter 4. In chapter 5, we experimentally evaluate the performance of the proposed artificial neural network model based PEMFC diagnosis framework. Concluding remarks, contribution and possible future directions of this research are eventually discussed in Chapter 6

Chapter 2

PEMFC (Fondamentals, materials and applications)

2.1 Introduction

Fuel cells (FC) are converters of chemical energy into electrical energy and heat. There are several types classified according to the nature of the electrolyte and/or the operating temperature. Among the different types of fuel cell, there are proton exchange membrane fuel cells, called PEMFC (Polymer Electrolyte Membrane Fuel Cell or Proton Exchange Membrane Fuel Cell) on which we will focus on. This chapter provides the literature review of fuel cell techniques (i.e. the necessary elements and the operation of the fuel cell as well as the deferent degradations).

2.2 Description of a PEMFC elementary cell

2.2.1 The elementary cell (The heart of the fuel cell)

Polymer Exchange Membrane Fuel Cell (PEMFC) represent an alternative energy conversion for stationary and automotive applications, where the electrolyte (i.e. polymer membrane) allows the transport of protons to the cathode side from the anode side. The electrons, meanwhile, move inside external load, thereby producing useful electrical power [28]. The overall electrochemical reaction occurring throughout the PEMFC is defined as follows 2.1:

$$O_2 + 2H_2 \rightarrow 2H_2O + energy + Heat \tag{2.1}$$

The enthalpy energy of the reaction can be calculated using Hess's law Eq. 2.2. Under standard conditions of pressure and temperature (1Bar and 298K or 25 ° C):

$$\Delta rH = \sum V_i \Delta H_i \tag{2.2}$$

The electrochemical reaction decomposed by the oxidize of hydrogen and the reduce of oxygen as the following half reactions 2.3, 2.4:

$$H_2 \rightarrow 2{H_2}^+ + 2e^- (Anode) \tag{2.3}$$

$$O_2 + 4H^+ + 4e^- \rightarrow H_2O(Cathode) \tag{2.4}$$

The membrane passes the protons to the cathode side; whilst, the electrons conducts inside external load to the cathode side, this process is displayed in Figure 2.1.

- **Electrolyte membrane** The thickness of the electrolyte mombran is about ten micrometers (from 20 to 200 ?m as a general rule). A low water content decreases the ionic conductivity and

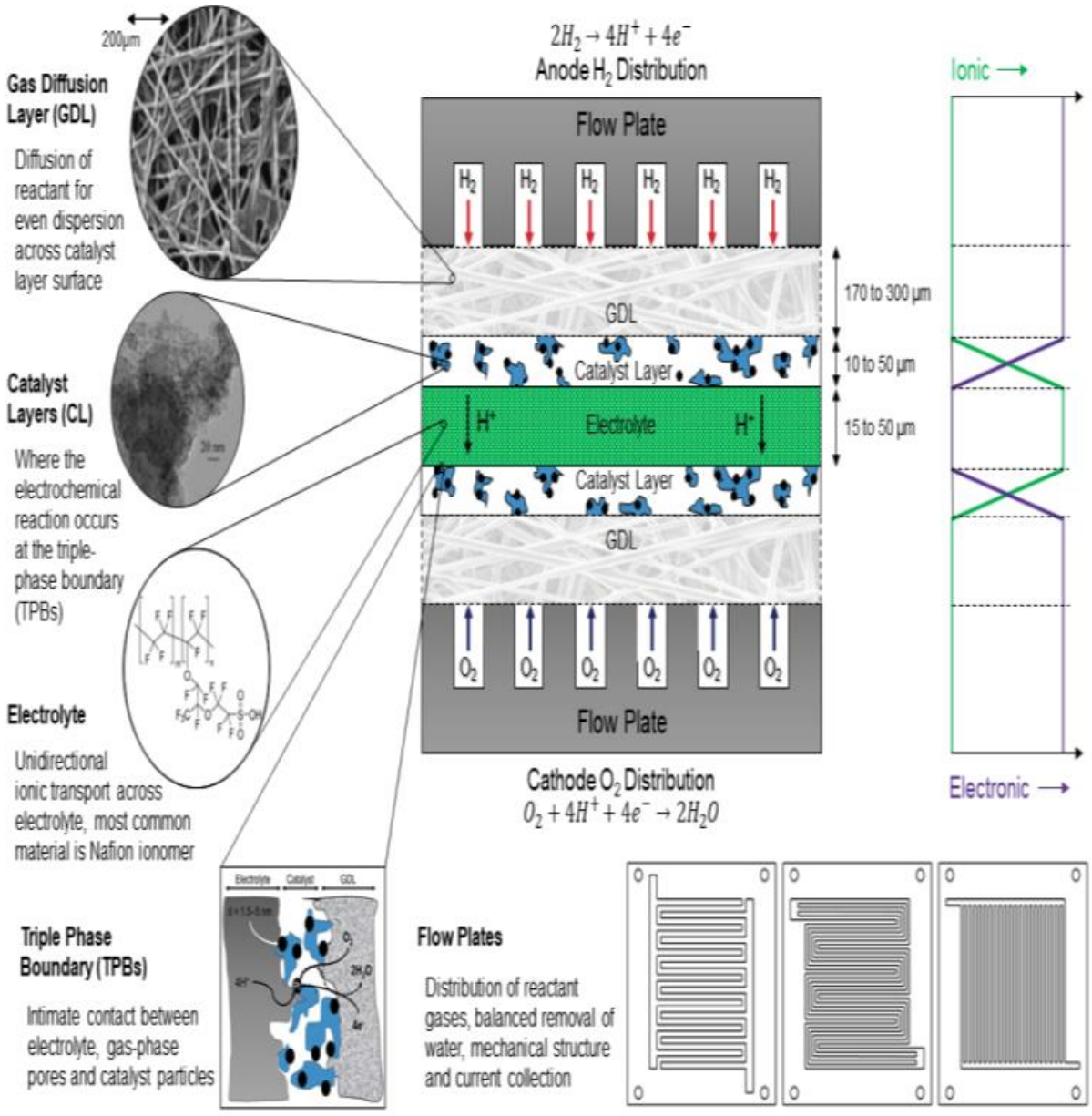

Fig. 2.1 *Overview of a PEFC single cell with highlighted microscopic images of the GDL and CL , illustrations of the electrolyte, TPBs and flow plates and a graphical representation of the ionic and electronic transport across the cell.*

increases its gas permeability. On the other hand, too high water contents can cause mechanical stresses due to the swelling of the membrane [29, 30].

• **Catalyst layer** The membrane is placed between two electrodes which constitute the catalyst layer (CL), seat of the oxidation-reduction half-reactions. The two active layers associated with the membrane constitute the Membrane Electrodes Assembly (MEA) [31].

• **Gas diffusion layer (GDL)** The AME, which is the heart of the PEMFC, is sandwiched between two gas diffusion layers (GDL for Gas Diffusion Layer) [32]. The diffusion layer provides several functions: (i) serves to supply reactants (H2 and O2/air to the anode and cathode respectively), (ii) provides electrical conduction between the bipolar plates and the active areas, (iii) evacuates the heat produced in the electrodes (resulting from reactions and ohmic losses), (iv) evacuates the water produced at the cathode towards the channel far from the electrodes, in order to prevent their flooding and drying (v) provide mechanical support for the MEA [33, 34, 35].

• **Bipolar plates** The external fluidic circuits are connected to the cell at the terminal plates and the reactant gases are distributed to the MEA on the surface of the bipolar plates via channels etched on them. Moreover, the low weight and high performance are important for manufacturing high-volume plats to be practical in industrial applications.

2.2.2 Transport mechanisms of ions and electrons

The two reactions on the anodic and cathodic side break down into several stages: the transport of the reactants towards the surface of the electrode, their adsorption on the surface of the catalyst, then, the catalyst accompanies the dissociation of molecules and the release/acceptance of protons and electrons. Finally, ionic transport is ensured by the membrane and electronic transport by the external circuit [36]. The membrane passes the protons to the cathode side; whilst, the electrons conducts inside external load to the cathode side, this process is displayed in Figure 2.2.

2.3 Sizing a PEMFC stack

To design the fuel cell corresponding to the book of terms of a given project, the designer has two degrees of freedom: The number N of the fuel cells placed in series and the surface A of a cell.

The stack's gross electrical power is calculated using the following relationship 2.5:

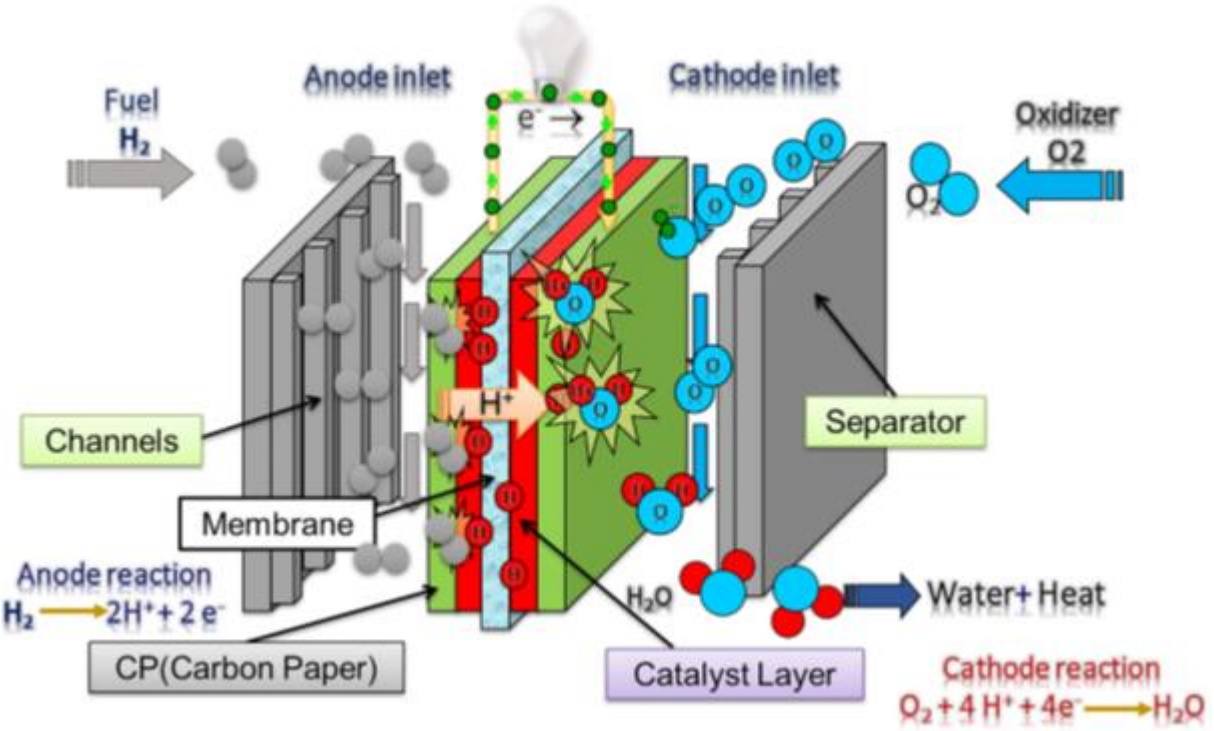

Fig. 2.2 *Basic PEM Fuel Cell process*

$$P_{ST} = V_{st}.I_{st} = N.V.J.A_s \tag{2.5}$$

Where P_{st} is gross electrical power of the stack (W), N is the number of stack cells, V is Voltage per cell (V), J is the current density A/m^2 and A_s is the active cell area m^2 [37, 38].

It is advantageous to have the highest voltage V_{st} and therefore the lowest possible current I_{st} because this limits the joule losses in the fuel cell.

2.4 Different types of fuel cells

The fuel cell applications can be categorized into three main areas (stationary, portable, and transportation power generation), which is why there are many types of fuel cells categorized by the features of each type as shown in Table 2.1 [9].The name of each fuel cell is directly related to the nature of the electrolyte.

2.5 PEMFC system

The overall system (core cell and auxiliaries) is called the fuel cell system. The auxiliaries of a fuel cell consume a significant part of the energy produced by it, thus causing the degradation of the efficiency of the system as shown in figure 2.3 [1]:

Table 2.1 *Fuel cell types.*

	PEMFCs	***AFCs***	***PAFCs***	***MCFCs***	***SOFCs***
Electrolyte	Polymeric membrane	Potassium hydroxide	Phosphoric acid	Molten carbonate	Ceramics
Charge carrier	H^+	OH^-	$H+$	CO_3^{-2}	O^{-2}
Operating temperature	$-40-120^0C$ $(150-180^0C$ in high temp PEMFCs)	$50-200^0C$	$150-220^0C$	$600-700^0C$	$500-1000^0C$
Electrical efficiency	Up to 65-72%	Up to 70%	Up to 45%	Up to 60%	Up to 65%
Primary fuel	H_2, reformed H_2, methanol in direct methanol fuel cells	H_2 or cracked ammonia	H_2 or reformed H_2	H_2, biogas, or methane	H_2, biogas, or methane
Primary applications	Portable, transportation, and small-scale stationary	Portable and stationary	Stationary	Stationary	Stationary
Shipments in 2019	934.2 *MW*	0 *MW*	106.7 *MW*	10.2 *MW*	78.1 *MW*

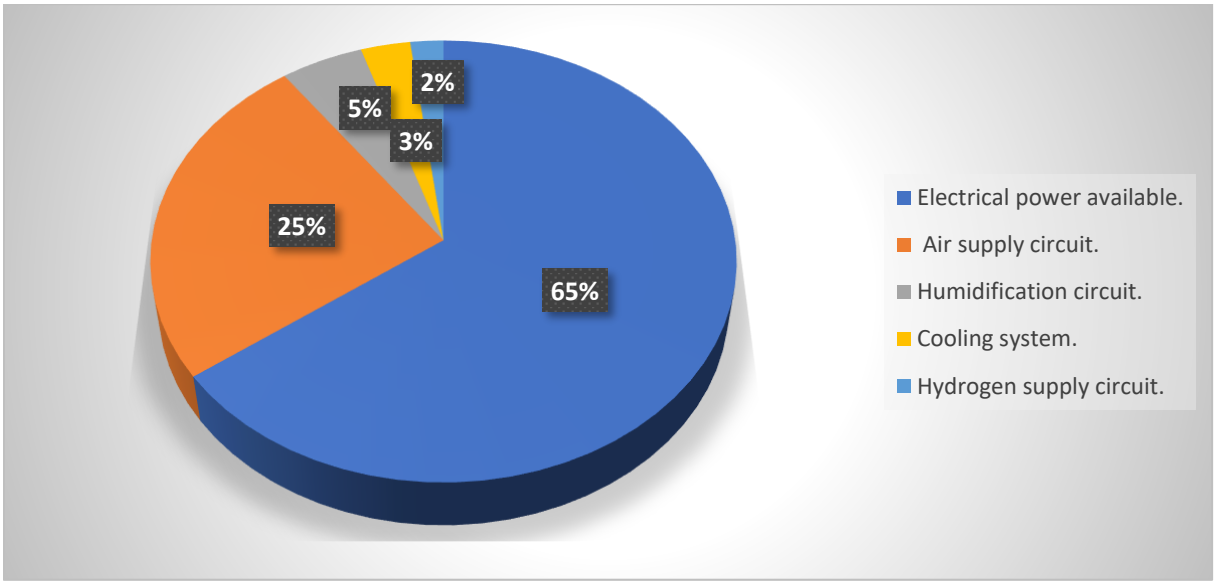

Fig. 2.3 *Division of electricity consumption in a fuel cell system. [1]*

2.5.1 Hydrogen supply circuit

The gas is stored in a tank at pressures ranging from 300 bar to 700 bar. In order to satisfy the pressure conditions at the fuel cell inlet (up to 3 bar), it is necessary to add a pressure reducer between the storage and the fuel cell.

2.5.2 Cooling system

For low powers, a fan can be made which can be the same as the one supplying the cell with air. In the case of higher power batteries, cooling plates are therefore inserted between the elementary cells of the stack and its temperature is thus regulated thanks to the flow rate of the fluid circulating in an independent circuit.

2.5.3 Humidification circuit

The role of the humidification circuit is to humidify the gases entering the cell, generally from the water produced by the cell, recovered by means of a condenser. Drying or over-wetting the membrane decreases electrical energy production and limits battery life.

2.5.4 Control system

To ensure proper operation (yield, battery safety, response time, mechanical constraints, etc.), it is necessary to have a global control system that acts on the various interacting subsystems:

✓**Control of static converters for energy management.**

✓**Control of the gas flow rate and the motor-compressor unit.**

✓**Control of the water pump and the fan necessary for cooling.**

✓**Humidifier temperature control.**

2.5.5 Air supply circuit

In the case of terrestrial, stationary or on-board applications, the fuel cells are mainly supplied with air. The air supply to the cell is ensured according to the required pressure level. The efficient processes of air supply are discussed in Figure 2.4.

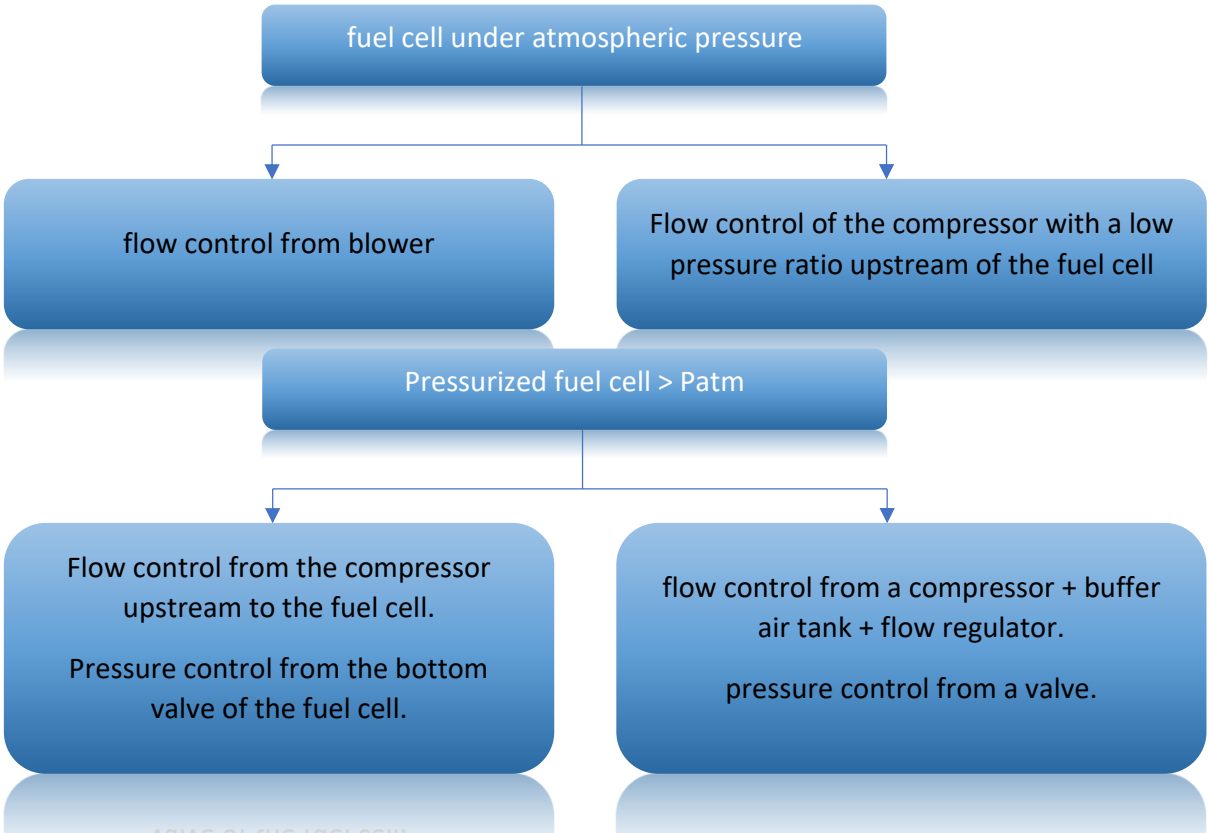

Fig. 2.4 *Different methods of supplying air to PEMFC.*

2.6 Principle of operation of an elementary cell

2.6.1 Thermodynamics

The two electrochemical reactions governing the operation of a fuel cell occur at the membrane/electrode interface. The electrochemical reaction decomposed by the oxidize of hydrogen

and the reduce of oxygen as the following halfreactions 2.6, 2.7:

- **On the anode side:**

$$H_2 \rightarrow 2H_2{}^+ + 2e^- \tag{2.6}$$

- **On the cathode side:**

$$O_2 + 4H^+ + 4e^- \rightarrow H_2O \tag{2.7}$$

- **The oxidation-reduction equation:**

$$O_2 + 2H_2 \rightarrow 2H_2O \tag{2.8}$$

The energy enthalpy of the reaction which can be calculated using Hess's law under standard conditions 2.2; In the case of water formation 2.9:

$$\begin{cases} \Delta rH = -\Delta H(H_2)gaz - (1/2)\Delta H(O_2)gaz + \Delta H(H_2O)liquide \\ \Delta rH = -285.83[Kj.mol^{-1}] \end{cases} \tag{2.9}$$

The equilibrium voltage is calculated using Nernst's law and it defines the open circuit voltage according to the gas concentrations 2.10.

$$Emax = E_{(ex,max)} + \frac{RT}{2F} ln\left(\frac{P_{(O_2)}{}^{1/2} P_{(H_2)}}{a_{(H_2O)}}\right) \tag{2.10}$$

Where:

- Eex,max =$(-\Delta rG/2F)$ = 1.2[V].
- ΔrG (Gibbs free energy or Gibbs energy)= -237.2 [kJ . mol-1].
- F (Faraday constant)= 96485 C/mol.
- PO_2, PH_2 : are the relative pressures of gases.
- a(H_2O): water activity.
- T: the temperature.
- R: the perfect gas constant (8.314 J/mol.K).

2.6.2 Polarization curve (Operating point)

2.6.2.1 Principle

The actual cell potential is decreased from the ideal potential due to several types of irreversible losses [39], as shown in Figure 2.5 [2]. Because of these different irreversibilities, the polarization curve of a fuel cell (cell voltage as a function of current density) exhibits a non-linear

electrochemical behavior [40, 41, 42]. This characteristic is called the law of polarization and is generally described by the following relation 2.11:

$$V(j) = E - R_0 j - \frac{RT}{anF}\ln\left(\frac{j}{j_0}\right) - \frac{RT}{anF}\ln\left(1 - \frac{j}{j_L}\right) \tag{2.11}$$

where:

- R_0: the surface resistance of the AME ($\Omega.m^2$).
- j: the current density (A/m^2).
- a: the charge transfer coefficient.
- n: the number of electrons exchanged.
- j_0: the exchange current density (A/m^2).
- j_L: the limit current density (A/m^2).

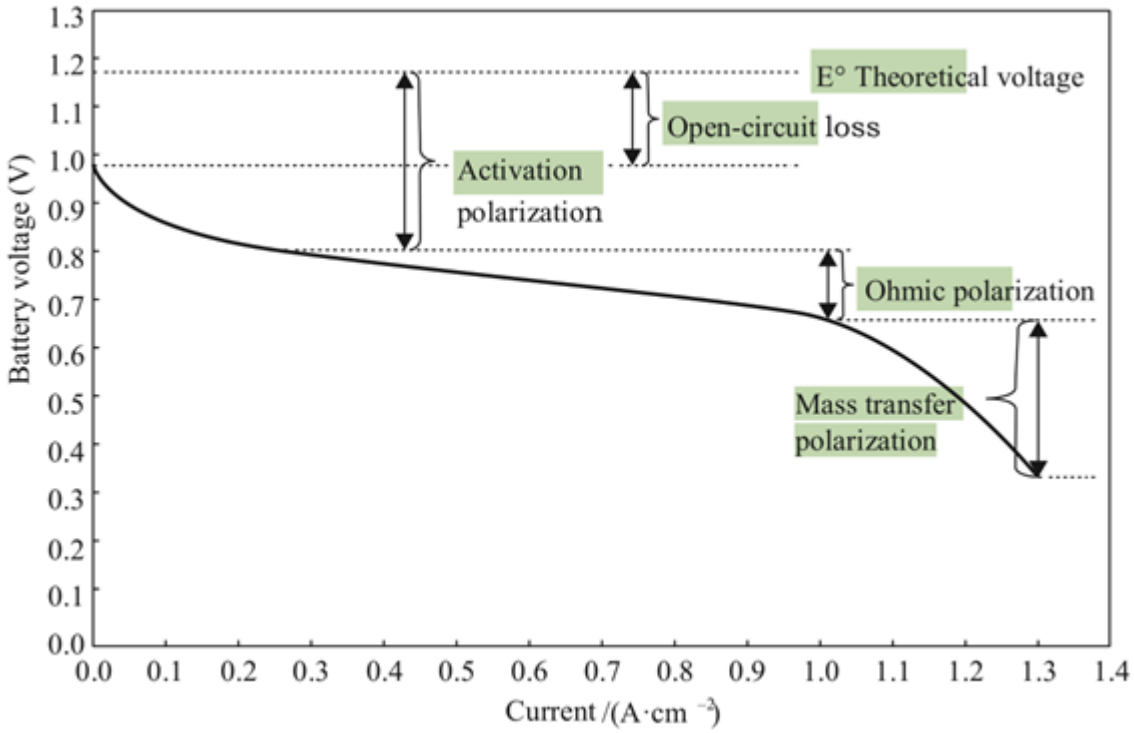

Fig. 2.5 *Typical polarization curve of a PEMFC.[2]*

2.6.2.2 Dynamic plotting of voltage-current curves

"Dynamic" reading, by current sweeping of high amplitude, at low frequencies, makes it possible to obtain very good results, with more information than point-to-point reading. Here, time, current and voltage information are thus retrieved, in much greater values than the traditional reading.

Compared to the point-to-point survey, this method allows a fairly easy reproducibility of

the tests and is much less dependent on the user. It also allows to obtain a very large number of points.

The notable difference between the point-to-point reading and the dynamic plotting is the time spent at each current value. In the case of the point-to-point survey, each point was surveyed by varying the current, then waiting for a stabilization time. In the case of dynamic tracing, the current only evolves on principle.

As shown in Figure 2.6 , the pressure was automatically regulated to 2bar and the H2 and O2 flows were set to satisfy the max current. The pressure and flow conditions were the same for the manual reading or current sweep reading tests [37].

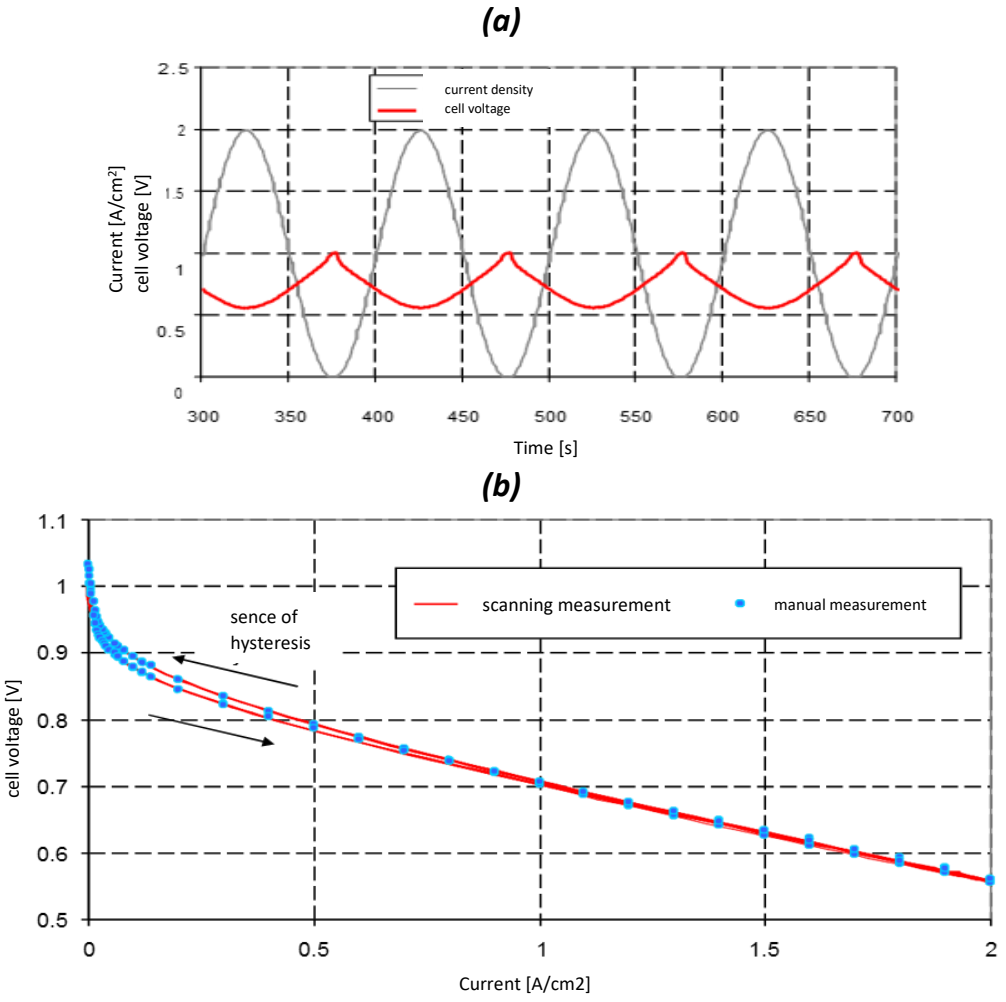

Fig. 2.6 *The sinusoidal current sweep at 10 mHz and the Comparison of the VI curves of a point-to-point reading "by hand" and that obtained by Monocell sweep supplied with H_2/O_2.*

2.6.3 Performance of the PEMFC

The maximum theoretical efficiency of the stack (without losses) is given by $\eta ex, max$ 2.12:

$$\eta_{ex,\max} = (\Delta rG/\Delta rH) = (228.2/285.82) = 0.79 \; or \; : 80\%. \tag{2.12}$$

The actual total electrical efficiency 2.13 [43]:

$$\begin{cases} \eta_{real,total} = \eta_{ex,max} \times \eta_{ex,elec} \times \eta_{farad} \times \eta_{mat} \times \eta_{sys} \\ \eta_{ex,elec} \,(\text{the electrical exergy efficiency}) = E_{mes}/E_{max} = 0.7/E_{max} = 60\% \\ \eta_{farad} \,(\text{the faradical yield}) = \eta_{farad} \; = I_{mes}/I_{theo} = I_{mes}/(2FDv/VmN) \end{cases} \tag{2.13}$$

where:
Dv is the hydrogen flow in l/s; Vm the molar volume of hydrogen in l/mol and N the number of cells.
ηmat (The material yield)= 95%.
ηsys (the system efficiency) takes into account the energy required for the pre-conditioning, humidification and compression of the reagents as well as for the control electronics.

2.7 State of the art of possible failures in the PEMFC

The PEMFC failure modes fall into two categories, depending on whether they are caused by internal or external causes associated to abnormal operating conditions. The internal causes stem from the operation of the cell itself: irreversible degradation due to aging, malfunctioning of water management, etc. The external causes are due to the pollutants brought into the cell, in particular by gases, in this case we will talk about poisoning. In order to achieve optimal efficiency, it is necessary to understand, detect, diagnose and isolate each of these failure modes in the PEMFC.

2.7.1 Reversible degradation

2.7.1.1 Flooding and drying out of a fuel cell

It's well known that fuel cell produces water when it delivers a current. The produced water is generally too much and therfore it will slow the diffusion of gases and distribute them well over the diffusion layers. Here, water management issue is particularly important in PEMFC [44, 45].

✓ **Flooding of the electrodes (active and diffusion layers)**

∗ **Causes that can be combined:**

- Gas flow too low to evacuate water.
- Operating temperature too low.
- Reactive gases too humidified.
- Loss of the hydrophobic character (provided by the addition of Teflon) of the electrode.

∗ **Consequences :** One of the most complex failures in diagnosis is the flood condition. When the reactive gases find it difficult to diffuse to the reactive sites, this failure results in a sudden voltage drop as shown in Figure 2.7 [46].

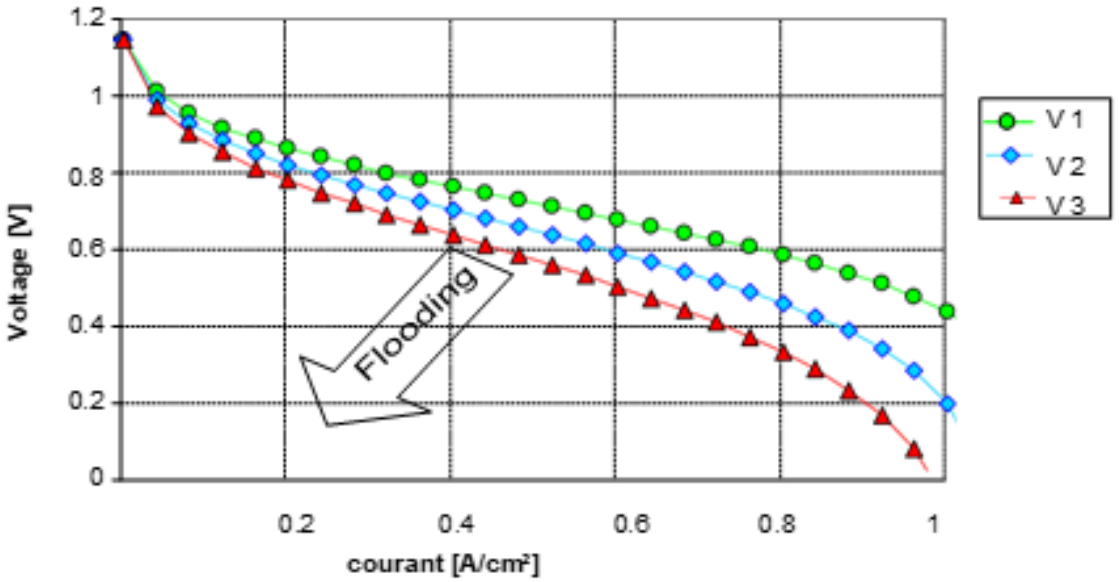

Fig. 2.7 *Voltage drop after RH is increased (during flooding).*

✓ **Canal congestion**

∗ **Causes that can be combined:**

- Electrode clogging.
- Gas flow too low to evacuate water.
- Purges do not take place.
- More problematic is poor channel design.

∗ **Consequences :** The reactive gases can no longer diffuse towards the reactive sites.

✓ **Dehydration of the membrane and the catalytic layers**

∗ **Causes that can be combined:**

- Gas flow too high.
- Insufficiently humidified reactive gases.
- Operating temperature too high.

∗ **Consequences :**

- Decreased proton conductivity (increased electrical conduction losses).
- Retraction of the membrane.
- Decrease and lack of water.
- Rupture of the membrane.

2.7.1.2 Malfunction of the gas supply to the electrodes

∗ **Causes that can be combined:**

- Engorgement.
- Gas supply fault.
- Gradual inerting of the electrode.

∗ **Consequences :**

- The risk is to consume the water in the membrane if the phenomenon continues.
- The cell functions as an oxygen pump, producing O_2 on the anode side and this can potentially be dangerous when resupplying with H_2.
- The cell then functions as a ”hydrogen pump”, producing H_2 on the cathode side and this can be dangerous when resupplied with O_2, fig 2.8 [47].

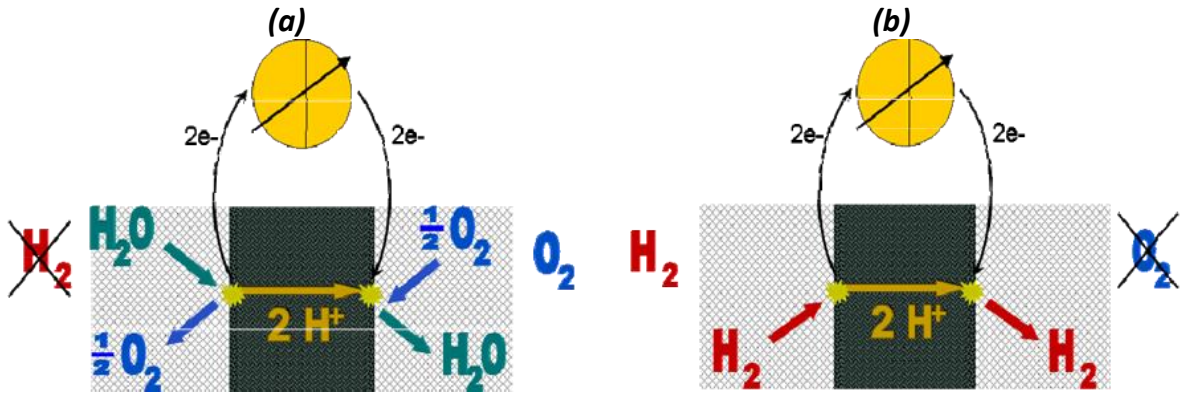

Fig. 2.8 *Power supply malfunction. (a) Depletion of H_2 at the anode. (b) Depletion of O_2 at the cathode.*

2.7.2 Irreversible degradation

2.7.2.1 Corrosion of carbon support catalyst

Carbon corrosion often occurs at the cathode depending on the reaction equation 2.14:

$$C + O_2 \rightarrow CO_2 \tag{2.14}$$

In some cases, it can also occur at the anode as following equation 2.15:

$$C + 2H_2O \rightarrow CO_2 + 4H^+ + 4e^{-4} \tag{2.15}$$

This reaction mainly occurs at high potentials. It leads to a loss of carbon mass. Endurance tests have shown a mass loss of up to 15% under 0.95 V (open circuit voltage) and up to 5% under 0.75 V. The carbon is then consumed on the anode side [48]. This phenomenon is limited in advance and is favored at the cathode.

2.7.2.2 Dissolution and migration of the platinum catalyst

There are several reaction mechanisms of dissolution:

- 1^{st} STEP:

$$Pt + 2H_2O \rightarrow PtO_2 + 4H^+ + 4e^- \tag{2.16}$$

- 2^{nd} STEP:

$$PtO_2 + 4H^+ + 4e^- \rightarrow Pt^{2+} + 2H_2O \tag{2.17}$$

This translates concretely into an irreversible loss of active surface and therefore of power

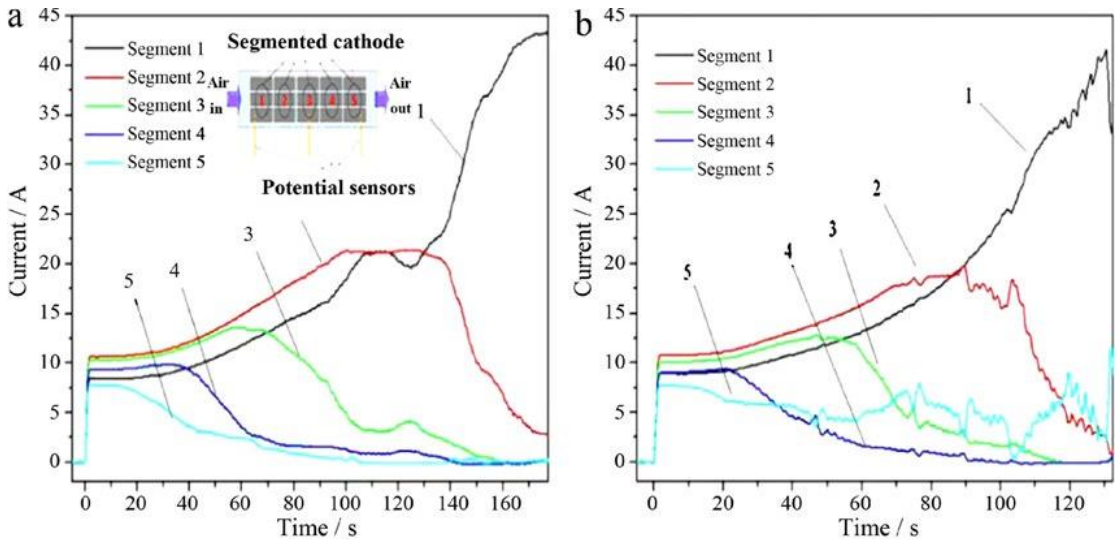

Fig. 2.9 *Evolutions of local current densities for a segmented cell: (a) H_2 stoichiometry at 1, (b) H_2 stoichiometry at 0.9 .[3]*

deliverable by the fuel cell [49, 50]. To overcome the problems related to platinum, in the works of [51] Authors suggested to replace platinum with platinum/gold clusters.

2.7.2.3 Membrane degradation

✓ **Mechanical damage** It can be caused by many factors such as thermal, cycles drying/humidification, large transient P, etc... [52].

✓ **Chemical damage** It leads to the appearance of free radicals (RH), that reduce the amount of beneficial substances.

A slow degradation of the membrane, for example, reduces its ability to transport ions, resulting in an increase in the electrical resistance of the fuel cell (therefore an increase in losses). In the case of storage, or not used for several weeks or several months, the membrane risks drying out too much.

2.7.3 Degradation and correlation with the current local distribution

The degradation mechanisms indirectly impact the current distribution in the cell in different ways; either by the local modification of the resistance of the fuel cells, or by reducing the active surface of the cell due to the degradation of the catalyst.

In the case of hydrogen depletion, the current density distribution of a cell subjected to different stoichiometric measurements of hydrogen (from 0.2 to 1) has been studied [3], and the current measurement is performed when using a segmented cathode (segment 1: gas inlets and segment 5: gas outlet) as shown in figure 2.9 [3].

2.8 Conclusion

There are different types of fuel cells which could be classified according to the nature of the electrolyte and/or the operating temperature.The name of each fuel cell is directly linked to the nature of the electrolyte. One of these categories is the PEM (Polymer Exchange Membrane) fuel cell. In this chapter, we have discussed the architecture and types of the fuel cells, their applications and potential in the development of fundamental knowledge and correlations, material selection and improvement, design and optimization of cells, fuel cell system, power management, monitoring of PEMFC operating status and possible failures. In order to achieve optimal efficiency, it is necessary to understand, detect, diagnose and isolate different failure modes that could be occured in the PEMFC, where it will be discussed in the next chapter.

Chapter 3

Advanced diagnosis techniques

3.1 Introduction

Behavior monitoring is a procedure performed manually or automatically, which aims to observe the state of a good service of the fuel cell. Automatic monitoring can be provided by sensors installed on the assets to be monitored and connected to a computer whose software has threshold values for these various sensors which can trigger the necessary alerts or shutdowns. We then talk about diagnostics to determine the procedure that consists in identifying the probable cause(s) of the failure(s) or the evolution of one or more significant parameters of degradation using logical reasoning based on a set of information. Diagnosis is used to confirm, complete or modify the assumptions made on the origin and cause of failures, and to specify the corrective actions or maintenance operations required. figure 3.1 displays a general monitoring and diagnosis diagram.

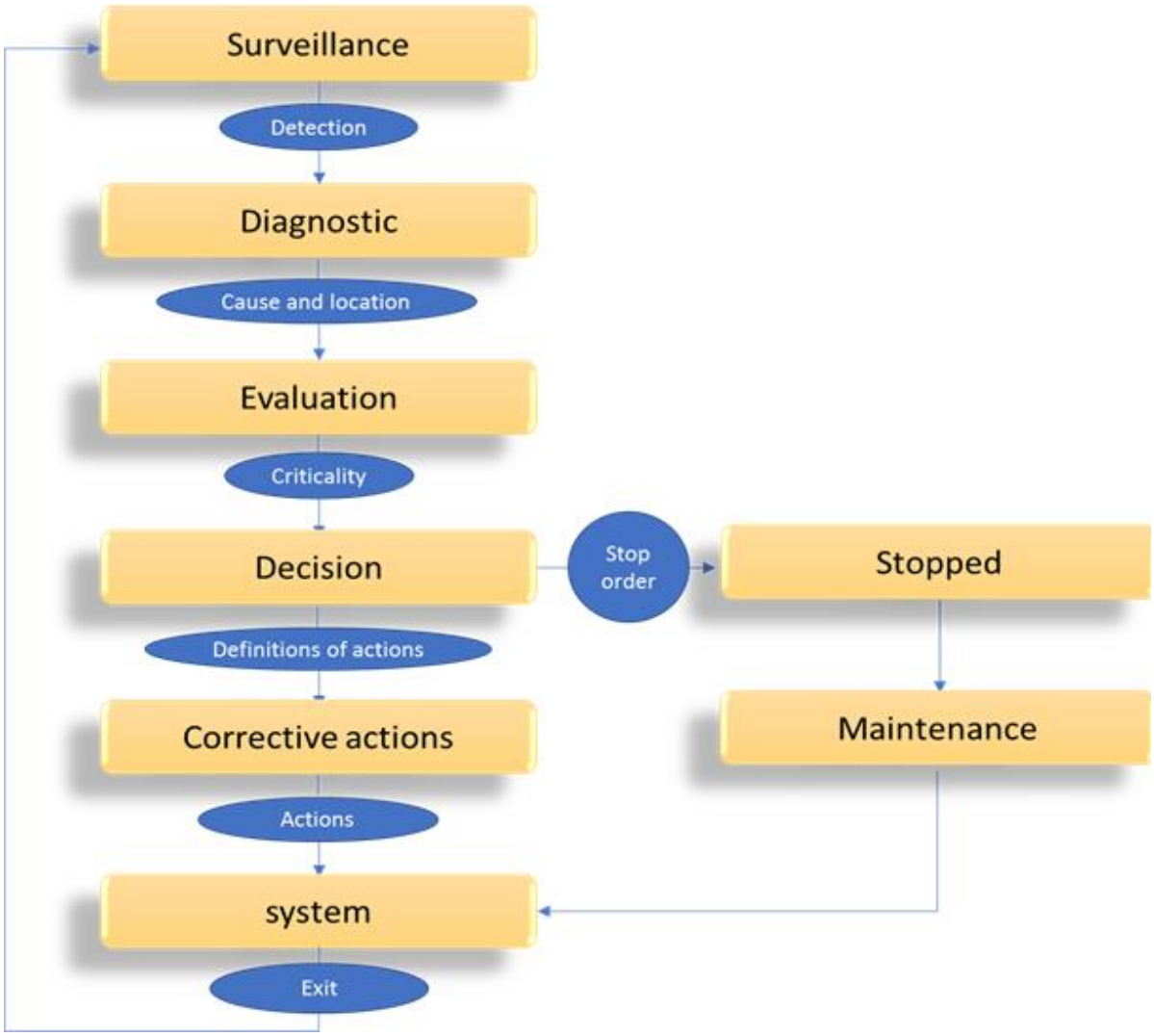

Fig. 3.1 *General monitoring and diagnostic diagram.*

3.2 Modeling and characterisation methodologies

There is a significant amount of methodological approaches that help to identify and diagnose a FC system. These approches can be classified into five families: knowledge models, semi-empirical models, black box models, empirical approaches and finally information processing techniques. The above-mentioned methodologies can be classified into two types: (static methods and dynamic methods). The static approach is particularly interesting for making a technological choice concerning, for example, the catalyst or for sizing fuel cell components. While dynamic methods are preferable when one wishes to analyze transient phenomena associated to a sudden change in a setpoint or a parameter.

3.2.1 Mechanistic Model

The first family of model is known under different names such as: knowledge model, mathematical model, physical model, or analytical model. This category of model calls upon precise relations describing in a physical way the various interactions between the input variables and the output vector according to the surrounding conditions (materials, boundary conditions, initial conditions). Even if more or less strong hypotheses make it possible to simplify the approach, the disadvantages of analytical models lie in the slowness of the temporal resolution of the equations, especially when the model is dynamic and in 3 dimensions (study on the 3 axes), as well as than in the validation of the model due to the large number of characteristic quantities to be estimated or measured. Finally, the need for experimental and sometimes invasive instrumentation is important in order to determine the characteristic quantities.

The use of equivalent electrical models involves passive electrical components to model the dynamic behavior of the fuel cell. This methodology is based on an experimental and multiparametric study allowing to determine the values of the model elements. Although mainly coupled with electrochemical impedance spectroscopy (EIS), some works has been undertaken using the current interruption (IC) method [53]. The advantage of this approach is the physical connection to the passive components of the model at a relatively low computational cost (parameter determination). Therefore, parameters cannot be determined in a single way as the impedance spectrum or current voltage reading that can be modeled by different equivalent circuits. However, using EIS as an equivalent model and complex nonlinear least squares algorithm allowed detection and identification of 3 defects (CO poisoning, immersion of electrodes and membrane drying) by varying model parameters [54]. On the contrary, there is a method to use the algorithm of multiparametric resolution, the use of the method by IC to wedge its model of Randles. The advantage of his approach lies in the fact that the solution found is unique with respect to the plot. Its disadvantage is that the IC method requires a fast acquisition system.

3.2.2 Black box model

The final interest of the black box approach is clearly to minimize the computation time linked to the model in order to be able to perform a control-command action on the system. The main disadvantage of this type of modeling is that there is no physical link between the model and the reality of things.

There are studies that use fuzzy logic and residue analysis as diagnostic vectors for two faults [55]: membrane drying out and water or nitrogen accumulation in the anode compartment. The residual values are calculated by considering the difference between the experimental operating point (current-voltage) and the current-voltage couple resulting from a reference polarization curve. The open-loop model is used to reduce computation time, which is combined with a genetic algorithm to increase detection sensitivity. The decision step is entrusted to an empirical probability threshold coupled with a logic circuit. This approach is interesting from a practical point of view since it only requires two low-cost sensors (current and voltage). While, authors in [56] have developed a model based on fuzzy logic with 3 inputs and one output according to the Standard additive model. In addition to the polarization curve, it uses electrochemical impedance spectroscopy to specifically identify the drying defect. In this perspective, the authors use the increase in the impedance amplitude as well as a decrease in the performance of the polarization curve to distinguish between drying and flooding respectively (fuzzy classification). The model is trained by an algorithm that classifies the health status of the generator into several levels (at least 3, one for each error). Although this method offers a good level of fault detection, it requires a large database to get an interesting level of detection. Another approach in [57] uses neural networks to diagnose any real-time change in the polarization curve due to aging effects, impurities contained in reactive gases and static or dynamic operation. The diagnosis is performed by comparing the polarization curve estimated by a model (through static or dynamic measurements) with a reference polarization curve. The polarization curve is estimated by an evolutionary learning algorithm (permanent learning) which transcribes the measured operating points into polarization curves. Neural networks have also been employed to detect the presence of contaminants in feed gases [10].

3.2.3 Semi-empirical model

Semi-empirical models occupy an intermediate place between physical models and behavioral models known as black boxes. This type has been used to diagnose the state of the fuel cell through the so-called current interruption method.

Researchers have suggested numerous models to diagnose the PEMFC. For instance the model developed by [58] is a simplification (reduction of the order) of a physical model using equivalent electrical circuits. The same method was used by [59] for diagnosing the presence of CO. Another semi-empirical model has been developed by [60] to study the effects of toluene

contamination on the polarization curve. Finally, authors in [61] used a semi-empirical approach combined with the current interruption method to detect the presence of the flooding phenomenon. The developed equivalent circuit is made up of a transmission line of three RC cells allowing modeling of the nonlinear equation linking the voltage to the current, the flaw detection is observed by varying certain parameters in the model.

The semi-empirical model has many advantages (e.g. increased convergence speed compared to physical models, preservation of part of the physical relations, etc.), and its interest in diagnostic context is informative and interesting.

3.2.4 Signal and information processing approaches

3.2.4.1 Signal approaches

The development of a physical, semi-empirical or black box model for diagnosis is relatively tedious, non-intuitive, costly in financial terms and in development time. To overcome these difficulties, the ”signal” approach has been proposed as an alternative to previously mentioned approches. In this case, it is actually a matter of finding one or more specific measurements (frequency, voltage, pressure, etc.) to characterize one or more defects it worth noting that. This approach has been widely implemented for fuel cell diagnostics.

An original method was proposed for detecting a possible accumulation of excessive water in the anode and cathode compartments [62]. The authors use the frequency response of the pressure sensor followed by a rung of current applied to the FC to estimate the water content in the cell (if there is for example flooding) using a local current density measurement in a segmented fuel cell. Furthermore, electrochemical impedance spectroscopy (EIS) is a technique capable of characterizing several physical and chemical processes provided that their time constants are distinct. The effect of drying being visible on the impedance spectrum in the frequency band 100 kHz-0.5 Hz. The effect of flooding being visible on a low frequency range starting at 100 Hz to 0.5Hz. The identification of frequency zones allowed the diagnosis and the determination of the defect. However, the measurement of several low-frequency points remains problematic. This problem was avoided by using three specific frequencies: 50 Hz, 500 Hz, and 5000 Hz to detect and identify poisoning, drying out and flooding faults [62, 21].

3.2.4.2 Information processing

The information processing approach is implemented in a way (logical, statistical or even probabilistic) based on the voltage distribution of the unit cells of the generator using a stochastic approach. The methodology allowed for a clear distinction between the different operating modes. Moreover, this approach has the advantage of remaining simple from the algorithmic point of view and thus, one can easily implement this method on embedded systems to get a

real-time diagnosis [63, 64].

The probabilistic approaches have also been considered for the diagnosis of FC [63]. This graphical method identifies or finds the logical cause and effect relationships present in the database through the various variables defined in the Bayesian network with five input parameters (voltage, current, electrical power, temperature and hydrogen pressure at the input of the stack) enabling the diagnosis of many faults. In addition, the graphical model of the Bayesian network was constructed using discriminating variables, observations, and diagnostics, these variables can only be defined by the network manufacturer.

3.3 Possible measurements on a fuel cell system for diagnosis

Fuel cell diagnostics is based on a measurement system that provides information on the performance of this system. When the available signals do not allow sufficient knowledge to be extracted or with the aim of deepening and reinforcing the diagnosis, excitation signals or test phases are imposed on the FC to allow information to be extracted through its response. The following figure 3.2 shows all the measurements that can be made on a fuel cell system [65, 66].

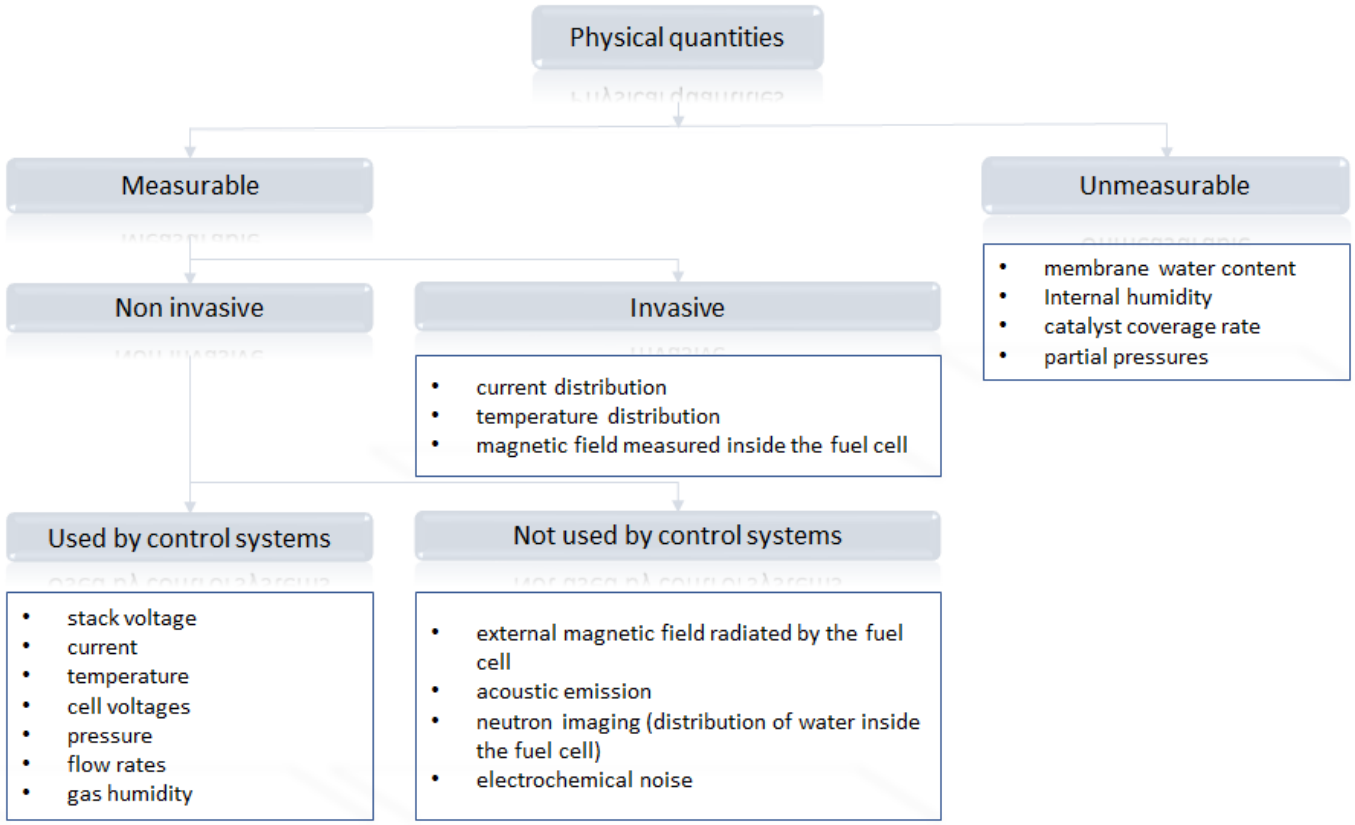

Fig. 3.2 *Fuel cell system measurements*

3.4 Invasive diagnostic technique

In order to collect information related to the behavior of the cell at particular locations, invasive techniques based on the insertion of active components inside the cell have been developed. The Membrane Electrodes Assembly (MEA) temperature measurements are performed in order to detect any hot spots. For instance, a film-formed gas temperature sensor was developed based on the use of thermistors. The local current density measurement card is marketed by a German company (S++ Simulation Services) which provides an image of the current distribution over the entire surface of the Membrane Electrodes Assembly. The internal magnetic field measurements have been explored in various works [67, 68, 69], where magnetic field sensors are inserted into the end plates of the stack. From the measurements of the fields, the current density is calculated directly using the Maxwell-Ampere equation.

The diagnosis by measuring the internal magnetic field is also studied by a Japanese team [69]. They use sensors at the end of which magnetic field sensors are attached (Figure 3.3) and inserted into the cooling channels of the PEMFC stack.

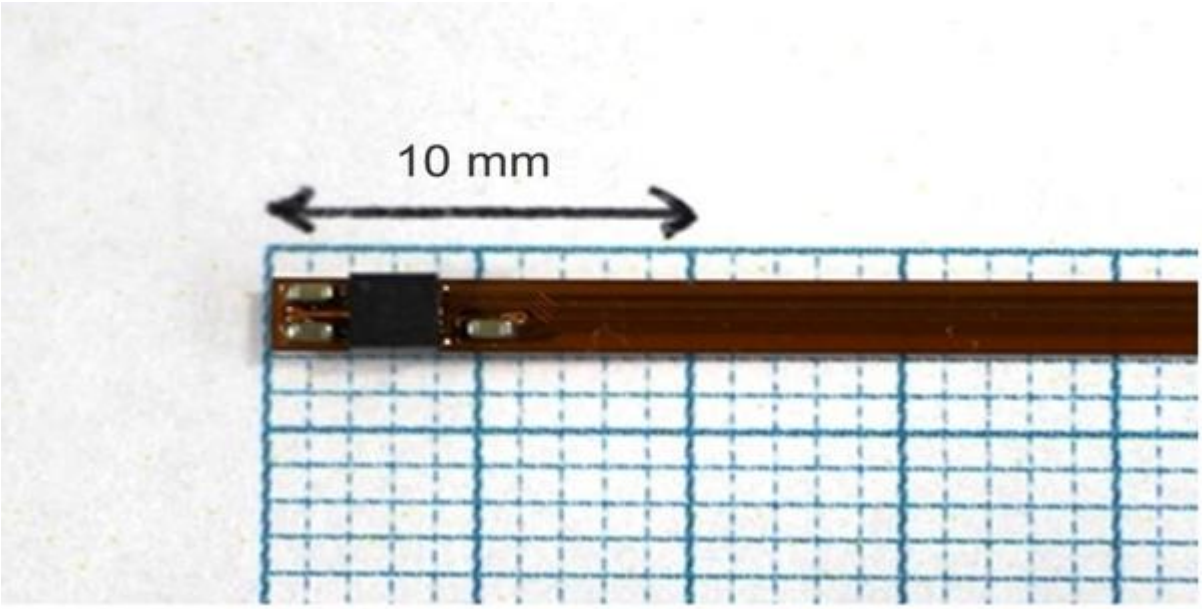

Fig. 3.3 *Magnetic sensor probe Picture.*

From each magnetic field measurement (Figure 3.4), the current density on the part of the cell where the probe was inserted is calculated.The technique was validated on a 300W stack, consisting of 20 cells, by inserting a network of 15 tri-axis sensors every 4 cells.

The invasive diagnostic methods are generally very effective because the measurement is carried out as close as possible to the fault and the exploitation is generally direct. On the other hand, an important disadvantage is that inserting the sensors into the PEMFC stack changes its intrinsic behavior. Therefore, it can be difficult to distinguish between the effect of the fault and the effect of the presence of the sensor. Thus, non-invasive approaches are preferred.

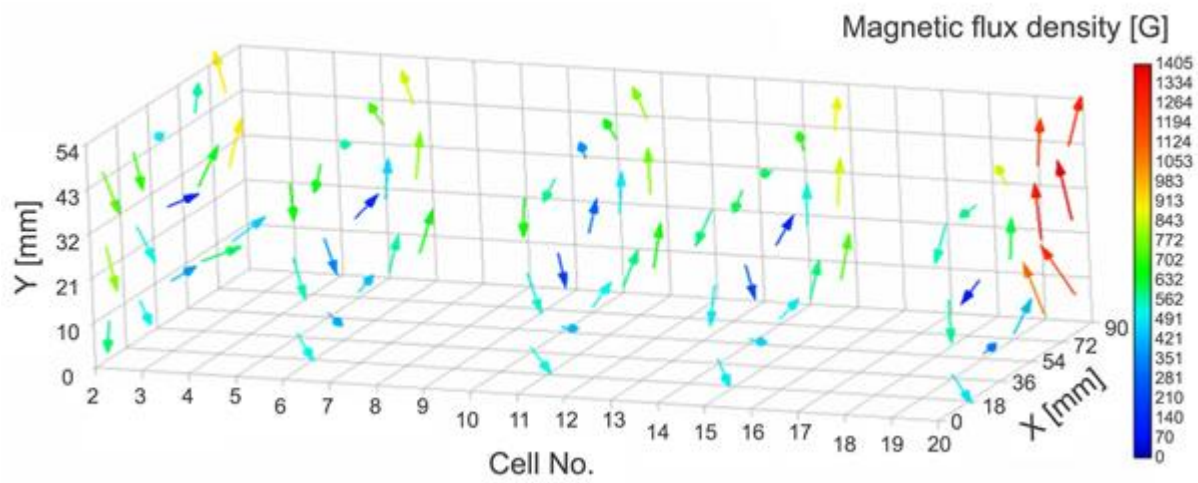

Fig. 3.4 *Vectors of magnetic flux density.*

3.5 Non-invasive diagnostic technique

3.5.1 Various experimental methods for performing diagnostics on the PEM fuel cell

Summary of the main characterization and diagnostic methods fig 3.5 [70].

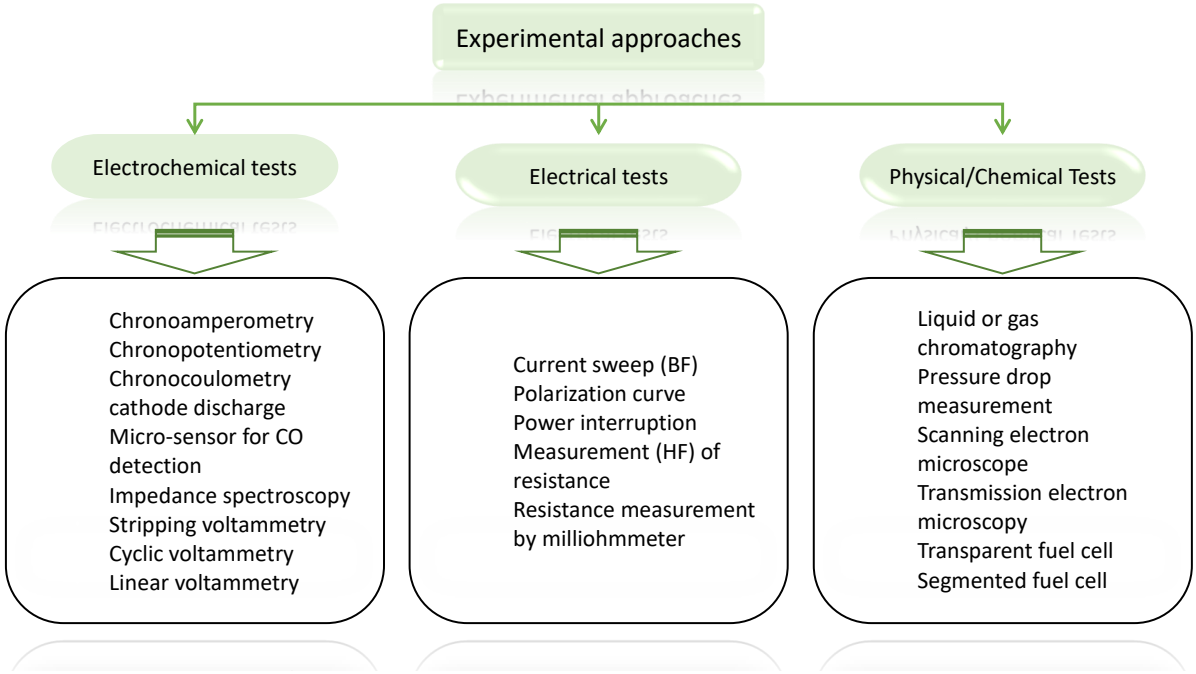

Fig. 3.5 *Summary of the main characterization and diagnosis methods applicable to a FC system or one of its elements.*

3.5.2 Voltammetry

3.5.2.1 Cyclic and stripping voltammetry

From an experimental point of view, the principle of cyclic voltammetry consists in applying a variation of "triangular potential" between two anodic and cathodic limit values (Ea and Ec) by the use of a potentatic assembly with three electrodes (i.e. a work electrode, reference electrode and auxiliary electrode). The work electrode and the auxiliary electrode are connected on both sides of the system in testing and allow the passage of the electric current. The reference electrode is immersed in an acid aqueous solution (typically H_2SO_4 sulfuric acid) which is used to simulate the proton conduction in the membrane [71]. Cyclic voltammetry is commonly used in electrochemistry to determine the catalytic activity of an electrode. As with the linear sweeping voltammetry, the potential in an experience by cyclic voltammetry is always controlled and the faradic current as well as the double layer current are measured. "We call Faradic current all current created by a redo chemical or electrochemical reaction". The intensity-potential curves obtained are called voltammograms.

Figure 3.6 displayed some examples of typical periodic voltammograms recorded on a five-cell PEMFC stack [4]. The voltammograms show multiple peaks of current associated with both redox reactions. The integration of these different low voltage peaks on the shaded area (fig. 3.6) provides information on the electrochemical active area.

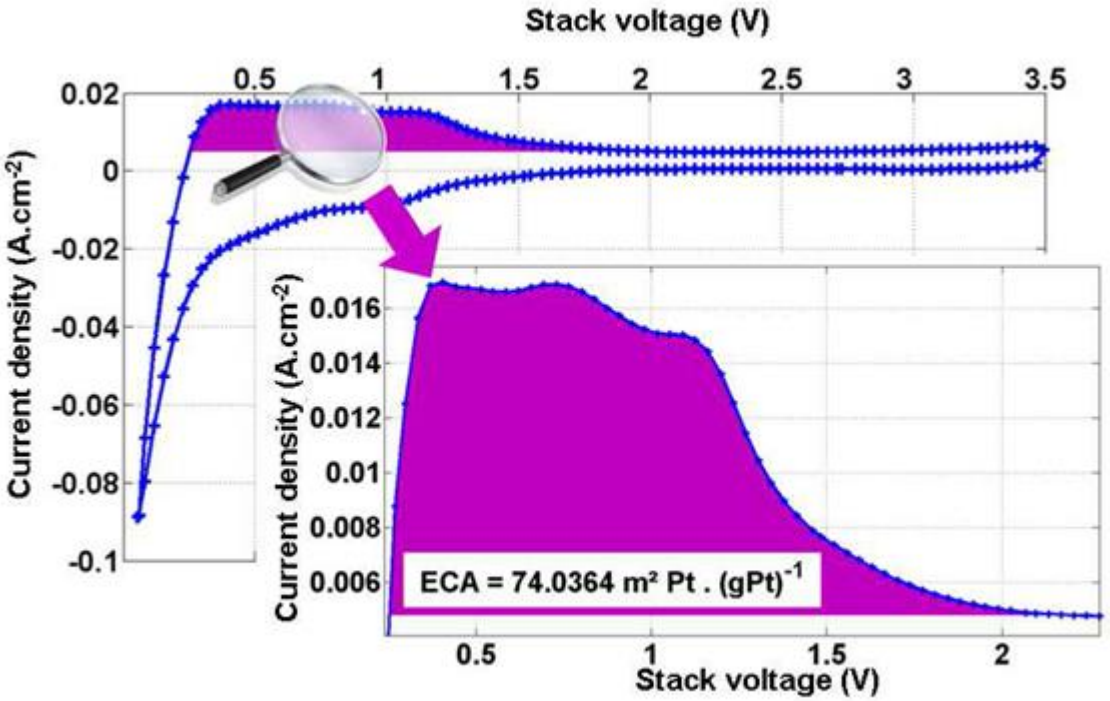

Fig. 3.6 *Example of cyclic voltammograms recorded at the boundaries of a stack of five cells .[4]*

In the figure 3.6, several areas can be distinguished: Disorption area: it corresponds to the release of H^+ions, also called desorption.

Central Zone: the measured current is only used to charge the double layer capacitor. Thus, a double-layer capacitor estimation can be made by measuring the lower limit of this current.

Oxide formation zone: corresponds to the surface oxidation of single oxygen species from the catalytic sites.

The cyclic voltammetry therefore allows a diagnosis of the battery, to know its really active platinum load, estimate the value of the double-layer capacitance, or even characterize the permeation of H_2 hydrogen through the membrane.

3.5.2.2 Linear voltammetry and chronocoulometry

The passage of reactant gases and electrons through the membrane over time usually results in a drop in potential. The current produced by these faults is generally called internal current since it does not serve the application powered by the FC. To measure its value, we can use a potentiostat and the method called linear sweeping voltammetry LSV. The potential of the system is swept linearly over time between two specific values, the maximum potential must not exceed a value of 1(V) in a humid environment in order to prevent any possible oxidation of the catalyst. The internal current could serve as alert data for off-line diagnosis of the membrane (permeation and short circuit), as shown in (figure 3.7) [4].

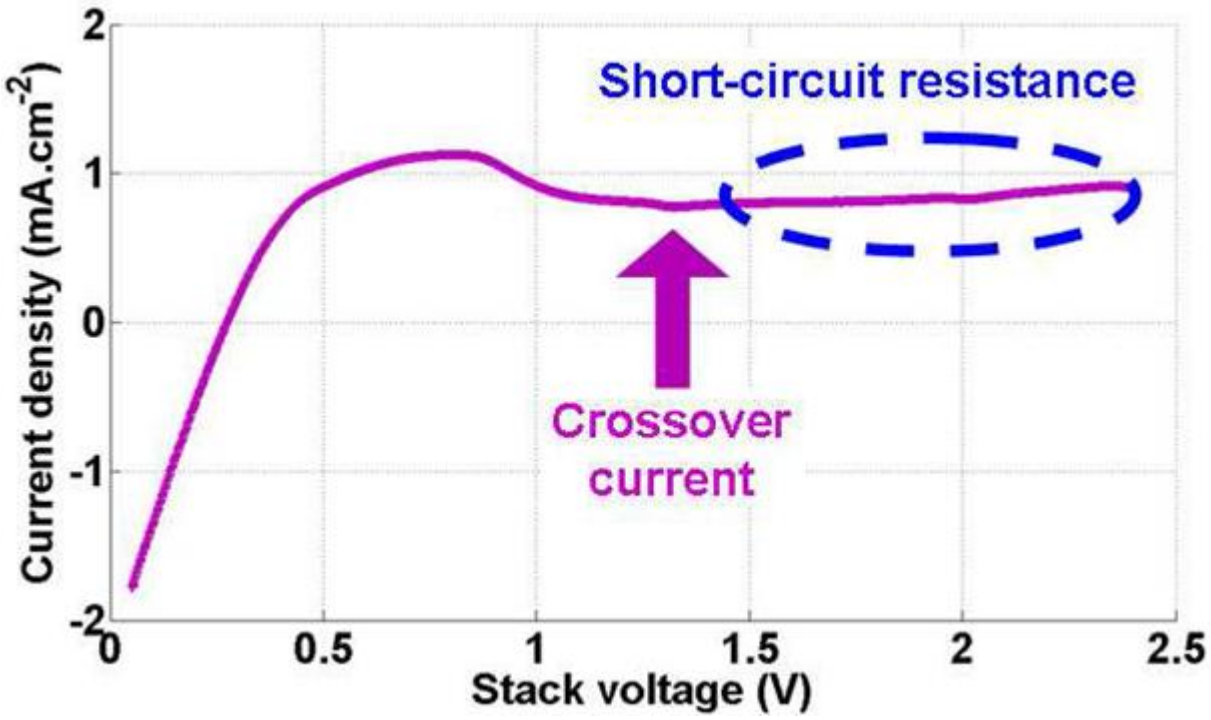

Fig. 3.7 *Example of linear sweeping voltammetry test result obtained on a three cell stack*

3.5.3 The step and the interruption of the current

This method used to identify the electrical and electrochemical parameters of the FC. The acquisition of values (current and voltage) must be done at a sampling frequency close to GHZ in order to separate ohmic losses from other losses [72, 73]. In addition, this method was then applied to study the effect of the cathode side dew temperature on the membrane resistance [74]. Moreover, the method of step and the interruption of the current requires very fast power acquisition and switching equipment if you want to have an accurate measurement of the ohmic resistance.

3.5.4 High amplitude and low frequency current sweep

The sweep can be sinusoidal or triangular with a frequency ranging from a few mHz to a few Hz, and amplitude of the current is usually between 0 A and its nominal value. The non-linear voltage response of the FC obtained in the I-U plane (the same as that of the polarization curves)is projected, its evolution as well as the hysteresis that it describes makes it possible to distinguish a deteriorating FC from a healthy FC. However, the strong difference in the current leads to large differences in certain parameters such as gas flow rates, temperature, pressure drops and the quantity of water in each of the compartments as well as in the membrane. The interpretation of the results can then be more complex.

3.5.5 Harmonic analysis

The basic principle of harmonic analysis is to send a signal to the fuel cell (e.g. a current respectively a voltage) very rich in harmonics, and to analyze its response in voltage (respectively in current). This measurement is fast and informative.

3.5.5.1 Harmonic analysis based on a chirp signal

A chirp signal is a pseudo-periodic signal whose frequency as a function of time used for certain electrical machine diagnostics, where the response to this signal is often exploited in time-frequency diagrams. This signal consists of a sinusoid, the frequency of which increases or decreases over time. Two classes are then differentiated:

- Linear chirps, whose frequency increases linearly over time equat 3.1.

$$\begin{cases} f(t) = f_0 + k * t \\ y_{lin}(t) = \sin(2\pi * f(t) * t) \\ f(t) = f_0 * k^t \end{cases} \tag{3.1}$$

- Geometric chirps, whose frequency varies geometrically equat 3.2.

$$y_{geo}(t) = \sin\left(\frac{2\pi}{\ln(k)} * (f(t) - f_0)\right) \tag{3.2}$$

Due to its frequency richness, this signal can also be used to measure the impedance of a fuel cell. For example, use it in combination with a rectangular signal, the current setpoint therefore consists of a rectangular excitation of a few periods, a few Hertz, immediately followed by a chirp signal.

3.5.5.2 Analysis from the total harmonic distortion (THD)

This method is used to be able to detect a fault in the fuel cell. In [5], they proposed the addition of a sinusoidal current of zero average value to the current delivered by the fuel cell. They were thus able to determine a frequency for the fundamental at which the detection of flooding or drying out is possible thanks to the THD calculation of the voltage produced by the injected current.

THD technology is viable during fuel cell operation without having to change or adapt the actual operating conditions of the FC system. Moreover, no conceptual changes to already developed stack designs are required to implement this system.

The harmonic analysis can also be performed by calculating the total harmonic distortion THD equat 3.3.

$$THD = \sqrt{\sum_{h=2}^{\infty} \left(\frac{Q_h}{Q_1}\right)^2} \tag{3.3}$$

where:

- Q_h: rms value of current / voltage.
- Q_1: fundamental component.
- h: harmonic rank.

In Figure 3.8 [5], an H_2 supply fault can easily be detected by monitoring the THD value.

3.5.5.3 Harmonic analysis from a square signal

The main goal is to determine the complex impedance value from the current and voltage signals, by analyzing these signals into Fourier series we can deduce the modulus and argument as a function of frequency, i.e. the complex impedance of the fuel cell. A square wave can be decomposed into a series of sinusoidal signals of multiple frequencies of the fundamental frequency. The advantage of this method is a very fast measurement of the complex impedance of the fuel cell, thanks to the harmonic richness of the signal sent.

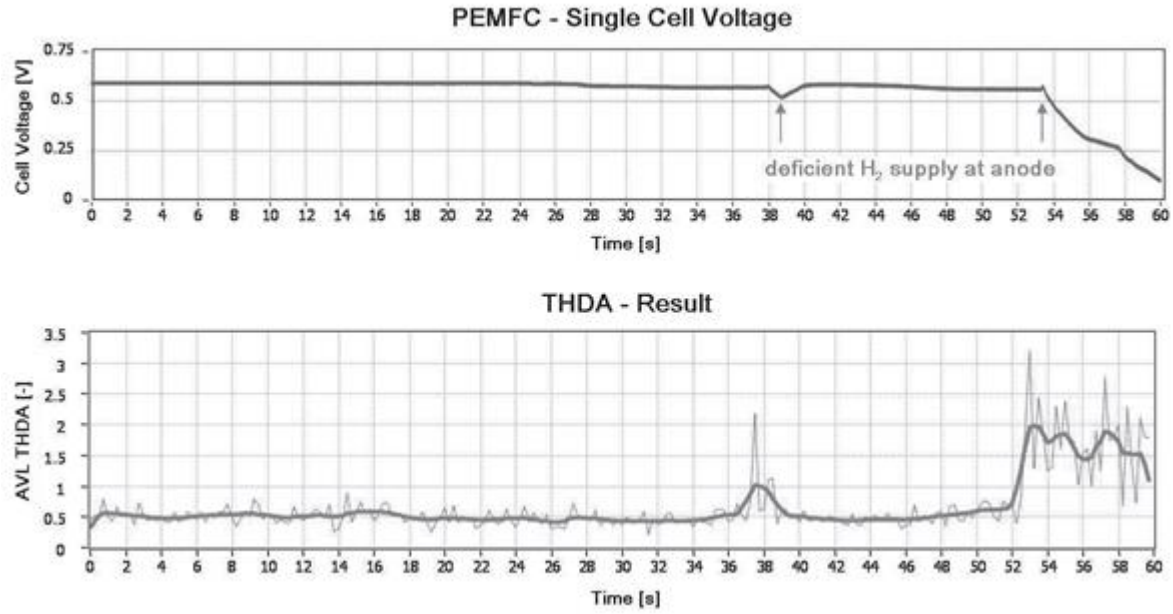

Fig. 3.8 *Example of using the THD for fault detection .[5]*

3.5.6 Impedance spectroscopy via a DC/AC/DC static converter

A static three-stage DC/AC/DC converter consisting of an inverter on the fuel cell side and a rectifier on the DC bus side was used to perform a measurement by impedance spectroscopy (figure 3.9) [75]. By using the PWM control of the power switches, it was possible to extract the impedance spectrum of the stack. However, the measurement of the individual impedances of each of the cells making up the generator has not been considered. Its duality (adapting the voltage between the FC and the load, electrochemical measurement system) makes its use interesting for embedded systems.

The integration of EIS functionality into the fuel cell system expands the onboard diagnostic strategies. This makes it possible to use EIS results for real-time diagnostic strategies to improve PEMFC usage conditions and extend its life time without any increase in its cost.

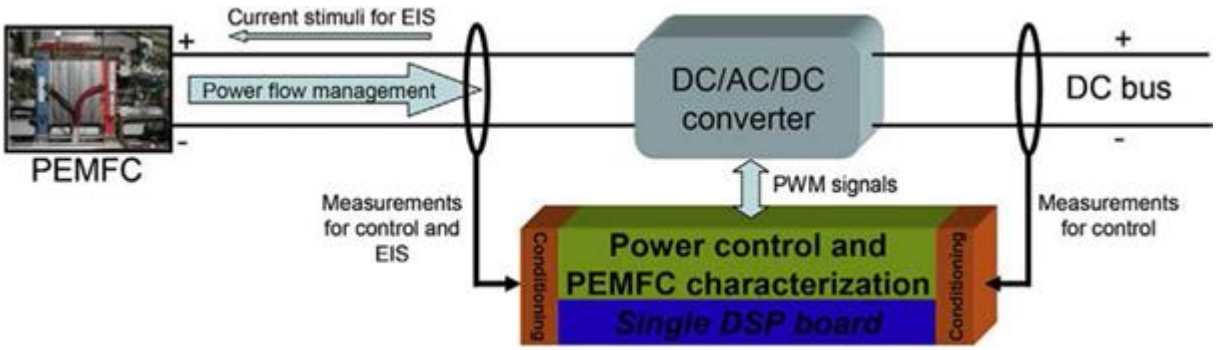

Fig. 3.9 *Principle of EIS integration in the power converter control.*

3.5.7 Measurement of the resistance by milliohmmeter

The resistance is determined by applying a high frequency alternating sinusoidal signal to the FC in normal operation, i.e. with a regulated or unregulated load in parallel. The choice of high frequency signal amplitude should not be arbitrary. The amplitude should be small relative to the FC bias voltage so as not to disturb the electrodes by causing them to operate away from their equilibrium potentials. The response of the system will then be an alternating sinusoidal signal of the same frequency as the incident signal with its own phase shift and amplitude. The presence of the load parallel to the FC can affect the measurement, especially if it is not regulated in current or voltage.

In the case of an unregulated load, it will then be necessary to determine the impedance of the load alone in order to subsequently extract the resistance of the FC.

In the case of a regulated load, the measurement of the resistance of the FC is immediate.

3.5.8 Measurement of high frequency resistance

The high frequency resistance measurement is a method of determining the resistance of the FC by using a high-frequency alternating sinusoidal signal generated by a dynamic load placed in parallel to the FC and the frequency which is imposed on the generator is variable. The advantage of modulation the frequency of the incident signal is to reduce the capacitive or inductive effects of the FC and thus to measure only the resistive component of the impedance. Therefore, this approach has been used to analyze the resistance at the membrane-electrode interface for various membranes.

3.5.9 Transmission or scanning electron microscopy

Electronic imaging techniques are the most widely used methods for post-mortem analysis of FC components. Scanning electron microscopy (SEM) is used to characterize materials at the micron scale while transmission electron microscopy is employed to visualize components at the nano scale. All of these methods and their variants have been extensively used to investigate the degradation processes and manufacturing processes of various components, i.e. the distribution of platinum on the membrane section, the morphology of the diffusion layer, the interface between the membrane and the electrodes, the morphology of the membrane, the formation of water drops on the fibers of the diffusion layer, and the catalyst losses etc [76, 77, 78].

3.5.10 Segmented fuel cell

The need for multiple electrical loads and an often overly complicated design for the bipolar plate makes this technique complex and difficult to implement on a technical level. To avoide

this difficulty, used a network of electrical resistors of identical values placed between the bipolar plate and the current collecting plate. The measurement of the voltage difference across the terminals of the resistance makes it possible via Ohm's law to estimate the local current density. This method, which is easier to set up, has been very often used.

3.5.11 Transparent fuel cell

The development of transparent fuel cell was motivated by the need to analyze and understand the physical phenomena associated with water management, e.g. production, water transfers, accumulation, etc. The transparency of the transmission channels allows a high spatial and temporal resolution of the water movements.The use of transparent fuel cell to visualize and study flooding in the case of PEMFC facilitates the understanding of the mechanisms of obstruction of the reactive gases.

3.5.12 Spectroscopy in the X-ray domain

The use of X-rays to characterize the structure and the chemical state of the various constituents of the fuel cell is particularly useful for detecting chemical degradation on the components during aging. There are many techniques depend on the use of X-rays e.g. (EXAFS), where the Extended X-Ray Absorption Fine Structure (EXAFS) provides information about the atomic environment of a particular element in any type (solid, liquid, gaseous, and interface environment).

3.5.13 Spectroscopy in the infrared range

This approach uses the infrared region of the electromagnetic spectrum to measure temperature. Most works use an infrared transparent glass that is positioned in such a way as to allow the electromagnetic radiation of the channels outside the FC; non-dispersive infrared spectroscopy was used to determine the rate of corrosion of the carbon support layer by measuring the molar concentration of CO and CO2 at the exhaust outlet. Fourier transform infrared spectroscopy was used ex-situ to visualize the degradation of the surface condition of silicone gaskets in a space simulating the FC environment (compression, temperature,etc) [79, 80].

3.5.14 Resonance spectroscopy

Magnetic resonance imaging (MRI) is a powerful analytical technology that provides cross-sectional and 3-D images with high anatomical resolution. This method is used to study the water distribution in the Nafion membrane as well as the difference in water content in the

anodic and cathodic compartments, observing the onset and slow propagation of the FC dehydration, and studying the effect of water supply in reactive gases on the electrical performance and the strategy of reactive gas supply.

3.5.15 Mass spectroscopy

Mass spectroscopy (MS) is an alternative or complementary method to gas or liquid phase chromatography. MS is a powerful physical method for analyzing compounds in liquid, gaseous or solid form, it makes it possible to determine the molecular structure as well as the molar amount of a molecule in a mixture. This technique has also been applied to study the degradation of electrodes and bipolar plates [81].

3.5.16 Measurement by acoustic emission

The acoustic emission method is used to study the membrane drying mechanism. Acoustic emission (AE) is a non-destructive, non-invasive and real-time method whose principle consists in measuring the energy released in the form of transient elastic waves following a mechanical deformation of a material. For instance, the plastic deformation of the membrane [82].

This technique opens the way for deeper investigations into the structural changes that occur during drying and flooding of membranes.

3.5.17 Diagnostics by measurement of the external magnetic field

The degradations at the Membrane Electrodes Assembly (MEA) levels essentially modify the impedance of these. This modification leads to a heterogeneous redistribution of current densities on the cell surface, according to Biot and Savart's law, the external magnetic signature of the fuel cell is then changed.

This study made it possible to determine an optimal positioning and orientation of the magnetic field sensors allowing only the information useful for diagnosis to be extracted. An inverse model of Biot and Savart's law was then developed, allowing reconstruction of the current densities in a fuel cell from external measurements of the magnetic field. This method focused on the identification of defects affecting all the cells and made it possible to reconstruct the average current density over the entire length of the FC stack.

In [83] the result of a two fault (i.e. Oxygen starvation of the stack, Ageing attempt) obtained by measuring the external magnetic field in a fuel cell was then compared to an "invasive measurement" of the current (Figure 3.10, 3.11).

Many studies have proposed the diagnostic method by measuring the external magnetic field, we distinguish:

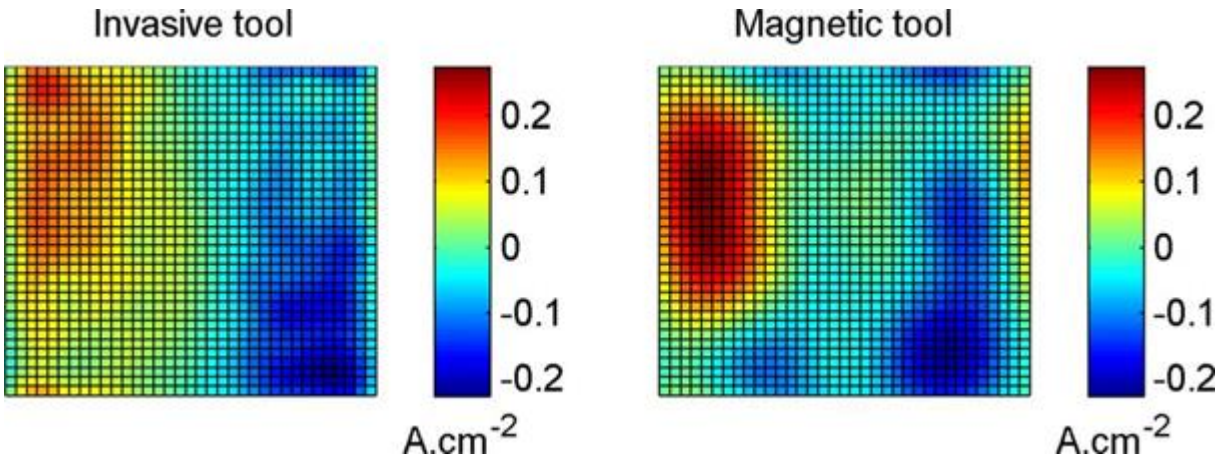

Fig. 3.10 *Oxygen starvation of the stack: comparisons between currents density obtained with internal measurements (left) and with magnetic inverse problem (right).*

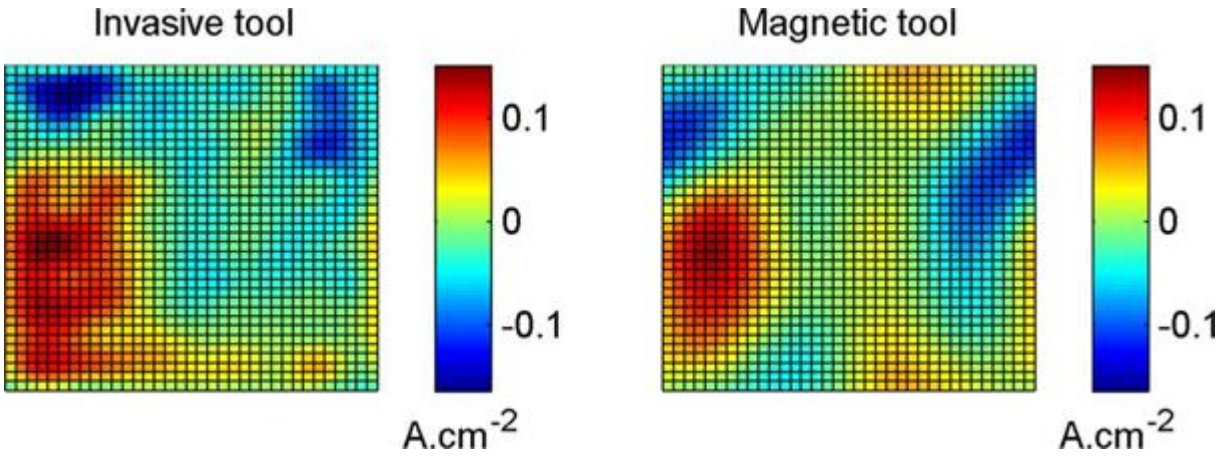

Fig. 3.11 *Ageing attempt: comparisons between the current densities obtained with internal measurements (on the left) and with the magnetic inverse problem (on the right).*

Karl-Heinz H et al. [84] developed a magnetic tomograph consisting of a robotic system on which two magnetic field sensors are installed. These sensors allow the field around the FC to be scanned in several positions.

The authors in [6, 85] imposed random current densities on a single fuel cell cell to construct a field base comprising 2000 elementary defects. Afterwards they calculate the magnetic field on 36 positions for each vector using a genetic algorithm. The inversion of the Biot and Savart operator linking the currents to the magnetic fields makes it possible to identify the current sources contributing to the measured field. (Figure 3.12) [6] shows the vector distribution of the static magnetic field measured by MI sensors for 108 position around the real fuel cell.

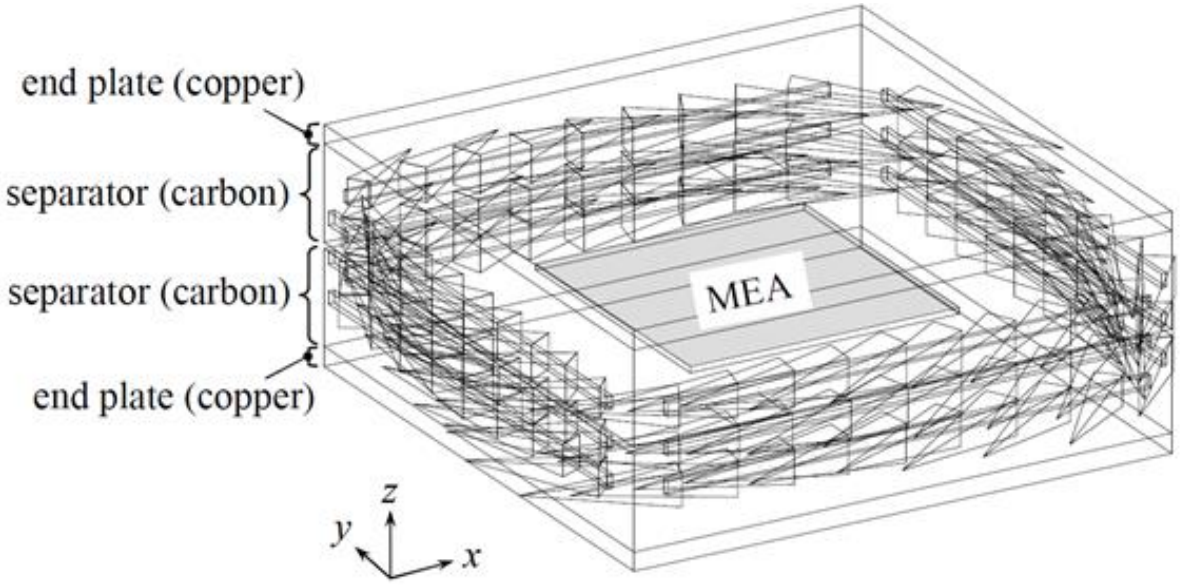

Fig. 3.12 *Bird's-eye view of the static flux density distribution measured by MI sensors for 108 position around the real fuel cell .[6]*

3.6 The basics of electrochemical impedance spectroscopy

3.6.1 Principle of impedance spectroscopy

3.6.1.1 Theoretical

The shape of the current injected/requested from the FC can be written as follow equat 3.4:

$$i(t) = i_{dc} + i_1 * \sin(w_1 t) \tag{3.4}$$

Where:

• W_1 the pulsation of the electric current, in [rad/s].

The response of the FC to this type of stimulus can be written(equat 3.5):

$$e(t) = e_{dc} + e_1 * \sin(w_1 t + \theta_1) + e_2 * \sin(2 * w_1 t + \theta_2) + ... \tag{3.5}$$

Where:

• $\theta_{(1,2,n)}$ the phase shift between current and voltage for each harmonic.

Using Euler's formulation and considering the system response as linear we find the following equations(equat 3.6, 3.7):

$$i(t) = i_{dc} + i_1 * \exp(jwt + j\theta_{i1}) \tag{3.6}$$

$$e(t) = e_{dc} + e_1 * \exp(jwt + j\theta_{e1}) \tag{3.7}$$

Since impedance is defined as the ratio between voltage and current in the frequency domain, the terms (idc and edc) can therefore be eliminated:

$$\left|\overline{Z}\right| = \frac{e_1}{i_1} \tag{3.8}$$

And :

$$\varphi = \theta_{e1} - \theta_{i1} \tag{3.9}$$

With :

$$\left|\overline{Z}\right| = \sqrt{\left[\mathrm{Re}\left(\overline{Z}(w)\right)\right]^2 + \left[\mathrm{Im}\left(\overline{Z}(w)\right)\right]^2} \tag{3.10}$$

And :

$$\varphi = \tan^{-1}\left(\frac{\mathrm{Im}\left(\overline{Z}(w)\right)}{\mathrm{Re}\left(\overline{Z}(w)\right)}\right) \tag{3.11}$$

The impedance thus defined for a frequency range can be plotted in a Nyquist diagram or in a dual Bode plane (phase and amplitude). The advantage of using a Bode plan is to be able to visualize explicitly the influence of the frequency.

3.6.1.2 Practical

a. **Measurement technique** There is an auxiliary electrode which supplies the electric current to the element under test, a working electrode which measures the electric current passing through the cell, a reference electrode, as its name suggests, that measures the reference potential and finally, a electrode allowing measurement of the potential of the element under investigation. With these four electrodes, several measurement methods called two, three or four electrodes can be thought of:

The two-electrode assembly used for high impedance measurement.

The three-electrode assembly using a reference electrode (low to medium impedance). (Figure 3.13) shows the schematics of the experimental setup [7, 8].

The four-electrode assembly is extremely useful for measuring very low impedances. These acquisition systems also offer the possibility of measuring the impedance of each of the cells of the stack. To do this, several electrodes are added to measure the potentials.

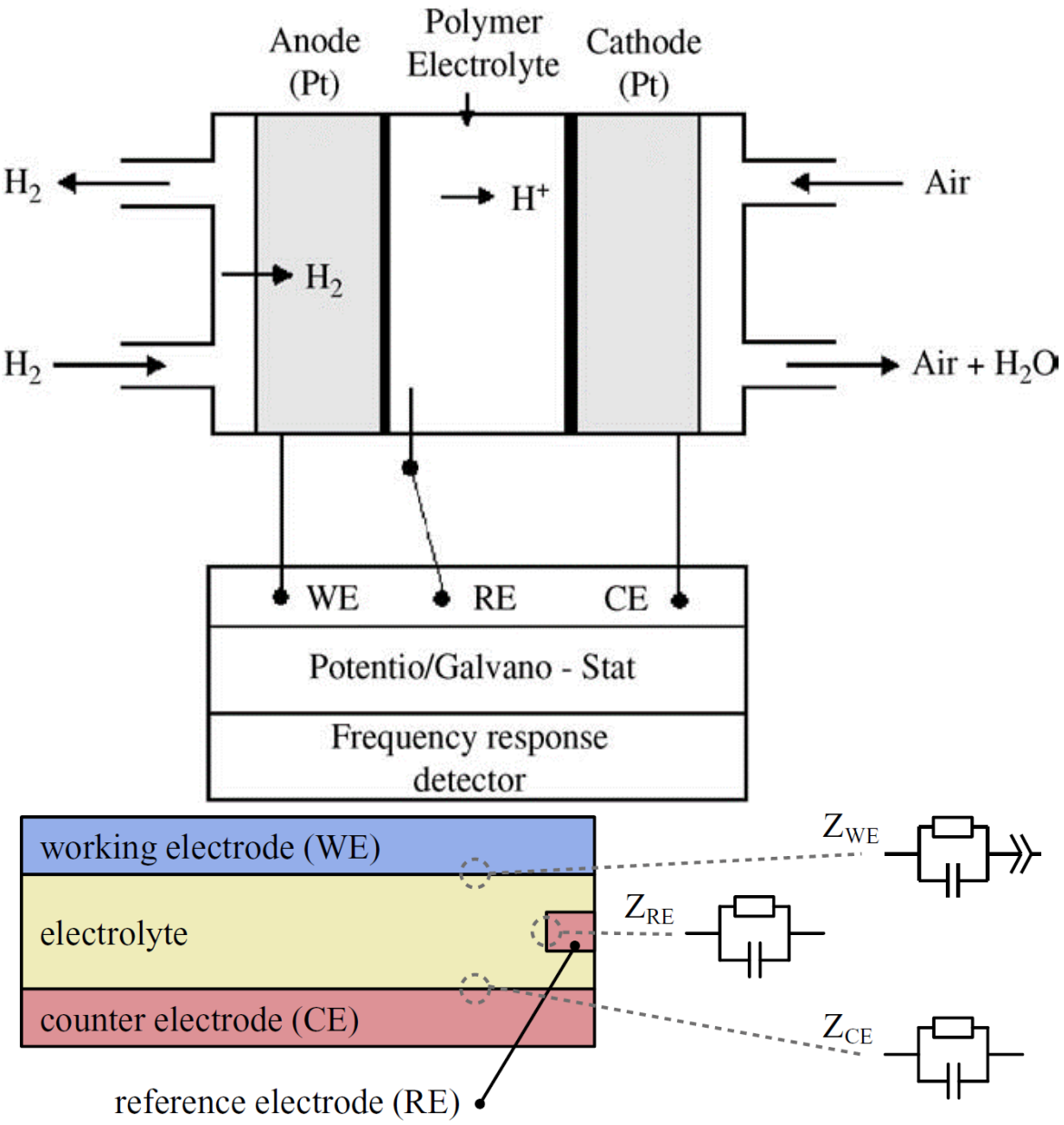

Fig. 3.13 *Schematics a) Employment of a reference electrode in the PEMFC. b)Representation of a three-electrode cell, consisting of working (WE), counter (CE) and reference electrode (RE), connected by the electrolyte .[7, 8]*

b. **Electromagnetic ambient noise** The use of shielded cables, crossed and of reduced length limits impedance measurement inaccuracies. Another possibility consists in using a Faraday cage to limit measurement errors.

c. **Impact of measurement cables** Theoretically, it is common to overlook the effects of measurement cables on the accuracy of the result. However, this assumption is only valid if the impedance of the cables is significantly lower than that of the FC, or when the four-electrode assembly is used.

d. **The input impedance of impedance meter** Data acquisition and processing is generally provided by a potentiostat or galvanostat. It is important that the current flowing through the FC is not diverted into the circuit that measures the potentials. For this reason, electrodes that measure potentials are usually connected to the potentiostat by very high impedance inputs.

3.6.2 Measurement by Equivalent Circuit Elements in the FC application

3.6.2.1 Inductance

High frequency inductive behavior is usually attributed to the electrical wiring between the load and the FC. While the inductive behavior at low frequencies is attributed to the formation of hydrogen peroxide on the cathode side. The impedance expression for a pure inductance as follows equa 3.12:

$$\overline{Z}(w) = jLw \tag{3.12}$$

3.6.2.2 Resistance

The membrane resistance can be defined as 3.13:

$$R_m = \frac{\rho * l}{S} \tag{3.13}$$

Where:

ρ the resistivity of the electrolyte, l the thickness of the membrane and S the active surface of the electrolyte.

The resistivity of the electrolyte varies strongly and non-linearly with the hydration level of the membrane.

The pure resistive circuit is also used to model charge transfer phenomena at each of the electrodes. Its value is generally determined by the partial derivative of the electrode potential ∂E_E with respect to the faradaic current of this same electrode ∂J_E equa 3.14:

$$R_{ct} = \frac{\partial E_E}{\partial J_E} \tag{3.14}$$

3.6.2.3 Condensator

The capacitor is used to define the double layer capacitance (an accumulation of negative and positive charges) equa 3.15.

$$\overline{Z}(w) = \frac{1}{jCw} \tag{3.15}$$

3.6.2.4 Constant Phase Element (CPE)

In general, the constant phase element is used to describe the double layer phenomenon on a porous or rough electrode equat 3.16.

$$\overline{Z} = \frac{1}{T_{CPE}(jw)^n} \tag{3.16}$$

The advantage of this circuit consists in being able to reproduce behaviors that are impossible to represent with classical elements.

3.6.2.5 Warburg impedance

The Warburg impedance is used describe the phenomenon of material diffusion from the dipole plates to the electrodes (in GDLs) based on the one-dimensional solution of Fick's second law. It can be represented by the following equation 3.17:

$$Z = \frac{R_W \times \tanh\left[(j \times T_W \times w)^{P_W}\right]}{(j \times T_W \times w)^{P_W}} \tag{3.17}$$

R_w and T_w are constants.

3.6.3 Determination of the key physical parameters of a PEMFC recorded in the Nyquist plane

Impedance spectroscopy is one of the most widely used characterization methods. Many studies use it to measure the value of the electrical resistance or for monitoring degradation. Used it to describe the evolution of a model's parameters throughout a drying out or a flooding they have deliberately caused. The variation of certain parameters thus made it possible to make the difference between flooding and drying out. During each degradation phase, they carried out impedance spectroscopies to characterize the impedance and monitor its evolution.

- At very low frequencies (a few mHz):

We can get a picture of the FC performance. The polarization resistance is determined for an imaginary part of the zero impedance. Theoretically, the slope of the polarization curve around a given operating point is equal to the polarization resistance noted by EIS for this same operating point.

- For frequencies ranging from a few mHz to a few Hz:

This arc can also reflect the diffusion of species in the oxidation/reduction reaction from the channels to the catalytic layer.

- At high frequencies:

The membrane resistance is determined by the intersection with the real axis. The second piece of information obtained is located in the so-called high frequency arc. This arc of a circle reflects the phenomena of transfer and accumulation of electric charges at the electrode-electrolyte interfaces.

The following figure 3.14 shows the dissociation of the physical zones modeled by a classical impedance measured on a PEMFC.

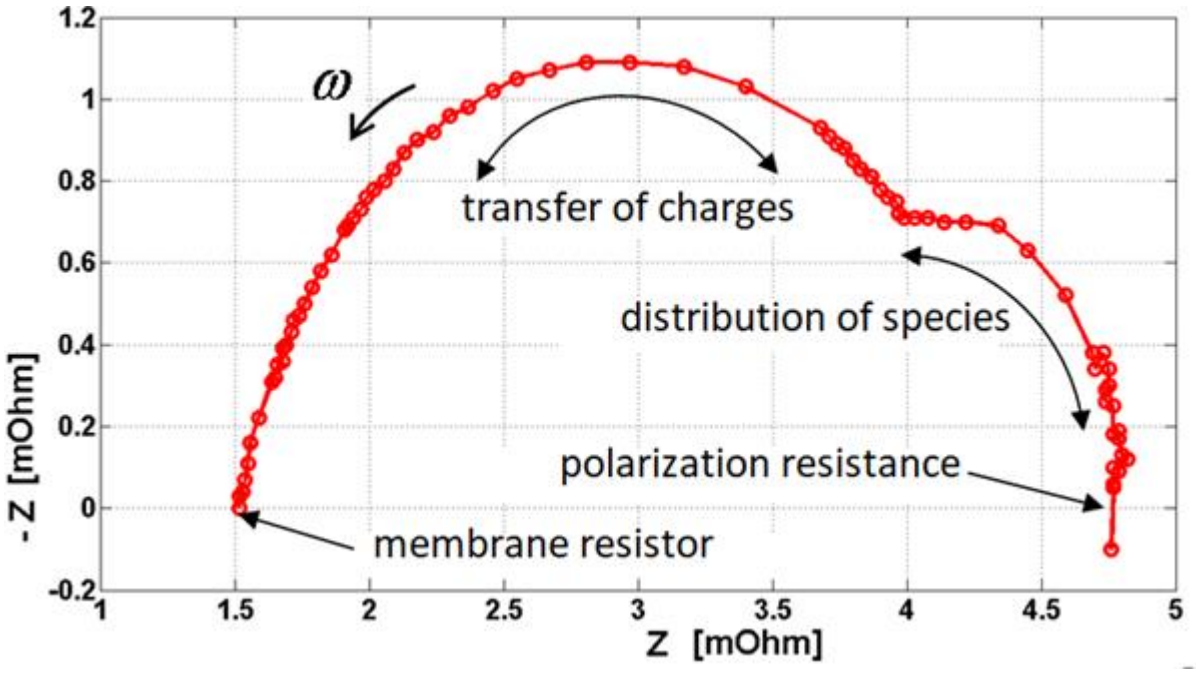

Fig. 3.14 *The classical impedance measured on a PEMFC.*

3.6.4 Implementation on systems, "on-line" diagnostics

The use of spectroscopies, which allows in particular to measure electrical resistance, generally requires equipment specific to a system: sensors of specific currents, an adequate load, the possibility of imposing a variation in current around the operating point (converter), etc. Several studies, have used the low amplitude and high frequency natural triangular current ripple gen-

erated by a BOOST converter around the operating point. Thus, by varying the frequency, or even the amplitude, it is possible to obtain an impedance spectrum.

3.7 Conclusion

The main obstacles to widespread deployment are premature fuel cell failures that limit the life of the PEM fuel cell, which brings us back to many difficulties. In this chapter, we have defined and discarded the main methodological approaches to identify and diagnose FC. In this context, and to deepen the understanding of PEMFC diagnostic behavior, we discussed possible measurement systems that provide information on the performance of this system with the aim of enhancing diagnostic techniques. The next chapter discusses artificial intelligence techniques (PEMFC Diagnostics Based on Learning Machine).

Chapter 4

AI technologies (machin lerning based PEMFC diagnosis)

4.1 Introduction

Artificial intelligence, a branch of basic information technology, was developed with the goal of simulating the behavior of the human brain. Artificial intelligence and machine learning, two powerful tools for analysing and/or classifying data, are attracting increasing interest in materials development and power systems control/monitoring.

Figure 4.1 [9] represents the patent figures related to artificial intelligence, machine learning and deep learning in the field of energy since 2000.

Machine learning informed by AI and mathematics can facilitate the development of basic knowledge and correlations, material selection and progression, fuel cell design and optimization, system control, management energy and process state monitoring, showing great potential for improving PEMFC technology.

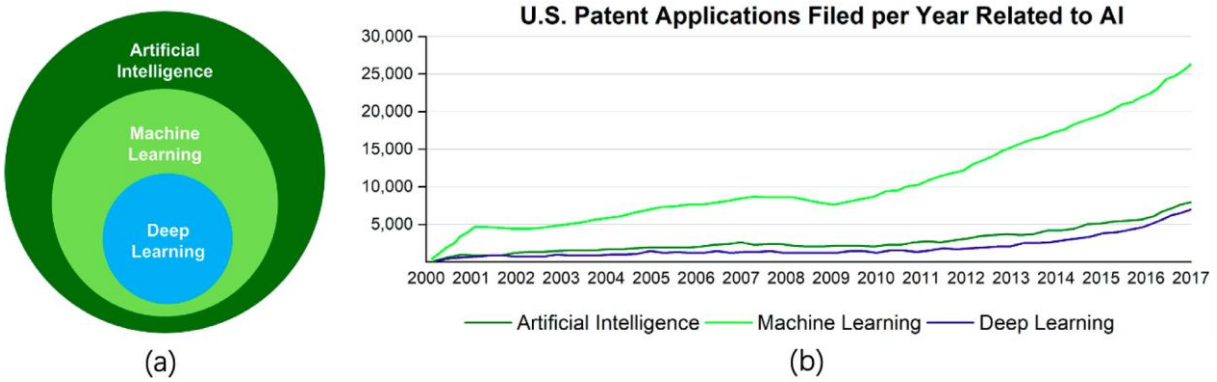

Fig. 4.1 *(a) the relationship between AI, machine learning, and deep learning and (b) the number of patent applications per year in the USA related to AI and deep learning.[9]*

4.2 Artificial neural networks

Neural networks are an artificial intelligence tool. Today many terms are used in the literature to designate the field of artificial neural networks, such as connectionism or neuromimetic etc.

The goal of researchers is to improve computing capabilities using models with tightly connected components. Neurosimulators technology tinker with models of artificial neural networks with the sole purpose of validating biological theories of central nervous system functioning.

Artificial neural networks are highly connected networks of elementary processors operating in parallel. Each elementary processor calculates a unique output based on the information it receives. The main networks are characterized by the organization of their architecture, their level of complexity (the number of neurons, the presence or absence of feedback loops in the network), the type of neurons (their transition or activation functions) and finally by the target goal: supervised or unsupervised learning, and optimization, dynamic systems.

4.3 Neuron networks overview

4.3.1 The biological neuron

The biological neuron is a biological cell mainly consists of the three parts "i.e. The dendrites, the soma which processes this information and the axon which transmits the signal" (fig. 4.2). In the human brain there are a large number of neurons, approximately 1011. There are about 1014 to 1015 interconnections between each neuron and other neurons [86].

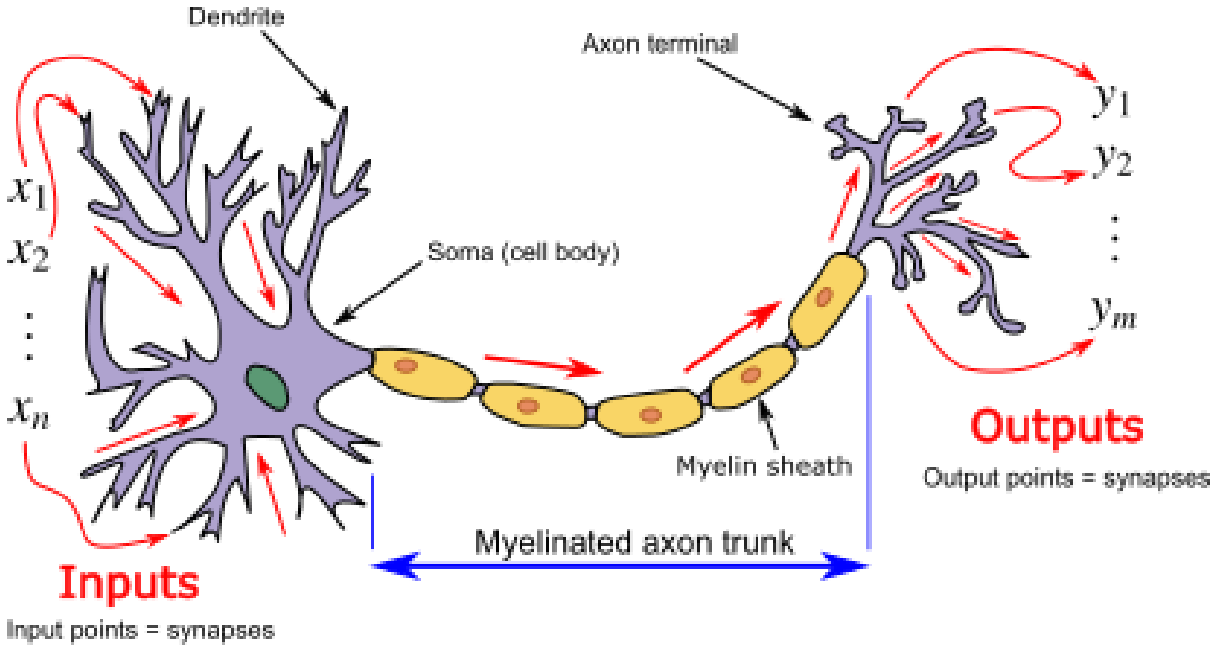

Fig. 4.2 *Representation of the biological neuron.*

4.3.2 The artificial neuron

The simple neuron or the formal neuron (Figure 4.3) [10] is a mathematical model that uses the principles of the functioning of the biological neuron. The artificial neuron is a basic processor, it receives a variable number of inputs $X1, X2, ...Xn$ coming from upstream neurons. Each of these inputs is associated with a weight W representing the strength of the connection. Each elementary processor has a single output, which then branches out to feed a variable number of downstream neurons. Each connection has a weight associated with it.

The mathematical formula for calculating the weighted sum of the inputs according to the following expression 4.1:

$$y_{in} = x_1 \cdot w_1 + x_2 \cdot w_2 + x_3 \cdot w_3 + ... + x_n \cdot w_n + b \tag{4.1}$$

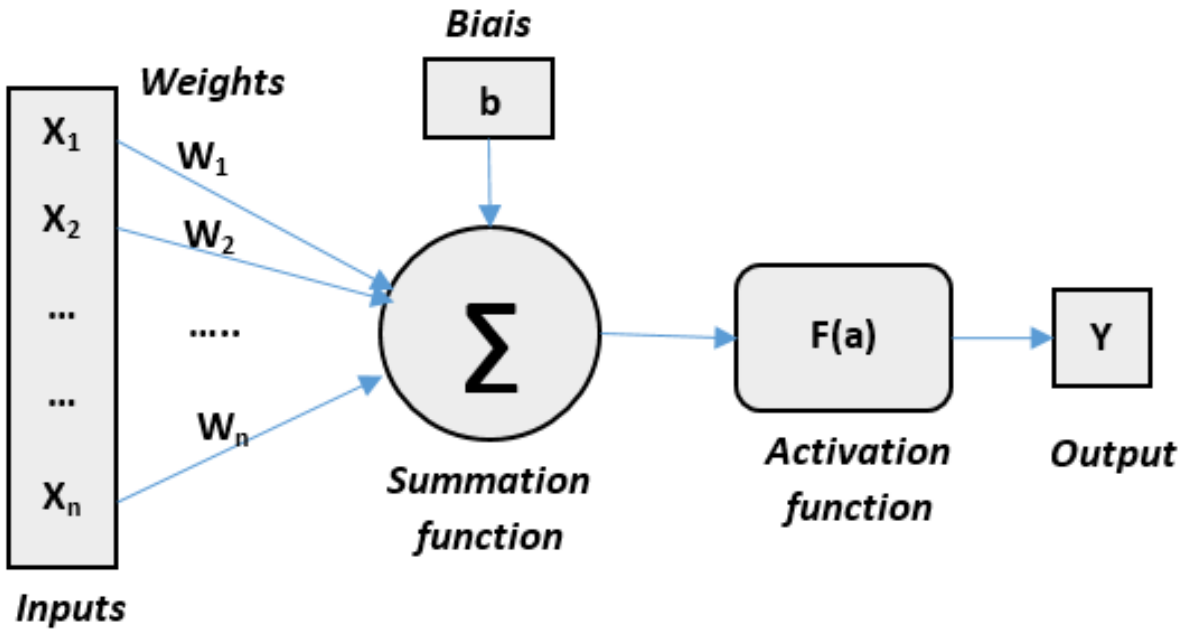

Fig. 4.3 *Representation of the formal neuron model.[10]*

4.3.3 The activation functions

The activation function is one of the most important parts that connects the weighted summation to the output signal. The activation function performs a transformation of an affine combination of input signals. This affine combination is determined by a weight vector associated with each neuron and whose values are estimated in the learning phase. most transfer functions are continuous, offering an infinity of possible values in the range [0, +1] (or [-1, +1]). There are many possible forms of the activation function.

- linear g is the identity function (fig 4.4):

$$g(x) = x \tag{4.2}$$

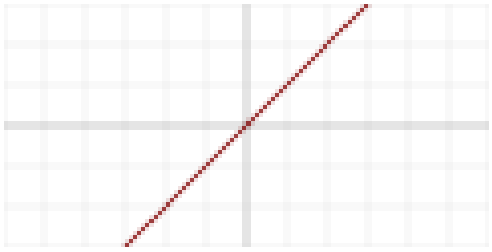

Fig. 4.4 *Linear g fonction.*

- sigmoid (fig 4.5):

$$g(x) = \frac{1}{(1+e^{x})} \tag{4.3}$$

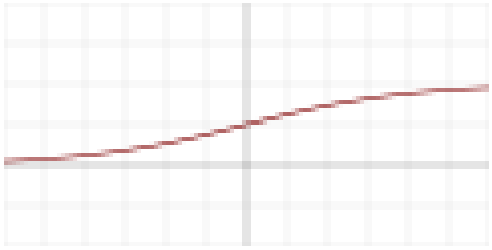

Fig. 4.5 *Sigmoid fonction.*

- Rectified linear unit (ReLU) (fig 4.6):

$$g(x) = \max(0; x) \tag{4.4}$$

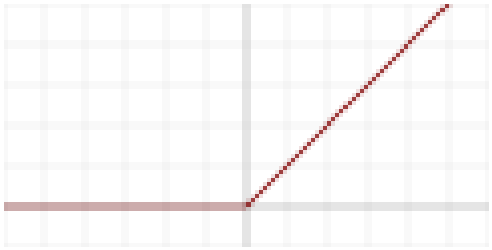

Fig. 4.6 *(ReLU) fonction.*

- Gaussian (fig 4.7):

$$g(x) = e^{-x^2} \tag{4.5}$$

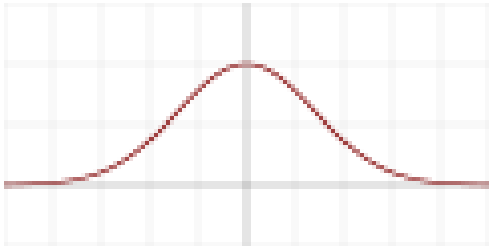

Fig. 4.7 *Gaussian fonction.*

- Softmax:

$$g(x)_j = \frac{e^x j}{\sum_{K=1}^{K} e^{xK}} \quad \text{for k=[1,...,K].} \tag{4.6}$$

- Radial:

$$g(x) = \sqrt{\frac{1}{2\pi}} e^{-x^2/2} \tag{4.7}$$

4.4 Some neural network architectures

4.4.1 Multilayer network

The multilayer network is a set of perceptron distributed in successive layers. It is an input layer reads the incoming signals, a number of hidden layers participate in the transfer and an output layer provides the response of the system. A layer is a set of neurons having no connection between them "i.e. There is no connection between neurons of the same layer and the connections are only made with the neurons of the downstream layers", as shown in figure 4.8.

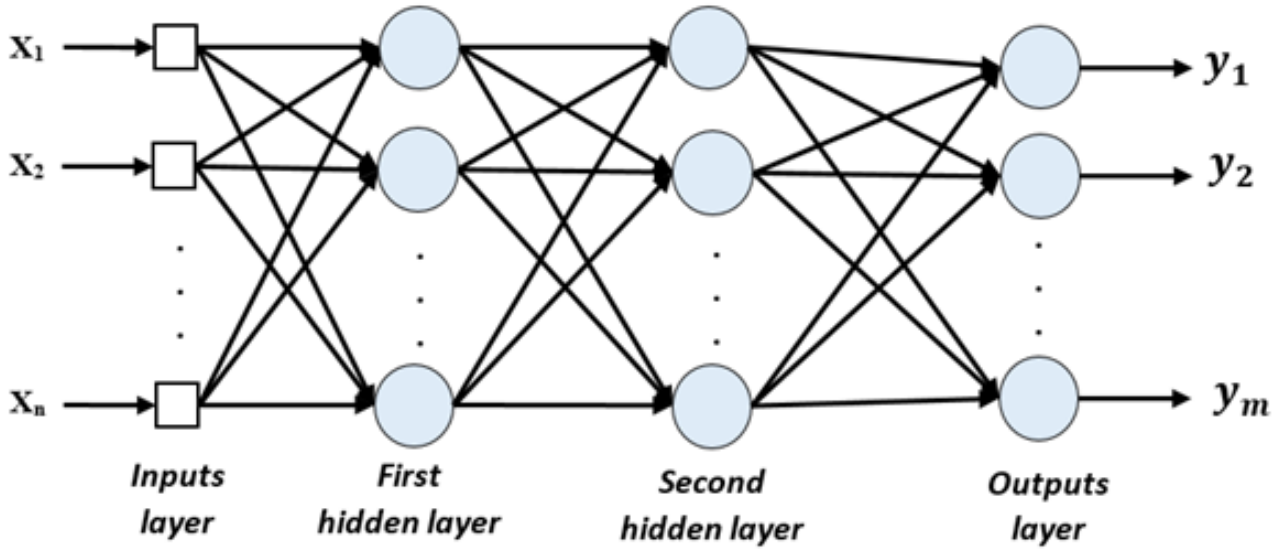

Fig. 4.8 *A typical architecture of multilayer network.*

Different optimization algorithms are proposed to train multilayer perceptron network, they are generally based on an evaluation of the gradient by back-propagation and minimizing the squared-error function in classification. In the literature, the most common squared-error function is defined as follows equat 4.8:

$$e(t) = yd(t) - ym(t) \tag{4.8}$$

The technique of back-propagation can reduce the mean square error by the gradient descent method by using the following relation equat 4.9:

$$E_g(t) = \frac{1}{2}\sum_{i=1}^{n} \left(y_{di}(t) - y_{mi}(t)\right)^2 \tag{4.9}$$

Where $y_d(t)$ denotes the desired output, $y_m(t)$ the measured output of the neuron.

4.4.2 Locally Connected Network

It is a multi-layered structure, but retains some topology. Each neuron maintains relations with a reduced and localized number of neurons in the downstream layer. There are therefore fewer connections than in the case of a conventional multilayer network, as shown in figure 4.9.

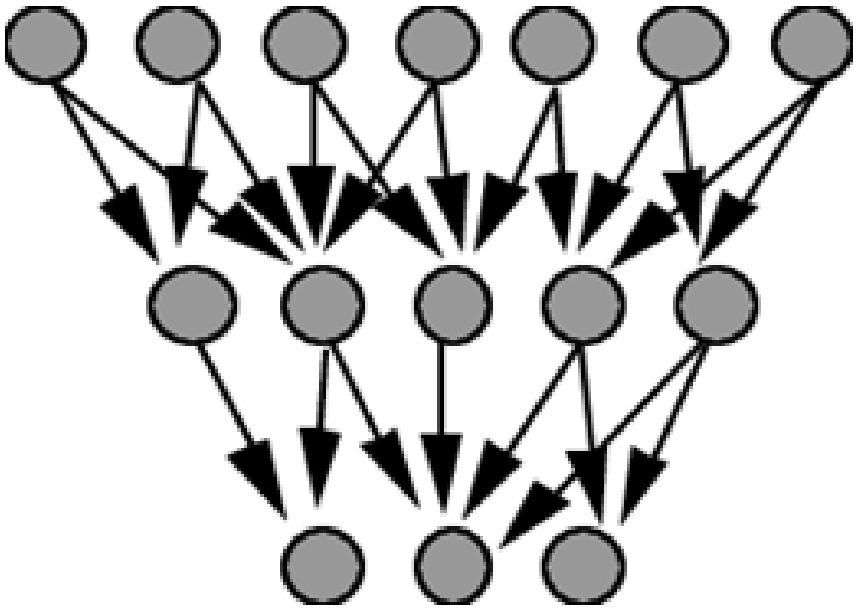

Fig. 4.9 *Locally Connected Network*

4.4.3 Recurrent neural network

The recurrent network contains at least one cycle in the structure bring the information back with respect to the direction of propagation defined in a multilayer network (see figure 4.10). These connections are usually local with the same techniques used in local networks for network training. recurring networks are generally used in pattern recognition (i.e. speech recognition, machine translation etc).

4.4.4 Full-Connection Network

The full-connection network is a set of series of fully connected layers and consists of multiple CNNs which aid in the problem learning process. All inputs/outputs being connected to each other, the number of neurons depends on the number of categories (see figure 4.11). The main feature of this topology is that it is structure agnostic capable of learning any function, which means that the full connection network is fully applicable, e.g. image analysis, speaker identification, etc.

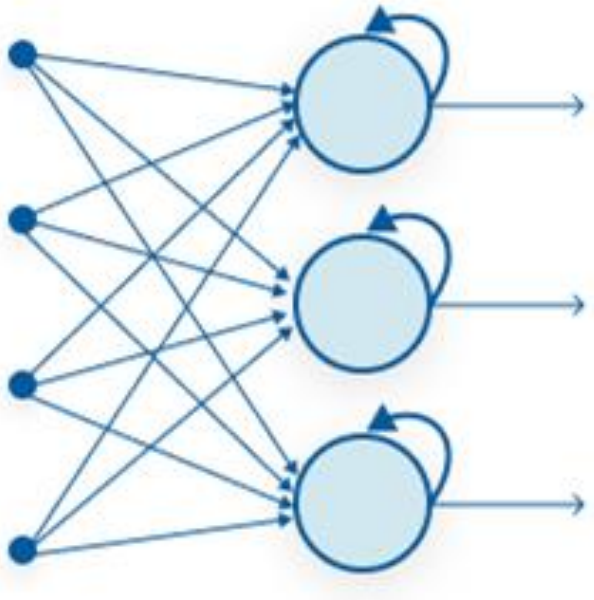

Fig. 4.10 *Recurrent neural network.*

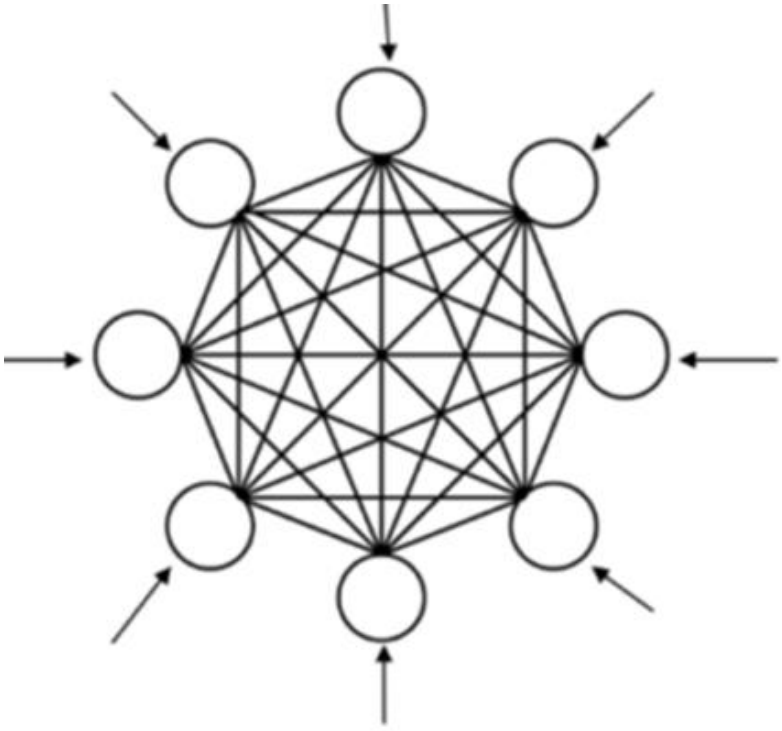

Fig. 4.11 *Full-connection network.*

4.5 Learning

Learning is a stage in the development of a neural network during which the network behavior is modified by a specific algorithm until the desired behavior is achieved. The following diagram 4.12 shows the hierarchical ranking of the learning methods.

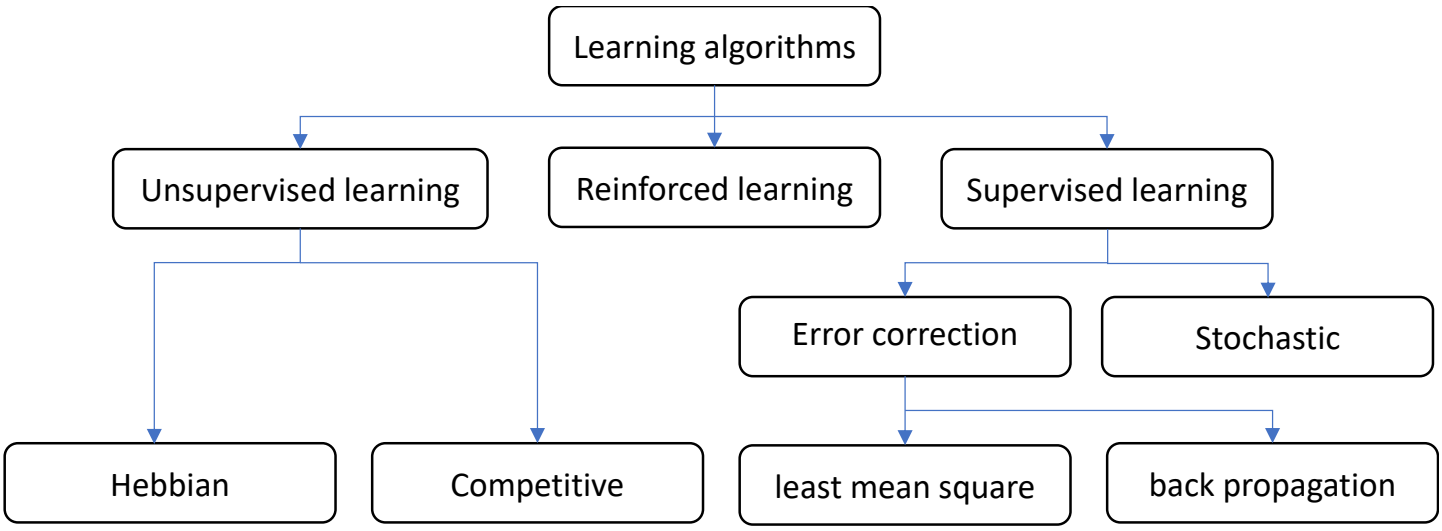

Fig. 4.12 *Diagram of the hierarchical ranking of the learning methods.*

4.5.1 Unsupervised learning

Unsupervised or self-organized learning is used in ANN which has less computational complexity than supervised learning.

The weights are adjusted by the algorithm of learning between neurons to improve the quality of the input classification.

4.5.2 Supervised learning

supervised learning is used only when we know the desired combinations of inputs and outputs.

The input/output (database) is used during the training phase to train the network and exhibits the expected results.

The learning process is based on the generated error by the comparison between the obtained output by the network and the desired output.

The error is used to adjust network parameters (weights), which will improve performance.

The learning algorithms that can be used are:

- Perceptron learning algorithms, back-propagation, adaline and madaline for the single or multi-layer perceptron.

- Boltzmane learning algorithm, for the recurrent architecture.
- Linear discriminant analysis, for the multilayer feed forward.
- Learning vector quantization, for the competitive architecture.

4.5.3 Reinforced learning

The weights are adjusted in a more or less random way to know if the outputs of the ANN are approaching or away from the intended goal and the modification is retained if the impact is positive or rejected, although the ideal outputs are not known directly.

4.5.4 Learning rules and choice of parameters

A simple way to avoid overfitting consists in regularization or introducing a penalty, in the scale to be optimized. when the value of the parameter is increased, the inputs weights of the neurons less and can take on chaotic values, consequently, helping to limit the risks of over-learning.

Therefore, the user must:

- Determine the input/output variables to subject them to possible transformations and normalizations, as for all statistical methods.
- Determine the network architecture: the number of hidden layers and the number of neurons in each hidden layer, which proportionate to an ability to accord with non-linearity problems. The weights are directly corresponding directly to these two choices to be estimated the complexity of the model. The balance between learning quality and prediction quality leads to a good compromise of bias/variance.
- Define the rate of learning as well as a possible strategy for its evolution.
- Set the size of the observation sets or batches taken into account at each iteration.
- Illustrate the parameters maximum number of iterations.
- Determine the maximum tolerated error.

4.6 Machin learning based PEMFC diagnosis

Recently, artificial neural networks (ANNs) based diagnosing method is widely employed. Many researchers have proposed the use of neural network method to diagnosis the PEM fuel cells [20, 87, 88, 89, 89]. For instance:

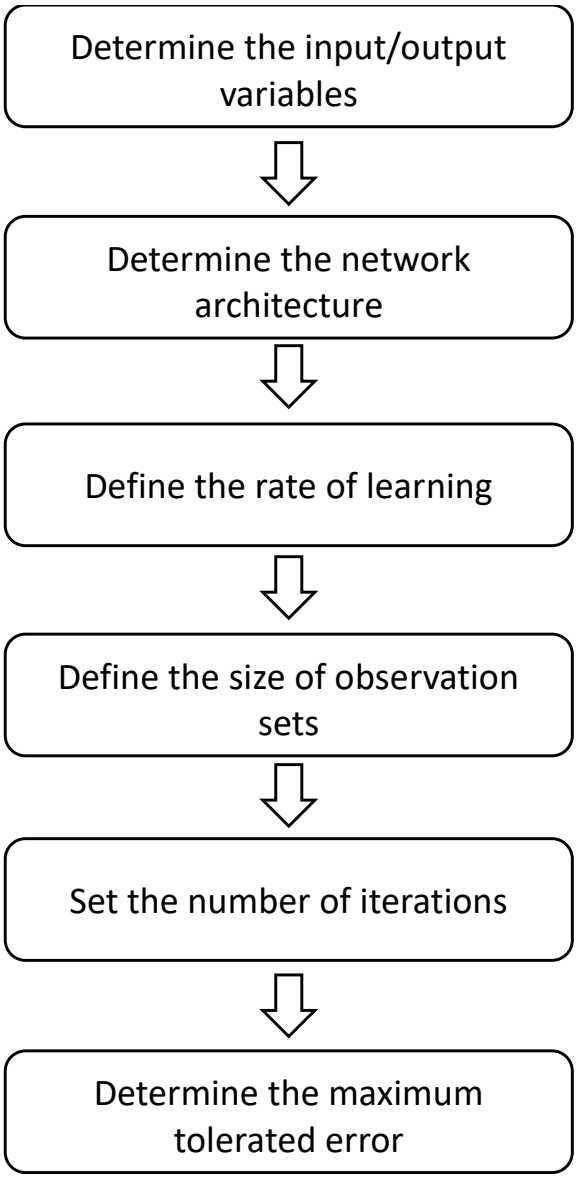

Fig. 4.13 *Learning rules diagram.*

The PEMFC approach of controlling a dynamic neural network was investigated by the authors of [90]. Their research's goal is to track the changes made to the system, commencing with the addition of a delay line to the (NNT)'s input to create a dynamic (NNT) control model.

For the purpose of categorizing the health states (SOH) of the fuel cells (flood, normal functioning, and drying out), Steiner et al. [20] suggested a model employing (NNT) and they showed the distinction between the normal functioning designed by a neural network and the real functioning.

In their investigation of diagnostic methods, Jonghoon et al. [89] used pattern recognition model identification (FCOV) based on Hamming NNT application. to choose the cell's (ΔRd) value and use it to determine the condition of the cell.

While Cadet et al. [88] have given indicators that can be used to evaluate diagnostic performances by providing precise equations to measure the degree of cell humidity. For the purpose of modeling the power supply for a (PEMFC) embedded system.

A neural network model has been created by Jeme et al. [87] that will allow for the control of energy transfer in fuel cell vehicles.

The PEMFC dynamic model was created by Meng Shao et al. [11] and is constructed and simulated using MATLAB. In order to increase the stability and reliability of PEMFC systems, the ANN ensemble for fault diagnosis (i.e., Fault in the stack cooling system; Increasing of fuel crossover; Fault in air delivery system; Fault in hydrogen delivery diagnosis) is constructed in their work.

The authors in [91] researched a method to estimate water activity in the PEMFC using the EIS and modified a neuro-fuzzy inference system (ANFIS).

In order to construct an ideal impedance model of the (PEMFC) that complies with the mass transfer theory and takes into account the physical parameters of the (EIS) model, Slimane Laribia et al. [92] have defined and put into practice a method using an artificial neural network. The authors have identified two PEM fuel cell failure modes (flooding and drying) using their ANN model. for additional studies on PEMFC diagnostics using the EIS approach.

The reader is advised to consult [26, 93, 94, 95].

4.7 Conclusion

Artificial intelligence and machine learning are attracting increasing interest in materials development and power systems control/monitoring. Machine learning informed by AI and mathematics can facilitate the development of basic knowledge, espicialy in the field of PEMFC technology. Today many terms are used in the literature to designate the field of artificial neural networks, such as connectionism or neuromimetic etc. In this chapter, we have provided an overview of neural networks, and the architectures of different neural networks. Then we described the main proprieties of learning and we have presented several related works that

rely on machine learning methods for the diagnosis of PEM fuel cells. The following chapter discusses the results obtained through applying an improved approach towards PEM fuel cell water management using artificial neural network.

Chapter 5

Implementation and results

5.1 Introduction

Given that the development of control systems for industrial applications must minimize the number of instruments for straightforward methodological diagnosis, we have used a neural network-based black box model in this chapter because it is simple and quick to implement. Specifically, the objective of this study is to ascertain the state of the electrochemical response during the use of a fuel cell by developing a neural network-based strategy for the diagnostics of PEM fuel cells in order to meet efficiency requirements.

This chapter concentrates on identifying a suitable, effective, and user-friendly method for preventing the frequent errors caused by the poor water flow inside the fuel cell during operation. Towards this end, the technology of artificial intelligence is proposed. Utilizing electrochemical impedance spectroscopy (EIS analysis) and a neural network model, Utilizing electrochemical impedance spectroscopy (EIS analysis) and a neural network model, it is possible to monitor the effect of the fuel cell membrane's humidity content. This method permits the examination and diagnosis of PEM fuel cell failure mechanisms (flooding and drying). The benefit of this work is summed up by the straightforward demonstration of the PEMFC's existence, which aids in defining its current state of health.

5.2 Structure of the PEMFC system

Figure 5.1 [11] depicts the operation of a fuel cell core, which necessitates a large number of essential auxiliaries for effective operation. The overall system is known as the fuel cell system, which consists of the cell core and the auxiliaries (i.e., the hydrogen system, which provides hydrogen gas to the anode, and the air system, which provides oxygen to the cathode). Through the pressure sensor, the valve's primary function is to modulate the pressure in the two systems (air compressor and hydrogen source). While the humidifier and refrigeration system maintain the fuel cell's humidity level and temperature, respectively [87]. The behaviour of the stack is significantly influenced by the behaviour of the auxiliaries; for example, the humidification subsystem (drying or over-humidification of the membrane) reduces the production of electrical energy and shortens the lifespan of the PEMFC.

5.3 Model of PEM fuel cell

The chosen model of the assembly is that presented by JC Amphlett et al [96]. This electrochemical model can be used to characterise the dynamic behaviour of a PEMFC assembly, and it allows for the consideration of the various parameters necessary for a successful outcome. At the level of an elementary cell, the quasi-static model is utilised to predict the voltage response of the cell as a function of current, temperature, partial pressures of reactive gases, and

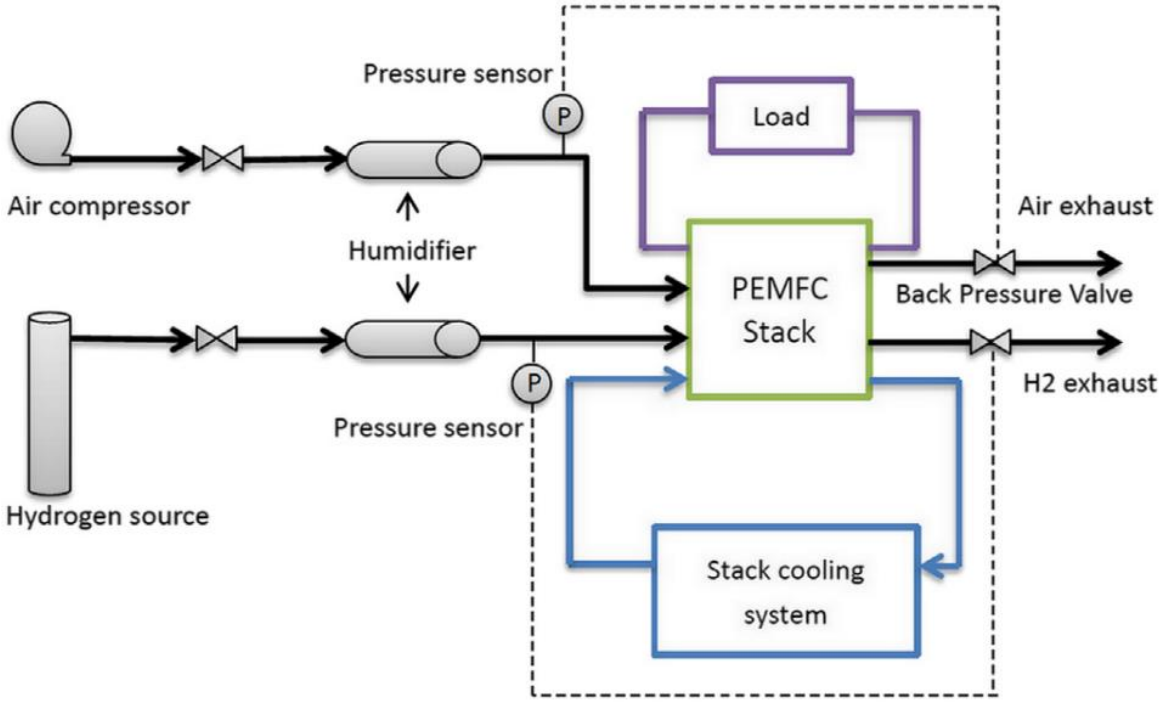

Fig. 5.1 *Structure of a PEM fuel cell system.[11]*

membrane hydration. Due to polarisations such as activation, ohmic, and concentration, the actual potential of a PEMFC is lower than its Nernst potential. This express is referred to as [11, 97, 98]:

$$V_{cell} = V_{Nerst} - V_{act} - V_{ohm} - V_{con} \tag{5.1}$$

The thermodynamic potential is defined by a Nernst equation in developed form as [22, 24, 11]:

$$V_{nerst} = 1.229 - 0.85 \cdot 10^{-3} (T - 298.15) + 4.31 \cdot 10^{-5} \cdot T \cdot \left[\ln (P_{H2}) + \frac{1}{2} \ln (P_{O2}) \right] \tag{5.2}$$

Where:

- T denotes the cell temperature [K].
- P_{H2} and P_{O2} are partial hydrogen and oxygen pressures [atm].

Note that the activation polarization at the anode increases with the current density, its expression can be written in the form [11, 99, 100] :

$$V_{act} = \xi_1 + \xi_2 \cdot T + \xi_3 \cdot T \cdot \ln (C_{O2}) + \xi_4 \cdot T \cdot \ln (I_{stack}) \tag{5.3}$$

Where:

- I stack are the operating current of the fuel cell (A).

• ξ_1; ξ_2; ξ_3; ξ_4 are the parametric coefficients appropriate to each fuel cell model, Table 5.1 identifies the exact parametric coefficients used in this work.

• T are the temperature of fuel cell.

• CO_2 is the concentration of oxygen in the catalytic interface.

The concentration of oxygen in the catalytic interface is expressed by Henry's law as follows equat 5.4:

$$C_{O2} = \frac{P_{O2}}{5.08 \cdot 10^6 \cdot e^{\left(\frac{-498}{T}\right)}} \tag{5.4}$$

The losses of the concentration polarization are given by the following relation (equat 5.5):

$$V_{con} = -B \cdot \ln\left(1 - \frac{J}{J_{\max}}\right) \tag{5.5}$$

Where:

• B is an empirical constant that depends on the type of FC and its operating state [12, 101].

• J is the current density of the permanent operation.

• J_{max} is the maximum current density.

The electrolyte and the electrodes obey Ohm's law. We can express the ohmic losses by the following equation 5.6:

$$V_{ohmic} = I_{stack}\left(\frac{t_m}{\sigma_m} + R_c\right) \tag{5.6}$$

Steam diffusion coefficient of water vapor in the membrane is calculated by (equat 5.7) [22, 91]:

$$\sigma_m = (0.00519\lambda - 0.00324)\exp\left(1268\left(\frac{1}{303} - \frac{1}{r_{fc}(K)}\right)\right) \tag{5.7}$$

The water content of the membrane is presented as:

$$\begin{cases} \lambda = 0.043 + 17.81\phi - 39.85\phi^2 + 36\phi^3, 0 \leq \phi \leq 1 \\ \lambda = 14 + 1.4(\phi - 1), \phi \leq 3 \end{cases} \tag{5.8}$$

The challenge of water management is to maintain a constant membrane hydration coefficient. The latter is sensitive to drying and flooding [102]; these two constraints reduce the membrane's gas-transmission rate and degrade it. Therefore, it is crucial to maintain the membrane's correct hydration by adhering to the relative humidity given as (equat 5.9)[91, 103, 100].

$$\varphi = \frac{P_{wout}}{P_{sat}} \tag{5.9}$$

The water vapour partial pressure Pw_{out} is related to the absolute pressure at the output of

the stack P_{exit} (atm), as represented by the following equation 5.10:

$$P_{wout} = \frac{(0.42 + \lambda\,\psi)\,P_{exit}}{\lambda\,(1+\psi) + 0.21} \tag{5.10}$$

The saturated vapour pressure P_{sat}(atm) depends on the temperature, which is given by the following relation 5.11.

$$P_{sat} = 10^5 \exp\left(13.7 - \left(\frac{5120}{T_{air} + 273.15}\right)\right) \tag{5.11}$$

ψ is calculated by (equat 5.12):

$$\begin{cases} \psi = \left(\frac{q_{win}}{q_{O_2 in} + q_{rest}}\right) \\ q_{O_2 in} = \frac{\lambda I_{stack}}{4 \cdot F} \\ q_{rest} = 3.76 \frac{\lambda \cdot I_{stack}}{4 \cdot F} \end{cases} \tag{5.12}$$

Where:

- q_{win} molar flow air in the inlet.
- q_{O2in} the molar oxygen flow rate at the inlet.
- q_{rest} the molar flow rate of non-oxygen N_2 in the air.

The humidity of the membrane is affected in several parameters like humid airflow q_{win}.

Figure 5.2 depicts the relationship between the change in humidity caused by a change in q_{win} and the state of PEMFC when the temperature remains constant. During the fluctuation of the value of q_{win}, there are three distinct regions based on the relative humidity percentage:

- $q_{win} < 0.4 * 10^{-5}$: too dry.
- $q_{win} > 1.5 * 10^{-5}$: too wet.

To make fuel cell operates in normal conditions, the humid air flow must be between these two mentioned values.

Figure 5.3 displays PEMFC as an electrical circuit with a simple structure, consisting of a voltage source representing the Nernst potential in series with resistances representing voltage fluctuations. Using equations 5.13, which involve the partial pressure of hydrogen (respective oxygen) and the flux of hydrogen entering the cell (respective oxygen), the fluid dynamics have also been considered.

The global dynamic models aid in predicting the electrical response (voltage or current) of the [101] stack.

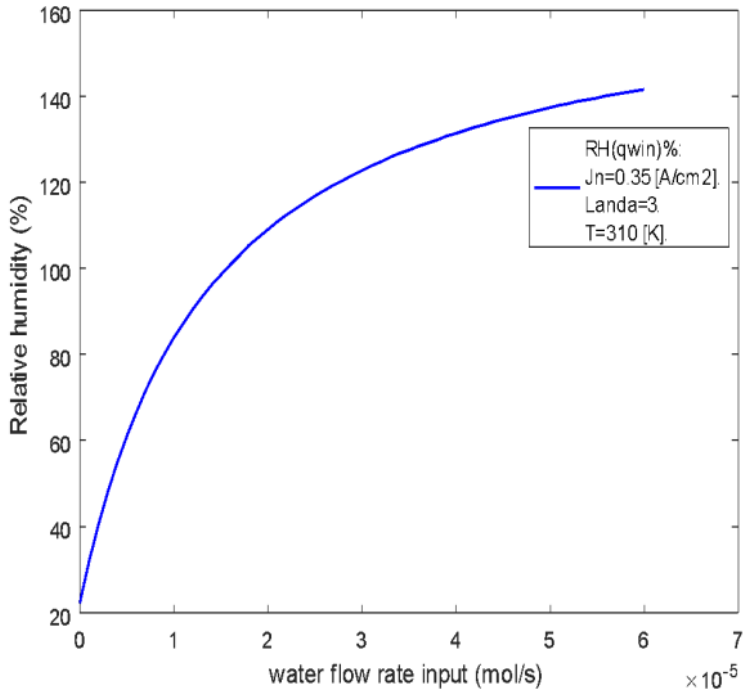

Fig. 5.2 *Relative humidity (%) curve as a function of the water flow rate input in PEMFC.*

$$\begin{cases} P_{H2} = \frac{{}^{1}/_{K_{H_2}}}{1+\tau_{H_2}\cdot S}\left(q_{H_2} - 2K_r \cdot I_{stack}\right) \\ \tau_{H_2} = \frac{V_{an}}{R\cdot T\cdot K_{H_2}} \\ P_{O2} = \frac{{}^{1}/_{K_{O_2}}}{1+\tau_{O_2}\cdot S}\left(q_{O_2 in} - 2K_r \cdot I_{stack}\right) \\ \tau_{O_2} = \frac{V_{an}}{R\cdot T\cdot K_{O_2}} \end{cases} \tag{5.13}$$

Where:

- K_{H2} gain of the hydrogen flow.
- K_{O2} gain of the oxygen flow.
- τ_{H2} time constant of the hydrogen flow.
- τ_{O2} time constant of the oxygen flow.

5.4 Modeling of the PEMFC impedance model

Electrochemical Impedance Spectroscopy is a common technique for the fundamental analysis of electrochemical device phenomena. In a PEMFC, equivalent impedances are used to determine the electrochemical parameters (double layer capacity, membrane and connection resistances, charge transfer resistance, etc.) or to analyse the internal behaviour of the PEMFC (influence of humidification and drying of the membranes [20], monitoring of the lifetime of

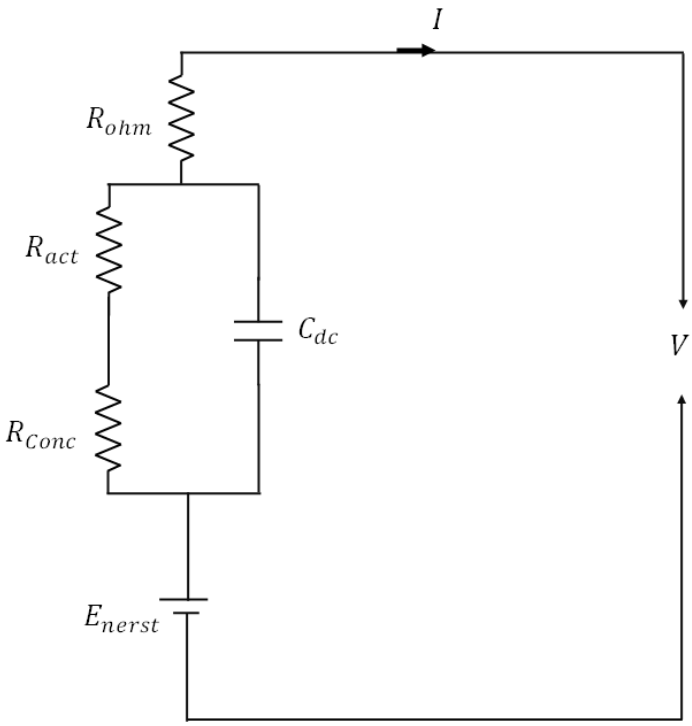

Fig. 5.3 *Simplified dynamic model*

the PEMFC [93]. The Randles circuit [12] is the most commonly used equivalent circuit in measurement models. Figure 5.4 illustrates a comparable Using the PEMFC stack model, the impedance of the fuel cell is expressed by (equat. 5.14):

$$Z_{cell}(jw) = R_m + \frac{1}{Z_{CPE} + ({}^{1}/_{(R_P+Z_W)})} \tag{5.14}$$

The Warburg impedance is defined as follows (equat 5.15) [24, 12, 26]:

$$Z_W(jw) = R_d \frac{\tanh\sqrt{(jw(\tau_d))}}{C\sqrt{\tau_d}} \tag{5.15}$$

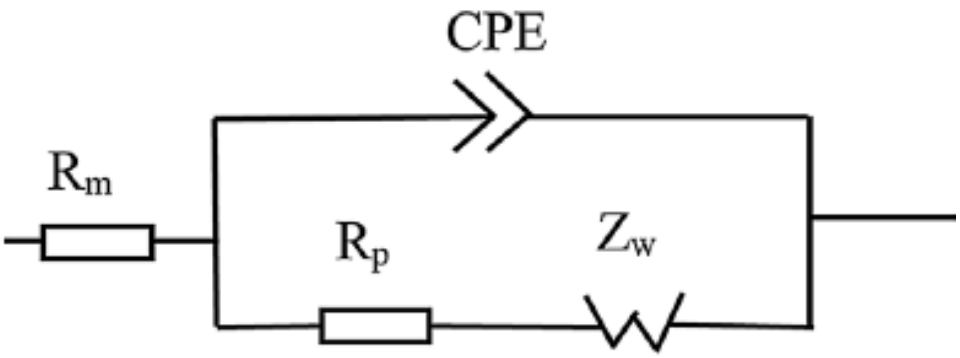

Fig. 5.4 *Randles cell with CPE impedance.*

The constant (τ_d), (R_d) and Z_{CPE} are given as follows (equat 5.16):

$$\begin{cases} \tau_d = \frac{\delta^2}{D} \\ R_d = \frac{RT\,\delta}{n^2F^2SCD} \\ Z_{CPE}\,(jw) = \frac{1}{Q(jw)^{\alpha}} \end{cases} \tag{5.16}$$

Therefore, the equivalent PEMFC impedance is calculated by the following equation 5.17:

$$Z_T\,(jw) = R_m + \frac{1}{Q(jw)^{\alpha} + {}^{1}/_{(R_P+Z_W))}} \tag{5.17}$$

If α = 1, CPE is an ideal capacity.

When α = 0.5, CPE is the Warburg impedance.

Figure 5.5. depicts the spectroscopy impedance for a fuel cell in a distinct PEMFC state, as presented by the (CPE) model and confirmed by experimental data for [12, 101]. In the normal state, there is a minor arc at low and high frequencies, whereas in the case of flooding, there is a large arc, whereas in the drought state, the arc on the right side of the Nyquist plot disappears. Studying the parameters Rm, Rp, and Rd (equation 5.17) allows us to determine the state of the fuel cell based on these observations.

5.5 Controller model by NNT for diagnostic PEMFC

Under the moniker deep learning, neural networks are experiencing a resurgence of interest and even a massive fad. An artificial neural network is a learning system that is modelled after the human brain. Typically, an artificial neural network is used to receive input-output relationships in a neural network model developed for a specific application. Using a well-defined training rule, the transfer function can alter the weights to assure the connection between the three layers of the neuron network model. To train the NNT, its parameters, including its architecture, data, and activation function, must be precisely defined. This phase is crucial because it entails an iterative procedure for estimating the parameters of network neurons in order for the latter to perform its function. After the training phase concludes, the trained network model must be able to make the correct decision for unlearned input vectors. Here, the NNT training performance is estimated using the Mean Squared Error (MSE); the MSE is computed by comparing the NNT output values to the desired value, which is then used to update the weights using the dynamic gradient descent algorithm

The water flow rate input (q_{win}) and operating time (t) are input into the NNT to diagnose the state of fuel cell health (PEMFC) using the NNT model. The condition of the fuel cell can be diagnosed based on the outputs of the NNT model, which are the values of the physical parameters of the EIS model (R_m, R_p and R_d). Finally, the experimental results obtained by

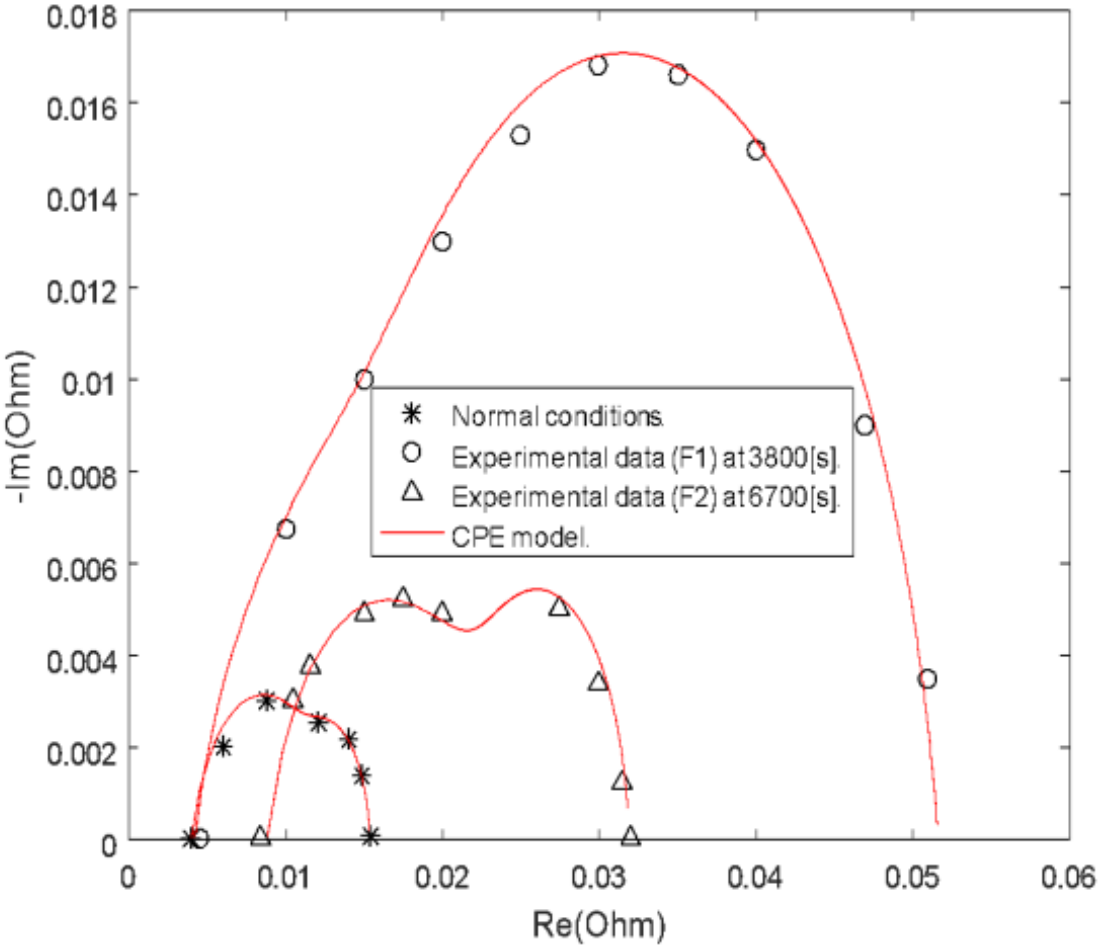

Fig. 5.5 *The Nyquist plot of the fuel cell impedance.*

Fouquet et al. [12] are compared with the results obtained by the NNT model.

5.5.1 PEMFC and ANN Architecture

The sub-models of the fuel cell system (pressure, voltage and relative humidity calculator) are presented in Figure 5.6, whilst, the parameters of this model presented in Table 5.1 [12].

Table 5.1 *Parameters of a normal operating condition of the PEMFC model .*

Parameters	***Value***
curent density : Jn	0.35 $[A/cm^2]$
Temperature: T	320 [K]
Active area : S	200 $[cm^2]$
Aair stoichimetry :λa	3
Nember of fuel cells :N_0	10
ξ_1	-0.948
ξ_2	0.00286+0.0002.lnS + $(4.3.10^{-5})$ lnC_{H2}
ξ_3	7.6×10^{-5}
ξ_4	-1.93×10^{-4}
Hydrogen valve constant : k_{H2}	$4.22 \times 10^{-5}[kmol]/[s.A]$
Oxygen valve constant : k_{O2}	$2.11 \times 10^{-5}[kmol]/[s.atm]$
Hydrogen time constant: τ_{H2}	3.37 [s]
Oxygen time constant : τ_{O2}	6.74 [s]
Hydrogen-Oxygen flow ratio : rH-O	1.168
Kr constant =N_0/4F	$0.996 \times 10^{-6}[kmol]/[s.A]$
$Vn_{(cell)}$	0.72 [V]
Water flow molare : q_{win}	$[0-3] \times 10^{-4}[mole/s]$

The multilayer perceptron is a network of neurons arranged in successive layers. An input layer interprets incoming signals, while an output layer generates the system's response. In addition, one or more concealed layers contribute to the transfer of information. A neuron from a hidden layer is connected as an input to each neuron of the preceding layer and as an output to each neuron of the following layer in a perceptron.

The concealed layer transfer function is defined by the following equation 5.18:

$$f(u) = \frac{1}{1+e^{-(d.u)}} \tag{5.18}$$

Where u represents the input of the hidden layer and calculated as (equat 5.19):

$$u = \sum_{j=1}^{n} \left(W_{ij}X_i + b_i\right) \tag{5.19}$$

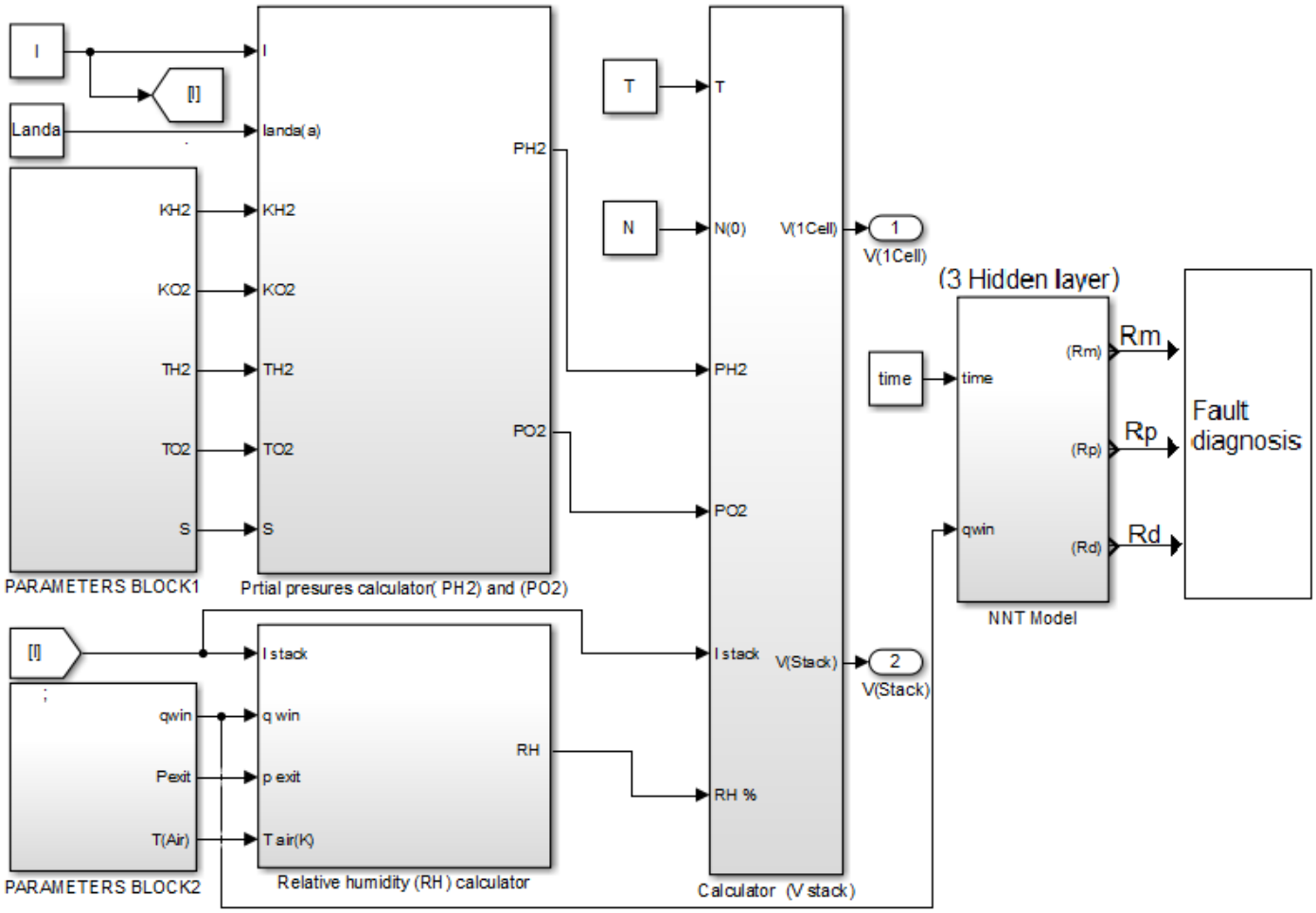

Fig. 5.6 *PEMFC and ANN block diagram.*

For the output layer, the equation that represents the network model is expressed as (equat 5.20):

$$y_K u = \sum_{j=1}^{N} \left(w_{ij}^0 u_i + b_i\right) = \sum_{j=1}^{N} w_{ij}^0 f\left(\sum_{j=1}^{N} \left(w_{ij} x_i + b_i\right)\right) \tag{5.20}$$

Where:

- y_k indicates the output signal from k^{th} output neuron.
- w_{ki}^0 represents the weight of i^{th} output ui to the k^{th} neuron in the output layer.
- u_i is the activation value of the j^{th} neuron in the i^{th} layer.

The next two choices (the number of hidden layers and the number of neurons per hidden layer) directly condition the number of parameters (weight W) to estimate the complexity of the model; they contribute to the search for a good compromise (bias/variance), i.e. the balance between learning quality and forecasting quality. The decision primarily concerns the control of over-learning limits the number of neurons or the learning duration, or even the increase of the parameter norm's penalization coefficient. This necessitates identifying a technique for error estimation, such as validation or test sample, cross-validation, or rap boots.

5.5.2 Neural network-based controller model

To simulate in Matlab how humidity affects the state of the fuel cell and how the values of the *Rm*, *Rp*, and *Rd* change when the fuel cell is operating, we developed a neural network model as depicted in Figure 5.6, which consists of two inputs q_{win} and t, three outputs representing the values of *Rm*, *Rp*, and *Rd* to express the state of the fuel cell, and three hidden layers for each (10, 5, 5) neuron. In addition, activation functions such as tansig, purelin, and purelin were utilised in each concealed layer. Our neural network's parameters are listed in Table 5.2. We then proceeded to implement the parameter values shown in Table 5.3. Notably, these values were derived from the experiments of Fouquet et al. [12]

Figure 5.7 shows the performance of the ANN training and the number of epochs, whereas Figure 5.8 illustrates the correlation between the experimental results and those obtained by the NNT model. Figure 5.9 depicts the output errors of the ANN model, which are approximately 10^{-9}; this demonstrates the ANN model's learning reliability.

5.6 Results and discussion

Based on what we observed in Figure 5.2, we set the value of q_{win} in three phases in order to examine the effect of RH % on the fuel cell's state. As shown in Figure 5.10, q_{win} is maintained at a constant value of 2 mol/s between 0 and 500 s. In this instance, the fuel cell is operating

Table 5.2 *ANN Parameters and training.*

ANN model		**Parameters**
Input		2
Output		3
Number of neuron	HL 1	10
	HL 2	5
	HL 3	5
Activation functions	HL 1	tansig
	HL 2	purelin
	HL 3	purelin
	Output layer	tansig
Epouch		1000
Performance		$3.73 * 10^{-08}$
Gradient		$1.31 * 10^{-06}$
Mu		$1.00 * 10^{-09}$

Table 5.3 *Physical parameters of fuel cell in different state.[12]*

Test	**Time[s]**	**Rm [*Ohm*]**	**Rp [*Ohm*]**	**Rd [*Ohm*]**
1(Normal state)	50	0.00398	0.0080	0.0034
2	1000	0.00406	0.00123	0.0094
3	1600	0.00400	0.0147	0.0172
4	3800	0.00416	0.0163	0.0312
5	3980	0.00512	0.0099	0.0051
6	5400	0.00685	0.0108	0.0056
7	6700	0.00880	0.0130	0.0101

* Slow increase of current (around 0.35 [A]).

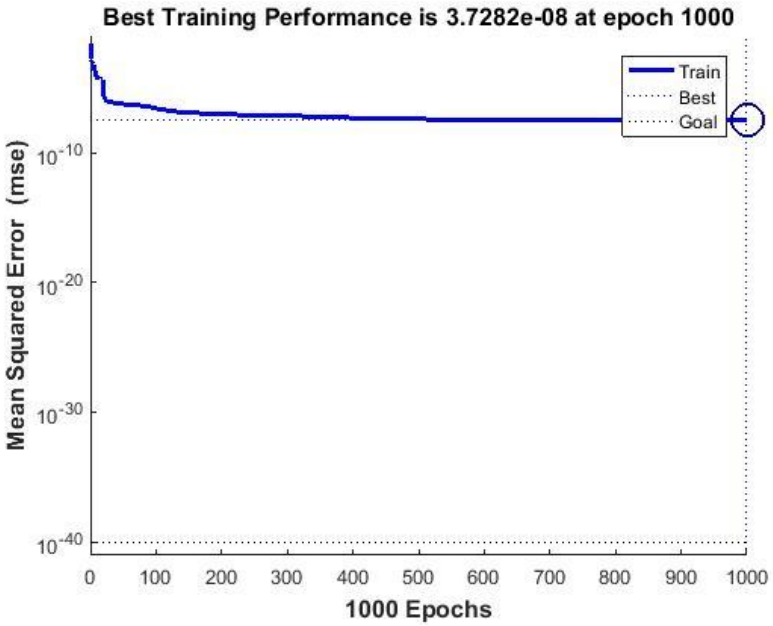

Fig. 5.7 *The performance of the NNT training.*

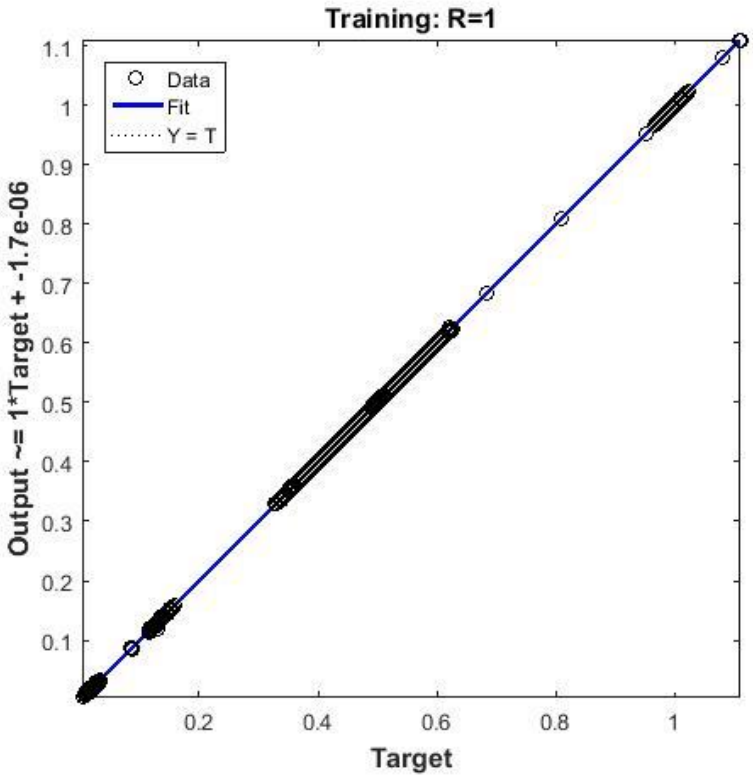

Fig. 5.8 *Linear regression*

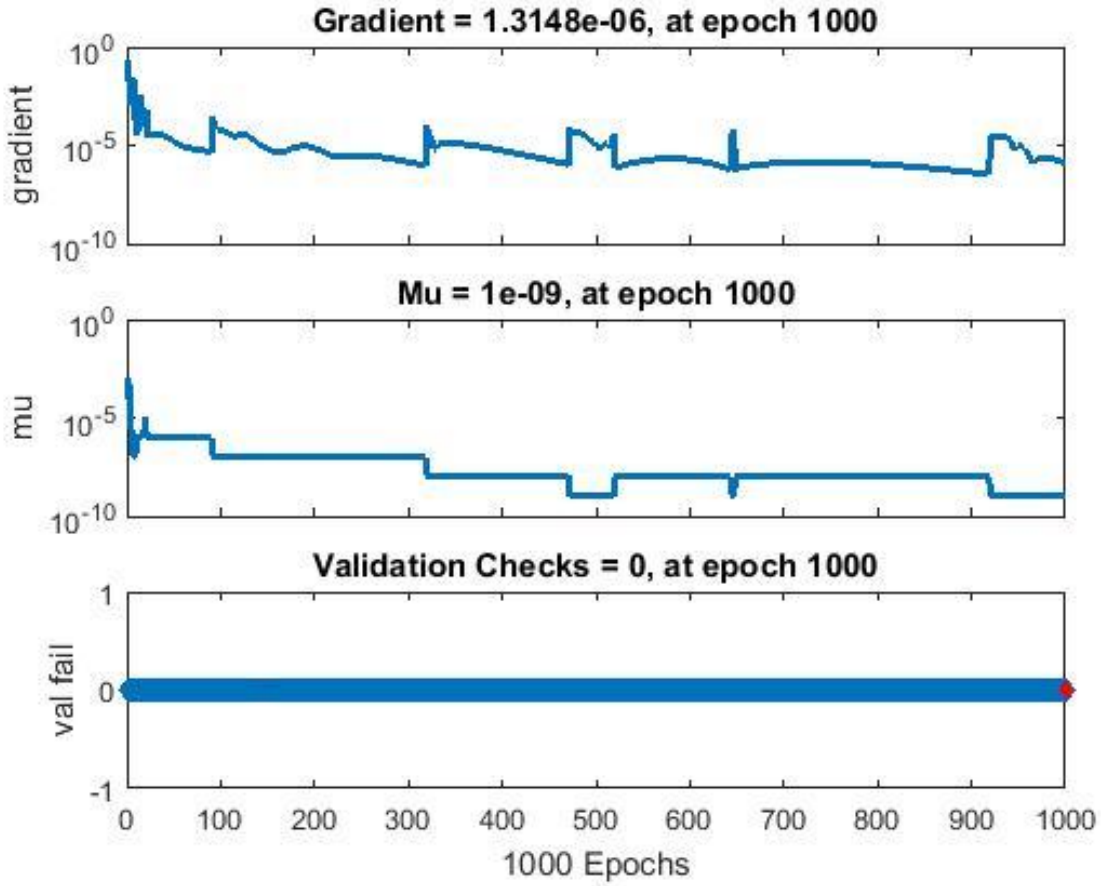

Fig. 5.9 *The output errors of the NNT.*

under normal conditions (T and λ are constant in all instances). However, the value of $q_w in$ between 500 and 3800 s is 5 mol/s. The fuel cell is therefore in a flooded state. After that, $q_w in$ falls to 0.2 mol/s, indicating that the fuel cell is in a dry state.

By analysing the results obtained using the neural network model under various operating conditions (see Figure 5.11, 5.12, 5.13), the following is observed:

- During the normal phase [0, 500] s, the values of R_m, R_p, and R_d are constant, indicating system stability.
- Between 500 s and 3800 s, it is observed that the value of R_m remains constant; however, the values of R_p and R_d increase by a large percentage in a short period of time due to the increase in humidity within the fuel cell.
- The value of qwin has been decreased to 0.2 mol/s to determine the impact of drought on the fuel cell's properties. During this phase, the value of R_m increases progressively; this corresponds to the fuel cell's drought. While the angle of inclination of the R_p and R_d curves in this case is less than the state of drowning, this also indicates that the fuel cell is in a state of drying.

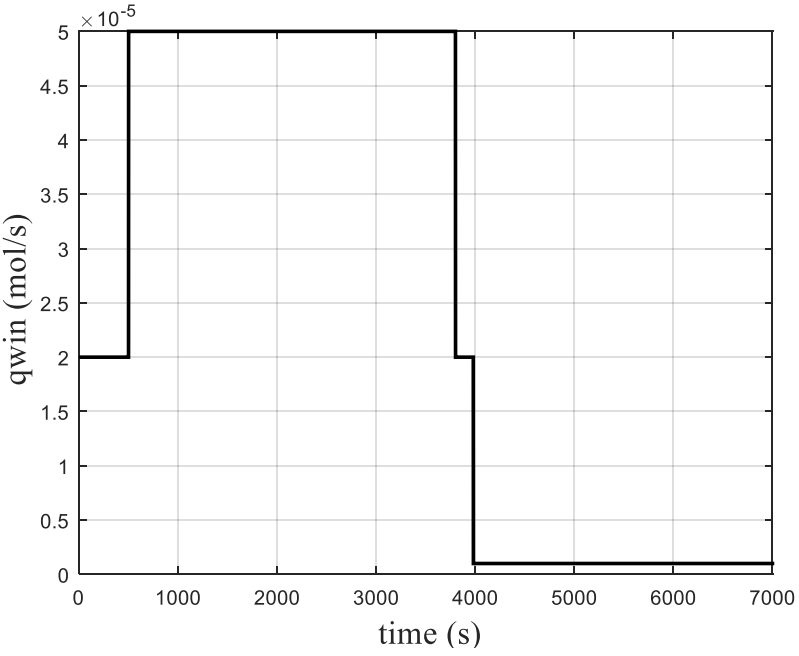

Fig. 5.10 *Molar flow air in the inlet.*

Figure 5.14 displays the values R_m, R_p, and R_d obtained from the neural network model after 3000 s for both drowning and dehydration. It is evident from this graph that the value of R_m remains unchanged in the normal and flooded states, while it increases by 20% in the drying state. Also, the value of polarisation resistance increases by 25% in the case of drying and by 40% in the case of drowning compared to the typical state of the fuel cell.

The difference in R_d values is a result of the difference in S caused by the accumulation of water within the PEMFC.

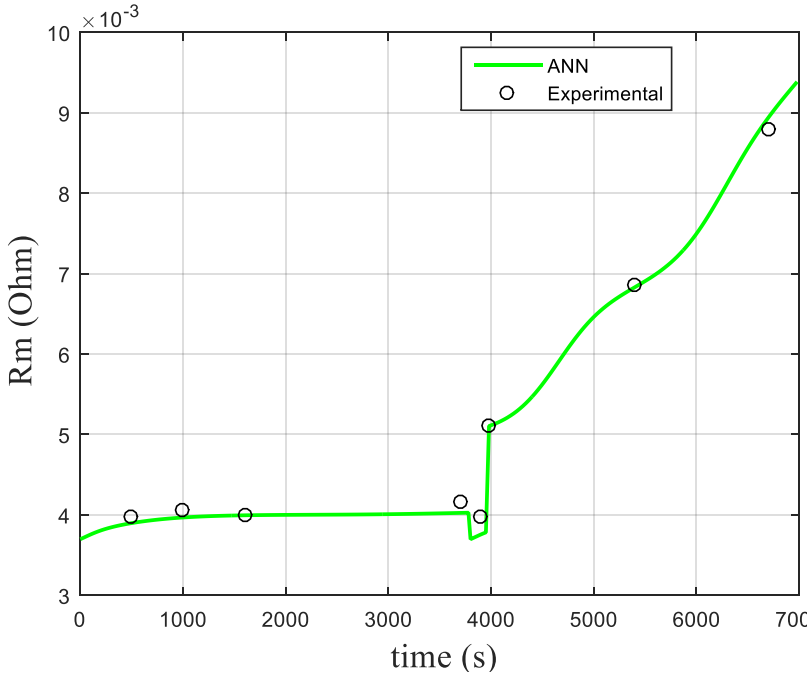

Fig. 5.11 *Membrane resistance.*

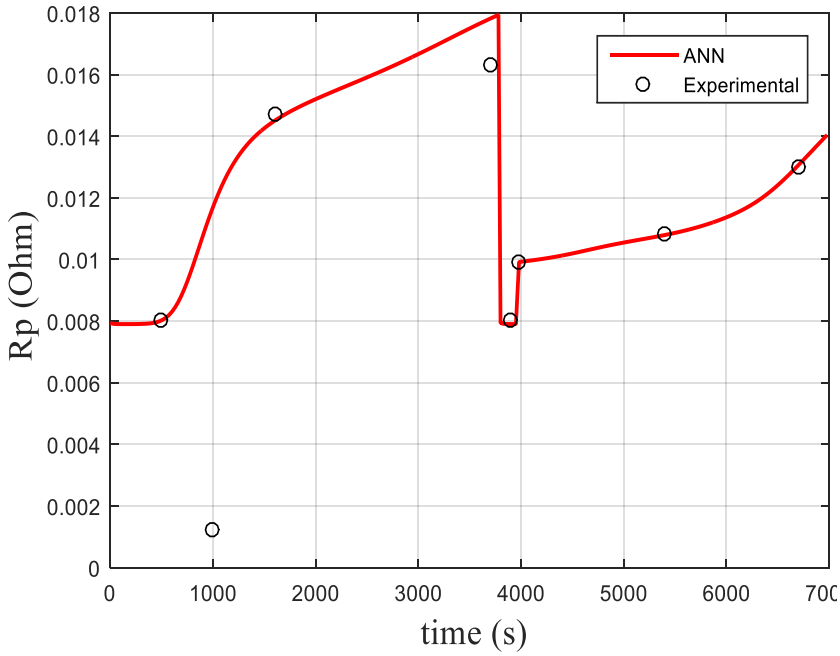

Fig. 5.12 *Polarisation resistance.*

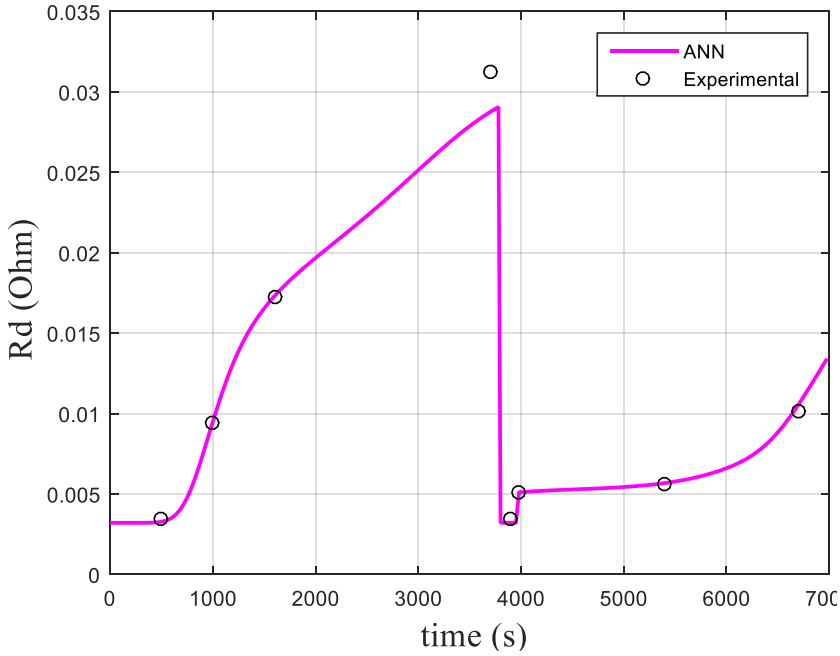

Fig. 5.13 *Electrical resistance.*

In three-dimensional space, Figure 5.15 depicts the values of R_m, R_d, and R_p. There appear to be three regions: region A (between 0 s and 500 s) represents the normal state, region B (between 2000 s and 3800 s) alludes to the case of the flood, and region C (between 5800 s and 6800 s) indicates that the fuel cell is in a state of drought. We can estimate the condition of the fuel cell based on these disparities.

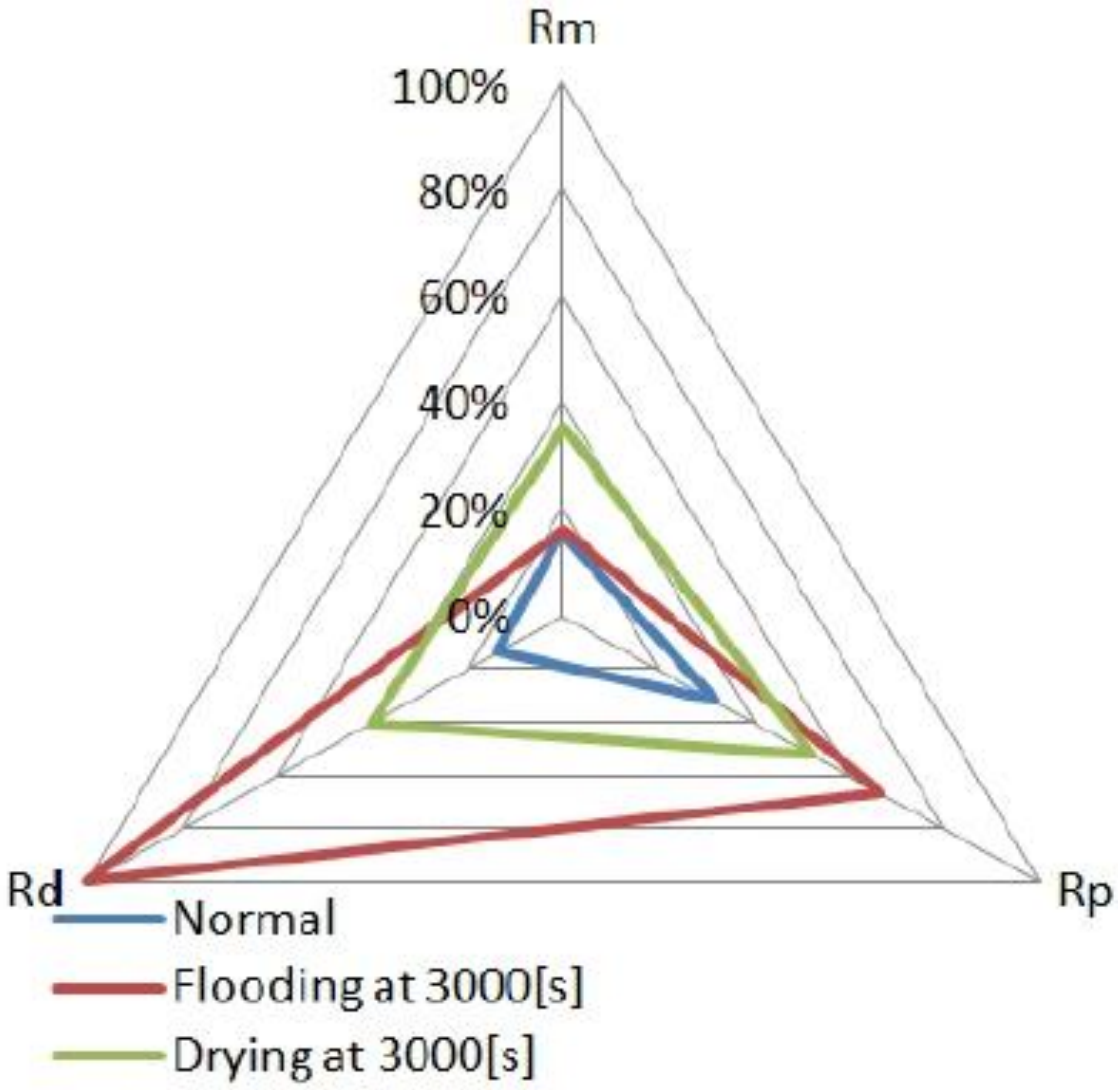

Fig. 5.14 *Radar diagram for classification of the state of health in different operating conditions.*

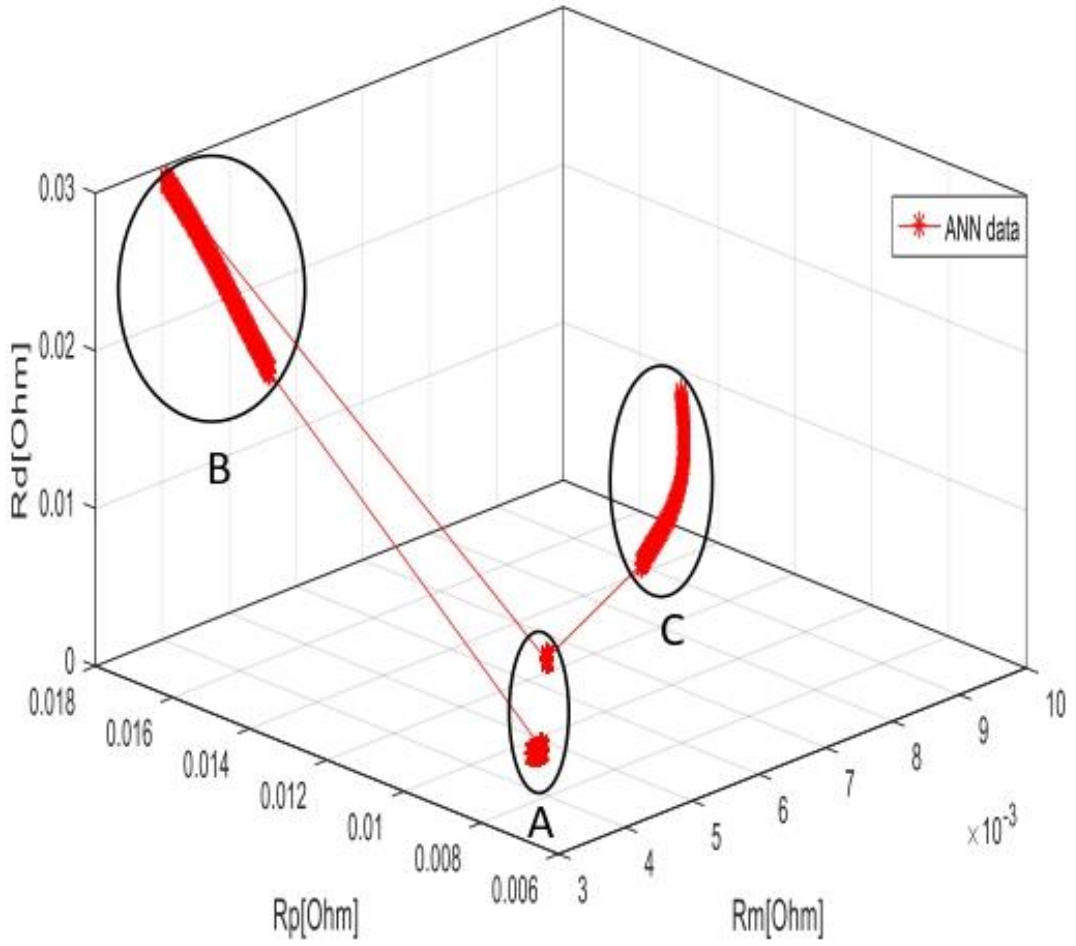

Fig. 5.15 *3D simulation of changing the fuel cell state during different time periods.*

5.7 Accurate Estimation of PEMFC State of Health using Modified Hybrid Artificial NNT Models

The Randles physical model with CPE and the fuel cell output voltage (FCOV) patterns served as the foundation for two techniques that make up the hybrid ANN model. Therefore, using statistical analysis of Rm, Rp, Rd, and FCOV losses, this model is able to pinpoint the hydration state (flooding and drying) and diagnose PEMFC failure types. The neuron network system's dependability and capabilities are provided by the integration of two sub-NNT models. The suggested approach can let various models run free to find their optimal performance for use in industrial applications.

5.7.1 ANN Architecture

The structure of the neuron network used in this investigation is depicted in Figure 5.16. The experimental data from study of Fouquet [12] are used to train the first sub-NNT model. The output of the second subNNT is created by combining the outputs of this subNNT. The input of the first NNT model is constrained by the operation period and the molar flow of air entering the fuel cell (qwin). Three under-layers (10, 5, and 5 neuron) are present in the hidden layer for each hidden layer, correspondingly. The Rm, Rp, and Rdvalues are additionally indicated by three neurons in the outputs layer. Each hidden layer's tansig, purelin, and purelin activation functions are distinct. The second NNT model's input layer is connected to the neurons in the first NNT model's output layer, and the fourth input stands in for the operation time. Two under-layers (5 and 4) of neurons are present in each hidden layer of the hidden layer. The output layer serves as a visual representation of the fuel cell's (SOH) V(CELL). The parameters of each layer are estimated using the logsig and tansig functions, respectively. As a result, in this study's ANN, experimental samples are used to train it in order to create a sensor for failure diagnosis. The test samples are then utilized to validate the defect diagnostic model's accuracy. The precision of the state of health can be greatly improved by this method. The experimental model's paramteres are illustrated in table 5.4.

5.7.2 Implementation and discussion

The fuel cell voltage is shown for each time period in Figure 5.17. Second sub-ANN provides the fuel cell voltage response in order to show how the parameters of the Randles model might vary and affect the fuel cell's state of health. The fuel cell's voltage remains constant between 0 and 500 seconds (i.e., under normal circumstances), and the Resistances of Randles model maintains its values, demonstrating the fuel cell's efficacy.

In addition, we see a decrease in fuel cell voltage in the flooding condition of the second

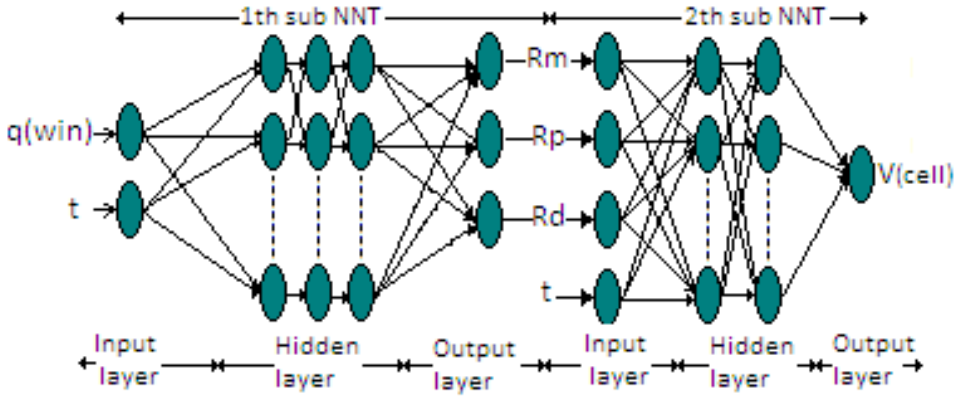

Fig. 5.16 *ANN model's schematic diagram.*

Table 5.4 *ANN Parameters and training.*

Parameters		**ANN 1**	**ANN 2**
Input		2	4
Output		3	1
Number of neuron	HL 1	10	5
	HL 2	5	4
	HL 3	5	/
Activation functions	HL 1	tansig	logsig
	HL 2	purelin	Logsig
	HL 3	purelin	/
	Output layer	tansig	tansig
Epouch		1000	664
Performance		$3.73 * 10^{-08}$	$9.99 * 10^{-7}$
Gradient		$1.31 * 10^{-06}$	$2.79 * 10^{-6}$
Mu		$1.00 * 10^{-09}$	$1.00 * 10^{-8}$

test. The rise in membrane ionic conductivity, as seen in Figure 5.17, is referred to as the drop voltage. Moreover, the gradual increase in (Rm, Rp, and Rd) coincides with the progressive voltage reduction that is immediately noticeable after 4000 s.

According to these findings, the decrease in voltage is directly related to the accumulation of water inside the fuel cell's channel due to the influence of water on the conductivity of the membrane. The flood phase is influenced by the sluggish drop in FC voltage because when RH rises, membrane conductivity rises as well.

Overall, the relative humidity variation into PEMFC and the change of the randles model parameters may be used to determine the state of hydration using the proposed method. As a result, the artificial neural network used in this study makes it possible to understand how humidity influences fuel cell voltage.

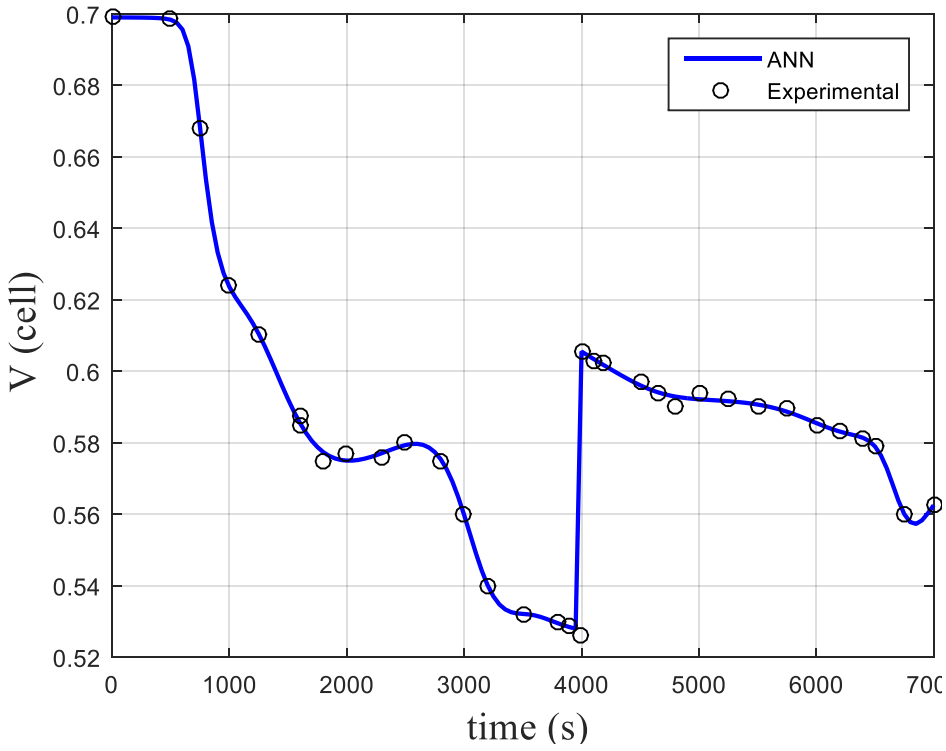

Fig. 5.17 *Fuel cell voltage at various states.*

5.8 Comparative methods

Table 5 5.5 provides an overview of the most important criteria of several research for PEMFC diagnostic in comparison to the advised approach. The suggested methodology in this study offers a lot of benefits over other methods that call for a lot of databases and tools, and this is supported by comparative analysis in terms of fast, accurate prognosis, quick implementation, and low cost.

Table 5.5 *Comparison of relevant and recent research on PEMFC diagnosis*

Approaches	Idea	Hard/ software	Advantages	Drawbacks	Ref
Neural networks technique.	✓ It has been suggested that the NNT model can estimate (RNNT_int, RNNT_pol) in both drying and flooding scenarios.	✓ NNT learning phase ✓ a back-propagation method used for data collecting.	✓ Its prediction is accurate.	✓ Numerous data are needed for it.	*[22]*
Invasive diagnostic procedure employing a new magnetic field measurement technique.	✓ The magnetic field sensors inside the stack are placed in the end plates. ✓ The density of the current can be determined from the field data itself. ✓ The spread of MEA current can be visualized using the magnetic field.	✓ Film-formed gas temperature sensor ✓S++ Simulation Services.	✓ The measurement is performed as closely as feasible to the defect. ✓ In most cases, exploitation is straightforward.	✓ Incorporating sensors into the PEMFC system affects its inherent behavior.	*[67]*
Aapplications for in-situ diagnosis that gauge changes in voltage and the magnetic field.	✓ This method was validated on a 300-watt stack. ✓ Every four cells, 15 tri-axis sensors were inserted. ✓ The current density was determined by measuring the magnetic field with PEMFC-equipped electrodes.	✓ In the PEMFC stack's cooling channels, magnetic field sensors have been installed.	✓ Non-destructive and enabling non-contact measurements.	✓ It is difficult to separate the impact of the problem from that of the sensor.	*[69]*
Analysis of THDA (Total Harmonic Distortion).	✓ (AVL) Total Harmonic Distortion technology can track voltage fluctuations in a single cell without requiring V (cell) readings.	✓ Databases containing up to a few hundred voltage channels.	✓ Significantly decreases the amount of wiring ✓ contacting and hardware required.	✓ There are no conceptual modifications required for existing stack designs to implement this system.	*[5]*
Utilisation of electrochemical impedance spectroscopy (EIS) in the administration of power transformers.	✓ Better diagnosis and management are made possible with this technology thanks to the proposed EIS. ✓ Real time EIS was used.	✓ The EIS is accomplished through the power converter.	✓ Variations can be monitored using EIS results for onboard diagnostics or control optimisation.	✓ costly in terms of computation. ✓ For EIS measurements, more equipment is needed.	*[75]*
The acoustic emission AE technique.	✓ The Nafion samples were measured for EIS and AE as they dried. ✓ After the loss of water, the resultant electrochemical parameters yield linear or exponential reactions.	✓Piezoelectric transducer. ✓ Specific measuring instruments.	✓ Analysis of fuel cell components using a Non-destructivetechnique shows promise.	✓ needs a sizable data set produced by PEMFC-based EIS experiments.	*[82]*
PEMFC diagnostic using AC impedance.	✓ In the typical EIS, both in situ and ex situ impedance measurements are discussed, investigated, and presented in a variety of scenarios.	✓Potentiostatic. ✓measurements at different modes of gas-feeding. ✓galvanostatic measurements.	✓ A quick AC impedance method is briefly discussed.	✓ The lack of a straightforward method to determine the impedance of a single electrode is usually negligible.	*[8]*
Applying a Neural Networks methodology to the EIS and polarization curves method.	✓ In this study, the ANN model employed a mixed approach based on stack voltage singularity measurement in addition to EIS measurement. ✓ AI technology is used to estimate and diagnose a fuel cell's health state in both cases of flooding and drying out.	✓ The backpropagation technique was used throughout the NNT's learning phase, and data collecting was done on an empirical basis.	✓ Predict fuel cell output voltage loss quickly with this prognostic tool. ✓ Predicting fuel cell breakdown due to insufficient water management (such as flooding or drying) may be possible with the proposed neural network model. ✓Easy, quick to implement ✓low cost.	✓ It is advised that more research be done to create a more focused control algorithm for this model so that it may be implemented as an intelligent water management controller with potentially adaptable targets for reconfiguration control and/or preventative maintenance.	*Proposed method*

5.9 conclusion

In this chapter, neural network technology is used to estimate and diagnose the state of health of the fuel cell by determining the electrochemical impedance parameters.
Based on the achieved results, we found that there are three parameters that help to identify the state of PEMFC, which are Rm, Rp, and Rd (as shown in the Randles model). In addition, this technology contributes to accurate diagnosis without requiring costly equipment, making it appropriate for practical applications. Overall, our model can be incorporated into the fuel cell's control system to improve water flow rate management in both inundation and drying scenarios.

Chapter 6

General conclusion and future works

6.1 General Conclusion

Global warming and the increase in the level of pollution incite the use of the renewable energy solutions rather than traditional sources of energy. Polymer electrolyte membrane fuel cells technology is become one of the main promising renewable power devices. PEMFC's accuracy, reliability, and durability are essential in the practical field and limiting factors to marketability. Therefore, it is important to avoid and diagnose early degradation.

Fault diagnostics "i.e. fault detect and isolate" are used to determine the procedure consisting in identifying the possible cause(s) of failure(s) or the evolution of one or more important degradation factors (flooding, drying, fuel or oxidizer starvation, catalyst poisoning, etc...). using logical reasoning based on a set of information, the corrective actions can be taken to increase the service life of PEMFC.

Artificial intelligence was developed with the goal of simulating the behaviour of the human brain. Artificial intelligence and machine learning are attracting increasing interest in materials development and power systems control/monitoring. To this aim, This study provides detailed analysis of pros and cons of several existing approaches for fuel cell diagnosis techniques and focuses in finding a suitable, effective, and easy to use method, to avoid the frequent mistakes that are presented by the poor flow of water inside the fuel cell during its operation. Towards this aim, the artificial intelligence technology is proposed. More specifically, a neural network model is used to enable monitoring the influence of the humidity content of the fuel cell membrane, through employing electrochemical impedance spectroscopy method (EIS analysis). This technique allows analyzing and diagnosing PEM fuel cell failure modes (flooding and drying). The benefit of this work is summed up in the demonstration of the existence in a simple way that helps to define the state of health of the PEMFC.

6.2 Author's contributions

One of the promising method based PEMFC diagnostics, becoming important for researchers, is ANNs, it provides many advantages compared to other traditional techniques that require a large number of instruments. -The neural network method proposed could be effective to predict the degradation caused by poor water management of the fuel cell (i.e. Flooding, Drying).

In this work, we suggested to employ the ANNs in the fuel cell system, we have several of inputs and outputs. Through the received inputs/outputs relationships the ANN model helps to diagnose the fuel cell status in a fast way based on three steps: learning, classification and testing. Typically, this process can be trained the data for any system to learn the ANN model without any physical equations. To simulate Matlab how humidity affects the state of the fuel cell and how to change the values of the Rm, Rp, and Rd when it is operating during periods, we formed a model of a neural network that is constituted of two inputs (qwin) and (t). Based

on the outputs of NNT model, which are the values of the physical parameters of the EIS model (Rm, Rp, and Rd), one can diagnose the state of the fuel cell.

We have presented a fast prognostic tool to predict the output voltage loss in the PEMFC. The main idea behind using output voltage loss to diagnose the SOH of PEMFC is that neural network approach presents a high sensitivity to identify the parameters of the Randles model and capable to predict response of voltage under a sudden change in relative humidity.

6.3 Future works

The future studies can be summarised as follows:

- Propose new diagnosis methods based on AI and publish results in peer-reviewed journals as well as in international conferences.
- We aim to adopte the magnetic tomography extracted from their magnetic fields of the PEMFC to estimate the useful information for the FC diagnosis, we will use the convolutional neural network (CNN) in the training and testing to classify each PEMFC's interior picture into a category, i.e. flooding, drying and anodic/cathodic starvation, thus obtaining the state of health of the fuel cell.

Finally, It is hoped that the proposed method can give free rein to different models get the best performance to be practical in the industrial applications. The proposed models will be exploited and explored for the development of diagnosis systems in this field as well as in different domains.

Bibliography

[1] Dubas, F. 'Conception d'un moteur rapide a aimants permanents pour l'entranement de compresseurs de piles a combustible'. Universite de Franche-Comte, 2006

[2] Hou, M., Shao, Z., Yi, B.: 'Technological approaches to increasing specific power of vehicular fuel cell stacks', *Strategic Study of Chinese Academy of Engineering*, 2019, **21**, (3), pp. 84–91

[3] Liang, D., Dou, M., Hou, M., Shen, Q., Shao, Z., Yi, B.: 'Behavior of a unit proton exchange membrane fuel cell in a stack under fuel starvation', *Journal of Power Sources*, 2011, **196**, (13), pp. 5595–5598

[4] Wasterlain, S., Candusso, D., Harel, F., Hissel, D., Francois, X.: 'Development of new test instruments and protocols for the diagnostic of fuel cell stacks', *Journal of Power Sources*, 2011, **196**, (12), pp. 5325–5333

[5] Ramschak, E., Peinecke, V., Prenninger, P., Schaffer, T., Baumgartner, W., Hacker, V.: 'Online stack monitoring tool for dynamically and stationary operated fuel cell systems', *Fuel Cells Bulletin*, 2006, **2006**, (10), pp. 12–15

[6] Yamanashi, R., Gotoh, Y., Izumi, M., Nara, T.: 'Evaluation of generation current inside membrane electrode assembly in polymer electrolyte fuel cell using static magnetic field around fuel cell', *ECS Transactions*, 2015, **65**, (1), pp. 219

[7] Ender, M., Illig, J., Ivers.Tiffe, E.: 'Three electrode setups for lithium ion batteries', *Journal of The Electrochemical Society*, 2016, **164**, (2), pp. A71

[8] Yuan, X., Wang, H., Sun, J.C., Zhang, J.: 'Ac impedance technique in pem fuel cell diagnosis a review', *International Journal of Hydrogen Energy*, 2007, **32**, (17), pp. 4365–4380

[9] Wang, Y., Seo, B., Wang, B., Zamel, N., Jiao, K., Adroher, X.C.: 'Fundamentals, materials, and machine learning of polymer electrolyte membrane fuel cell technology', *Energy and AI*, 2020, **1**, pp. 100014

[10] Saber, M., El.Rharras, A., Saadane, R., Aroussi, H.K., Wahbi, M.: 'Artificial neural networks, support vector machine and energy detection for spectrum sensing based on real signals', *International Journal of Communication Networks and Information Security*, 2019, **11**, (1), pp. 52–60

[11] Shao, M., Zhu, X.J., Cao, H.F., Shen, H.F.: 'An artificial neural network ensemble method for fault diagnosis of proton exchange membrane fuel cell system', *Energy*, 2014, **67**, pp. 268–275

[12] Fouquet, N., Doulet, C., Nouillant, C., Dauphin.Tanguy, G., Ould.Bouamama, B.: 'Model based pem fuel cell state-of-health monitoring via ac impedance measurements', *Journal of Power Sources*, 2006, **159**, (2), pp. 905–913

[13] Ahmed, N.A., Miyatake, M., Al.Othman, A.: 'Power fluctuations suppression of stand-alone hybrid generation combining solar photovoltaic/wind turbine and fuel cell systems', *Energy Conversion and management*, 2008, **49**, (10), pp. 2711–2719

[14] Wang, Y., Chen, K.S., Mishler, J., Cho, S.C., Adroher, X.C.: 'A review of polymer electrolyte membrane fuel cells: Technology, applications, and needs on fundamental research', *Applied energy*, 2011, **88**, (4), pp. 981–1007

[15] Petrone, R., Zheng, Z., Hissel, D., Péra, M.C., Pianese, C., Sorrentino, M., et al.: 'A review on model-based diagnosis methodologies for pemfcs', *International Journal of Hydrogen Energy*, 2013, **38**, (17), pp. 7077–7091

[16] Zheng, Z., Petrone, R., Péra, M.C., Hissel, D., Becherif, M., Pianese, C., et al.: 'A review on non-model based diagnosis methodologies for pem fuel cell stacks and systems', *International Journal of Hydrogen Energy*, 2013, **38**, (21), pp. 8914–8926

[17] Wu, J., Yuan, X.Z., Wang, H., Blanco, M., Martin, J.J., Zhang, J.: 'Diagnostic tools in pem fuel cell research: Part ii: Physical/chemical methods', *International Journal of Hydrogen Energy*, 2008, **33**, (6), pp. 1747–1757

[18] Wu, J., Yuan, X.Z., Wang, H., Blanco, M., Martin, J.J., Zhang, J.: 'Diagnostic tools in pem fuel cell research: Part i electrochemical techniques', *International journal of hydrogen energy*, 2008, **33**, (6), pp. 1735–1746

[19] Barbir, F., Gorgun, H., Wang, X.: 'Relationship between pressure drop and cell resistance as a diagnostic tool for pem fuel cells', *Journal of Power Sources*, 2005, **141**, (1), pp. 96–101

[20] Steiner, N.Y., Hissel, D., Moçotéguy, P., Candusso, D.: 'Diagnosis of polymer electrolyte fuel cells failure modes (flooding & drying out) by neural networks modeling', *International journal of hydrogen energy*, 2011, **36**, (4), pp. 3067–3075

[21] Mérida, W., Harrington, D., Le.Canut, J., McLean, G.: 'Characterisation of proton exchange membrane fuel cell (pemfc) failures via electrochemical impedance spectroscopy', *Journal of power sources*, 2006, **161**, (1), pp. 264–274

[22] Arama, F.Z., Mammar, K., Laribi, S., Necaibia, A., Ghaitaoui, T.: 'Implementation of sensor based on neural networks technique to predict the pem fuel cell hydration state', *Journal of Energy Storage*, 2020, **27**, pp. 101051

[23] Bethoux, O., Hilairet, M., Azib, T. 'A new on-line state-of-health monitoring technique dedicated to pem fuel cell'. In: 2009 35th Annual Conference of IEEE Industrial Electronics. (IEEE, 2009. pp. 2745–2750

[24] Saadi, A., Becherif, M., Hissel, D., Ramadan, H.S.: 'Dynamic modeling and experimental analysis of pemfcs: A comparative study', *International Journal of Hydrogen Energy*, 2017, **42**, (2), pp. 1544–1557

[25] Mitzel, J., Sanchez.Monreal, J., Garcia.Sanchez, D., Gazdzicki, P., Schulze, M., Häußler, F., et al.: 'Fault diagnostics in pemfc stacks by evaluation of local performance and cell impedance analysis', *Fuel Cells*, 2020, **20**, (4), pp. 403–412

[26] Lu, H., Chen, J., Yan, C., Liu, H.: 'On-line fault diagnosis for proton exchange membrane fuel cells based on a fast electrochemical impedance spectroscopy measurement', *Journal of Power Sources*, 2019, **430**, pp. 233–243

[27] Nara, H., Yokoshima, T., Osaka, T.: 'Technology of electrochemical impedance spectroscopy for an energy-sustainable society', *Current Opinion in Electrochemistry*, 2020, **20**, pp. 66–77

[28] Li, X.: 'Principles of fuel cells'. (CRC press, 2005)

[29] O'Hayre, R., Fabian, T., Litster, S., Prinz, F.B., Santiago, J.G.: 'Combined heat and mass transfer model of a passive air breathing fuel cell cathode', *ECS Transactions*, 2006, **3**, (1), pp. 1125

[30] Baschuk, J., Li, X.: 'Carbon monoxide poisoning of proton exchange membrane fuel cells', *International Journal of Energy Research*, 2001, **25**, (8), pp. 695–713

[31] Qi, Z.: 'Proton exchange membrane fuel cells'. (CRC Press, 2013)

[32] Spiegel, C.: 'Designing and building fuel cells'. vol. 87. (Mcgraw-hill New York, 2007)

[33] Sharaf, O.Z., Orhan, M.F.: 'An overview of fuel cell technology: Fundamentals and applications', *Renewable and sustainable energy reviews*, 2014, **32**, pp. 810–853

[34] Korner, A., Tam, C., Bennett, S., Gagne, J.: 'Technology roadmap-hydrogen and fuel cells', *International Energy Agency (IEA): Paris, France*, 2015,

[35] El.Kharouf, A., Mason, T.J., Brett, D.J., Pollet, B.G.: 'Ex-situ characterisation of gas diffusion layers for proton exchange membrane fuel cells', *Journal of Power sources*, 2012, **218**, pp. 393–404

[36] Liu, W., Zuckerbrod, D.: 'In situ detection of hydrogen peroxide in pem fuel cells', *Journal of The Electrochemical Society*, 2005, **152**, (6), pp. A1165

[37] Fontes, G. 'Modelisation et caracterisation de la pile PEM pour l'etude des interactions avec les convertisseurs statiques', 2005

[38] Lachaize, J. 'Etude des strategies et des structures de commande pour le pilotage des systemes energetiques a Pile a Combustible (PAC) destines a la traction', 2004

[39] Zhang, J., Wu, J., Zhang, H., Zhang, J.: 'PEM fuel cell testing and diagnosis'. (Newnes, 2013)

[40] Zhang, J., Tang, Y., Song, C., Zhang, J., Wang, H.: 'Pem fuel cell open circuit voltage (ocv) in the temperature range of 23 c to 120 c', *Journal of power sources*, 2006, **163**, (1), pp. 532–537

[41] Zhang, H., Li, J., Tang, H., Lin, Y., Pan, M.: 'Hydrogen crossover through perfluorosulfonic acid membranes with variable side chains and its influence in fuel cell lifetime', *International journal of hydrogen energy*, 2014, **39**, (28), pp. 15989–15995

[42] Cheng, X., Zhang, J., Tang, Y., Song, C., Shen, J., Song, D., et al.: 'Hydrogen crossover in high-temperature pem fuel cells', *Journal of Power Sources*, 2007, **167**, (1), pp. 25–31

[43] Prigent, M.: 'Les piles a combustible: etat du developpement et des recherches en cours', , 1997,

[44] Park, Y.H., Caton, J.A.: 'An experimental investigation of electro-osmotic drag coefficients in a polymer electrolyte membrane fuel cell', *International Journal of Hydrogen Energy*, 2008, **33**, (24), pp. 7513–7520

[45] Ge, S., Yi, B., Ming, P.: 'Experimental determination of electro-osmotic drag coefficient in nafion membrane for fuel cells', *Journal of The Electrochemical Society*, 2006, **153**, (8), pp. A1443

[46] Borup, R.L., Davey, J.R., Garzon, F.H., Wood, D.L., Inbody, M.A.: 'Pem fuel cell electrocatalyst durability measurements', *Journal of Power Sources*, 2006, **163**, (1), pp. 76–81

[47] Candusso, D., De.Bernardinis, A., Péra, M.C., Harel, F., François, X., Hissel, D., et al.: 'Fuel cell operation under degraded working modes and study of diode by-pass circuit dedicated to multi-stack association', *Energy Conversion and Management*, 2008, **49**, (4), pp. 880–895

[48] Kahia, H., Aicha, S., Herbadji, D., Herbadji, A., Bedda, S.: 'Neural network based diagnostic of pem fuel cell', *Journal of New Materials for Electrochemical Systems*, 2020, **23**, (4), pp. 225–234

[49] Yasuda, K., Taniguchi, A., Akita, T., Ioroi, T., Siroma, Z.: 'Platinum dissolution and deposition in the polymer electrolyte membrane of a pem fuel cell as studied by potential cycling', *Physical Chemistry Chemical Physics*, 2006, **8**, (6), pp. 746–752

[50] Wang, X., Kumar, R., Myers, D.J.: 'Effect of voltage on platinum dissolution: Relevance to polymer electrolyte fuel cells', *Electrochemical and Solid-State Letters*, 2006, **9**, (5), pp. A225

[51] Zhang, J., Sasaki, K., Sutter, E., Adzic, R.: 'Stabilization of platinum oxygen-reduction electrocatalysts using gold clusters', *Science*, 2007, **315**, (5809), pp. 220–222

[52] Cho, E.: 'A study on performance degradation of pemfc by water freezing', *J Electrochem Soc*, 2003, **150**, (12), pp. A1667–A1670

[53] Rubio, M., Urquia, A., Dormido, S.: 'Diagnosis of pem fuel cells through current interruption', *Journal of Power Sources*, 2007, **171**, (2), pp. 670–677

[54] Latham, R.A.: 'Algorithm development for electrochemical impedance spectroscopy diagnostics in pem fuel cells', , 2004,

[55] Hissel, D., Péra, M., Kauffmann, J.: 'Diagnosis of automotive fuel cell power generators', *Journal of Power sources*, 2004, **128**, (2), pp. 239–246

[56] Fennie, C., Reisner, D., Barbetta, J., Singh, P. 'Fuzzy logic-based state-of-health determination of pem fuel cells'. In: Proceeding of Electric Vehicle Symposium and Exhibition. (, 2001.

[57] Nitsche, C., Schroedl, S., Weiss, W. 'Onboard diagnostics concept for fuel cell vehicles using adaptive modelling'. In: IEEE Intelligent Vehicles Symposium, 2004. (IEEE, 2004. pp. 127–132

[58] Forrai, A., Funato, H., Yanagita, Y., Kato, Y.: 'Fuel-cell parameter estimation and diagnostics', *IEEE transactions on energy conversion*, 2005, **20**, (3), pp. 668–675

[59] Nakajima, H., Konomi, T., Kitahara, T., Tachibana, H.: 'Electrochemical impedance parameters for the diagnosis of a polymer electrolyte fuel cell poisoned by carbon monoxide in reformed hydrogen fuel', *Journal of fuel cell science and technology*, 2008, **5**, (4)

[60] Li, H., Zhang, J., Fatih, K., Wang, Z., Tang, Y., Shi, Z., et al.: 'Polymer electrolyte membrane fuel cell contamination: Testing and diagnosis of toluene-induced cathode degradation', *Journal of Power Sources*, 2008, **185**, (1), pp. 272–279

[61] Sugiura, K., Yamamoto, M., Yoshitani, Y., Tanimoto, K., Daigo, A., Murakami, T.: 'Performance diagnostics of pefc by current-pulse method', *Journal of power sources*, 2006, **157**, (2), pp. 695–702

[62] Mérida.Donis, W.R. 'Diagnosis of PEMFC stack failures via electrochemical impedance spectroscopy', 2002

[63] Hernandez, A. 'Diagnostic d une pile a combustible de type PEFC'. PhD thesis, Universite de Technologie de Belfort Montbelliard, 2006

[64] Hernandez, A., Hissel, D., Outbib, R. 'Fuel cell fault diagnosis: A stochastic approach'. In: 2006 IEEE international symposium on industrial electronics. vol. 3. (IEEE, 2006. pp. 1984–1989

[65] Park, J., Li, X., Tran, D., Abdel.Baset, T., Hussey, D.S., Jacobson, D.L., et al.: 'Neutron imaging investigation of liquid water distribution in and the performance of a pem fuel cell', *International Journal of Hydrogen Energy*, 2008, **33**, (13), pp. 3373–3384

[66] Chikahisa, T., Tabe, Y., Kikuta, K., Nohara, N., Shinohara, H. 'Measurement of water production behavior, temperature, and current density distributions in a polymer electrolyte fuel cell'. In: International Conference on Fuel Cell Science, Engineering and Technology. vol. 42479. (, 2006. pp. 25–30

[67] Candusso, D., Poirot.Crouvezier, J., Bador, B., Rullière, E., Soulier, R., Voyant, J.: 'Determination of current density distribution in proton exchange membrane fuel cells', *The European Physical Journal-Applied Physics*, 2004, **25**, (1), pp. 67–74

[68] He, S., Mench, M.M., Tadigadapa, S.: 'Thin film temperature sensor for real-time measurement of electrolyte temperature in a polymer electrolyte fuel cell', *Sensors and Actuators A: Physical*, 2006, **125**, (2), pp. 170–177

[69] Akimoto, Y., Okajima, K., et al.: 'Experimental study of non-destructive approach on pemfc stack using tri-axis magnetic sensor probe', *Journal of Power and Energy Engineering*, 2015, **3**, (03), pp. 1

[70] Vielstich, W., Lamm, A., Gasteiger, H.: 'Handbook of fuel cells. fundamentals, technology, applications', , 2003,

[71] Hinds, G.: 'Performance and durability of pem fuel cells: a review.', , 2004,

[72] Abe, T., Shima, H., Watanabe, K., Ito, Y.: 'Study of pefcs by ac impedance, current interrupt, and dew point measurements: I. effect of humidity in oxygen gas', *Journal of The Electrochemical Society*, 2003, **151**, (1), pp. A101

[73] Cooper, K., Smith, M.: 'Electrical test methods for on-line fuel cell ohmic resistance measurement', *Journal of Power Sources*, 2006, **160**, (2), pp. 1088–1095

[74] Jaouen, F., Lindbergh, G.: 'Transient techniques for investigating mass-transport limitations in gas diffusion electrodes: I. modeling the cathode', *Journal of The Electrochemical Society*, 2003, **150**, (12), pp. A1699

[75] Depernet, D., Narjiss, A., Gustin, F., Hissel, D., Péra, M.C.: 'Integration of electrochemical impedance spectroscopy functionality in proton exchange membrane fuel cell power converter', *International Journal of Hydrogen Energy*, 2016, **41**, (11), pp. 5378–5388

[76] Bi, W., Gray, G.E., Fuller, T.F.: 'Pem fuel cell pt/ c dissolution and deposition in nafion electrolyte', *Electrochemical and Solid-State Letters*, 2007, **10**, (5), pp. B101

[77] Medici, E., Allen, J.: 'Existence of the phase drainage diagram in proton exchange membrane fuel cell fibrous diffusion media', *Journal of Power Sources*, 2009, **191**, (2), pp. 417–427

[78] Nam, J.H., Kaviany, M.: 'Effective diffusivity and water-saturation distribution in single- and two-layer pemfc diffusion medium', *International Journal of Heat and Mass Transfer*, 2003, **46**, (24), pp. 4595–4611

[79] Wang, M., Guo, H., Ma, C.: 'Temperature distribution on the mea surface of a pemfc with serpentine channel flow bed', *Journal of Power Sources*, 2006, **157**, (1), pp. 181–187

[80] Tan, J., Chao, Y.J., Li, X., Van.Zee, J.: 'Degradation of silicone rubber under compression in a simulated pem fuel cell environment', *Journal of Power sources*, 2007, **172**, (2), pp. 782–789

[81] Hung, Y., Tawfik, H., Mahajan, D.: 'Durability and characterization studies of polymer electrolyte membrane fuel cells coated aluminum bipolar plates and membrane electrode assembly', *Journal of Power Sources*, 2009, **186**, (1), pp. 123–127

[82] Legros, B., Thivel, P.X., Bultel, Y., Boinet, M., Nogueira, R.P.: 'Electrochemical impedance and acoustic emission survey of water desorption in nafion membranes', *Electrochemical and Solid-State Letters*, 2009, **12**, (7), pp. B116

[83] Le.Ny, M., Chadebec, O., Cauffet, G., Dedulle, J.M., Bultel, Y., Rosini, S., et al.: 'Current distribution identification in fuel cell stacks from external magnetic field measurements', *IEEE transactions on magnetics*, 2013, **49**, (5), pp. 1925–1928

[84] Hauer, K.H., Potthast, R., Wannert, M.: 'Algorithms for magnetic tomography on the role of a priori knowledge and constraints', *Inverse Problems*, 2008, **24**, (4), pp. 045008

[85] Nara, T., Koike, M., Ando, S., Gotoh, Y., Izumi, M.: 'Estimation of localized current anomalies in polymer electrolyte fuel cells from magnetic flux density measurements', *AIP Advances*, 2016, **6**, (5), pp. 056603

[86] Jain, A.K., Mao, J., Mohiuddin, K.M.: 'Artificial neural networks: A tutorial', *Computer*, 1996, **29**, (3), pp. 31–44

[87] Jemeı, ä., Hissel, D., Péra, M.C., Kauffmann, J.M.: 'On-board fuel cell power supply modeling on the basis of neural network methodology', *Journal of Power Sources*, 2003, **124**, (2), pp. 479–486

[88] Cadet, C., Jemei, S., Druart, F., Hissel, D.: 'Diagnostic tools for pemfcs: from conception to implementation', *International Journal of Hydrogen Energy*, 2014, **39**, (20), pp. 10613–10626

[89] Kim, J., Lee, I., Tak, Y., Cho, B.: 'State-of-health diagnosis based on hamming neural network using output voltage pattern recognition for a pem fuel cell', *international journal of hydrogen energy*, 2012, **37**, (5), pp. 4280–4289

[90] Hatti, M., Tioursi, M.: 'Dynamic neural network controller model of pem fuel cell system', *International Journal of Hydrogen Energy*, 2009, **34**, (11), pp. 5015–5021

[91] Mammar, K., Saadaoui, F., Laribi, S.: 'Design of a pem fuel cell model for flooding and drying diagnosis using fuzzy logic clustering', *Renewable Energy Focus*, 2019, **30**, pp. 123–130

[92] Laribi, S., Mammar, K., Sahli, Y., Koussa, K.: 'Analysis and diagnosis of pem fuel cell failure modes (flooding & drying) across the physical parameters of electrochemical impedance model: Using neural networks method', *Sustainable Energy Technologies and Assessments*, 2019, **34**, pp. 35–42

[93] Wahdame, B., Candusso, D., Harel, F., François, X., Péra, M.C., Hissel, D., et al.: 'Analysis of a pemfc durability test under low humidity conditions and stack behaviour modelling using experimental design techniques', *Journal of Power Sources*, 2008, **182**, (2), pp. 429–440

[94] Halvorsen, I.J., Pivac, I., Bezmalinović, D., Barbir, F., Zenith, F.: 'Electrochemical low-frequency impedance spectroscopy algorithm for diagnostics of pem fuel cell degradation', *International Journal of Hydrogen Energy*, 2020, **45**, (2), pp. 1325–1334

[95] Chevalier, S., Trichet, D., Auvity, B., Olivier, J., Josset, C., Machmoum, M.: 'Multiphysics dc and ac models of a pemfc for the detection of degraded cell parameters', *International Journal of Hydrogen Energy*, 2013, **38**, (26), pp. 11609–11618

[96] Mann, R.F., Amphlett, J.C., Hooper, M.A., Jensen, H.M., Peppley, B.A., Roberge, P.R.: 'Development and application of a generalised steady-state electrochemical model for a pem fuel cell', *Journal of power sources*, 2000, **86**, (1-2), pp. 173–180

[97] Srinivasulu, G.N., Subrahmanyam, T., Rao, V.D.. 'Retracted: Parametric sensitivity analysis of pem fuel cell electrochemical model'. (Elsevier, 2011

[98] Mammar, K., Saadaoui, F., Hazzab, A.: 'Development and simulation of a pem fuel cell model for prediction of water content and power generation', *Iranian Journal of Hydrogen & Fuel Cell*, 2018, **4**, (4), pp. 289–299

[99] Amphlett, J., Baumert, R., Mann, R., Peppley, B., Roberge, P., Rodrigues, A.: 'Parametric modelling of the performance of a 5-kw proton-exchange membrane fuel cell stack', *Journal of Power Sources*, 1994, **49**, (1-3), pp. 349–356

[100] Agbossou, K., Dubé, Y., Hassanaly, N., Adzakpa, K.P., Ramousse, J.: 'Experimental validation of a state model for pemfc auxiliary control', *IEEE Transactions on Industry Applications*, 2009, **45**, (6), pp. 2098–2103

[101] Fouquet, N. 'Real time model-based monitoring of a pem fuel cell flooding and drying out'. In: 2010 IEEE Vehicle Power and Propulsion Conference. (IEEE, 2010. pp. 1–8

[102] McCain, B.A. 'Modeling and Analysis for Control of Reactant and Water Distributions in Fuel Cells.', 2008

[103] Boulon, L., Agbossou, K., Hissel, D., Hernandez, A., Bouscayrol, A., Sicard, P., et al. 'Energy management of a fuel cell system: influence of the air supply control on the water issues'. In: 2010 IEEE International Symposium on Industrial Electronics. (IEEE, 2010. pp. 161–166